



<http://researchspace.auckland.ac.nz>

ResearchSpace@Auckland

Copyright Statement

The digital copy of this thesis is protected by the Copyright Act 1994 (New Zealand).

This thesis may be consulted by you, provided you comply with the provisions of the Act and the following conditions of use:

- Any use you make of these documents or images must be for research or private study purposes only, and you may not make them available to any other person.
- Authors control the copyright of their thesis. You will recognise the author's right to be identified as the author of this thesis, and due acknowledgement will be made to the author where appropriate.
- You will obtain the author's permission before publishing any material from their thesis.

To request permissions please use the Feedback form on our webpage.

<http://researchspace.auckland.ac.nz/feedback>

General copyright and disclaimer

In addition to the above conditions, authors give their consent for the digital copy of their work to be used subject to the conditions specified on the [Library Thesis Consent Form](#) and [Deposit Licence](#).

Note : Masters Theses

The digital copy of a masters thesis is as submitted for examination and contains no corrections. The print copy, usually available in the University Library, may contain corrections made by hand, which have been requested by the supervisor.

Development and Evaluation of a Novel Probiotic Delivery System

Song Chen, MHS

*A thesis submitted in partial fulfilment of the requirements for the degree of Doctor of
Philosophy in Pharmacy, The University of Auckland, 2012.*

*This thesis is for examination purposes only and may not
be consulted or referred to by any persons other than
those involved in the examination process.*

Summary

Health-promoting benefits of probiotics after oral administration are challenged by antimicrobial bio-barriers in human gastrointestinal (GI) tract. The objective of this project was to develop an applicable delivery system based on chitosan-coated sub-100 μm Ca^{2+} -alginate gel microcapsules for improved colonic delivery of probiotic lactic acid bacteria (LAB).

Flow cytometric analysis (FCM) was utilized to evaluate sucrose and lecithin vesicle on six probiotic LAB strains for the protection against the GI defensive factors – gastric pH and bile acids, respectively. Three subpopulations (intact, injured and dead) could be clearly identified in each sample. In the presence of the protectants, significant expansion of the intact subpopulation was observed, whereas the dead subpopulation was highly decreased.

The protectants were then incorporated in Ca^{2+} -alginate microcapsules prepared by an internal-gelation/emulsification technique. With the protection of the reinforced sub-100 μm delivery system, all four examined probiotic strains showed improved survival through an 8-h sequential treatment of the simulated GI fluids. The degradation of the delivery system was also found to respond to the extracted enzymes from human faeces. Approximately 80% of the embedded probiotic bacteria were released within 8-h suspension in the simulated colonic fluid, whereas the release ratio was only 10% in the absence of the colonic enzymes. Additionally, the probiotic delivery system was further confirmed to enhance the storage stability of the probiotic LAB strains and have no obvious adverse influence on the probiotic (e.g. antimicrobial) effect of the embedded probiotic bacteria.

The mucoadhesive property of the probiotic delivery system was modified by coating with chitosan. The coated system could retain markedly more probiotic bacteria on HT29-MTX colonic epithelial monolayer. The coatings were further demonstrated in an innovative tensile test to exert stronger mucoadhesion to the colonic mucosa tissues at

near neutral pH and with less ambient water, which highly conforms to the physiological environment of the colon.

In conclusion, the novel probiotic delivery system was proved to be an efficient vehicle for the colonic delivery of a variety of LAB probiotic strains. The developed probiotic delivery system also indicates the readiness for future research on in vivo confirmation and clinical trials.

Acknowledgements

I would like to dedicate this thesis to the two important women in my life - my late mother, who unfortunately is not able to see it coming out, and also to my wife, who supported me consistently at those dark moments of the loss of my mother during my PhD study. Words cannot express my deep love towards you.

I wish to take this opportunity to convey my utmost gratitude to my chief supervisor Prof. Sanjay Garg, for his guidance, kind encouragement and support throughout my study. His professional attitude, knowledge and passion have always been an inspiration for me.

I am also heartily thankful to my supervisor Prof. Lynnette R. Ferguson for her constant guidance, advice, and motivation.

I am sincerely grateful to my company mentors Dr. Quan Shu and Prof. Yi-huai Gao for giving me valuable advice and instructions during this research.

Additionally, I am deeply indebted to the following institutions and people for their kind assistance with my project during the past four years. They are the staff at Food Safety and Preservation team of Plant and Food Research led by Mr. Graham Fletcher, the staff at AnQual laboratory of the School of Pharmacy (UoA), Mr. Sairam Behera, Mrs. Amanda Collocott, Mrs. Asma Othman, Ms. Sabrina Tian, Ms. Qian Zhao, Ms. Vivien Zhang, Ms. Cristina Cruz, Mr. Graeme Summers, Ms. Michel Nieuwoudt and Dr. Darren Svirskis for their invaluable assistance with my experimental works.

Funding for this project was provided by the Technology in Industry Fellowship (TIF, the Ministry of Science and Innovation) and the University of Auckland scholarships. I am sincerely grateful for their providing me the scholarships to support my study.

Table of Content

Summary.....	ii
Acknowledgements	iv
Table of Content.....	v
List of Figures.....	xi
List of Tables	xv
Chapter 1. General introduction	1
1.1. General introduction.....	1
1.2. The scope of the current project.....	3
Chapter 2. Literature review	6
2.1. Probiotics as functional food ingredients and therapeutic agents	6
2.1.1. Probiotics	6
2.1.2. Administering routes of probiotics	7
2.1.3. Mechanisms of probiosis	8
2.2. Solutions to the obstacles facing production, storage and <i>in vivo</i> delivery of probiotic products.....	9
2.2.1. Obstacles challenging the effectiveness of administering probiotics.....	9
2.2.1.1. During manufacture and processing	9
2.2.1.2. During storage.....	11
2.2.1.3. Gastric acidity	12
2.2.1.4. Bile challenge in intestine.....	13
2.2.1.5. Challenge at mucosal surfaces especially in the GI tract.....	14

2.2.2. Strategies for overcoming the obstacles	15
2.2.2.1. Strain selection.....	15
2.2.2.2. Stress responses	16
2.2.2.3. Packaging and formulae.....	17
2.2.2.4. Microencapsulation.....	18
2.2.3. Advantageous fluorescent-probe-based flow cytometric methods for probiotics research.....	22
2.2.3.1. Various fluorescent probes feature a physical/chemical multiparametric observation by FCM	23
2.2.3.2. FCM is a powerful tool for probiotic strain selection (studies based on pH and bile salt tolerance)	26
2.2.3.3. FCM is a valuable tool in evaluation of stress on probiotic cells during process and storage	27
2.3. Strategies for colon-specific delivery.....	28
2.3.1. Physiology of colon and the benefits of colon delivery	29
2.3.2. pH-controlled colonic delivery system.....	30
2.3.3. Time-controlled colonic delivery system	31
2.3.4. Pressure-controlled colonic delivery system	32
2.3.5. Microbiota-controlled polysaccharide colonic delivery system.....	32
2.4. Prolonged colonic retention by mucoadhesion	35
2.4.1. Physiological role of colonic mucus.....	35
2.4.2. Mucoadhesion and its advantages	38
2.4.3. Theories of mucoadhesion.....	39
2.4.4. Conventional mucoadhesive polymers.....	41
2.4.5. Novel strategies for enhanced mucoadhesion	43
2.4.5.1. Lectins.....	43
2.4.5.2. Thiomers	44

2.4.5.3. pH-responsive mucoadhesive polymers	45
2.4.6. Methods for mucoadhesion analysis	47
2.4.6.1. <i>In vitro</i> methods	47
2.4.6.2. <i>In vivo</i> methods	50
Chapter 3. Flow cytometric assessment of protectants for enhanced survival of probiotic lactic acid bacteria through human gastro-intestinal environment	51
3.1. Introduction	51
3.2. Materials and methods	54
3.2.1. Materials	54
3.2.2. Strains and culturing conditions	55
3.2.3. Simulated gastric fluid and sucrose supplement	55
3.2.4. Simulated intestinal fluid and lecithin vesicle supplement	56
3.2.5. Time course study of bile salts challenge to <i>L. reuteri</i> DPC16 at serial concentrations	56
3.2.6. Fluorescence labelling and FCM analysis	57
3.2.7. Cell sorting	58
3.2.8. Statistical analysis	58
3.3. Results	59
3.3.1. SGF challenge and sucrose supplement	59
3.3.2. Bile-salt SIF challenge and lecithin vesicle supplement	63
3.3.3. Cell sorting	65
3.3.4. Time course study of bile salts challenge to DPC16 at serial concentrations	67
3.4. Discussion	69
Chapter 4. Development of the probiotic colonic delivery system based on microencapsulation with protectants	73
4.1. Introduction	73
4.2. Materials and methods	76

4.2.1. Materials	76
4.2.2. Strains and culturing conditions	77
4.2.3. Preparation of microcapsules	77
4.2.4. Particle size analysis.....	78
4.2.5. Challenge of simulated gastric fluid.....	78
4.2.6. Inactivation of the F ₁ F ₀ -ATPases of <i>L. reuteri</i> DPC16 and <i>Bf. lactis</i> HN019 in microcapsules	79
4.2.7. Challenge of bile salt solution	79
4.2.8. Probiotics release from chitosan-coated alginate microcapsules and plate count	80
4.2.9. Epifluorescent microscopy of bile salt challenged samples	80
4.2.10. Sequential challenge of SGF and SIF.....	80
4.2.11. <i>In vitro</i> release of the microencapsulated <i>L. reuteri</i> DPC16 in simulated GI fluids	81
4.2.12. Statistical analysis	83
4.3. Results	83
4.3.1. Microcapsule size analysis	83
4.3.2. Challenge of simulated gastric fluid.....	83
4.3.3. F ₁ F ₀ -ATPase inhibitor treatment	86
4.3.4. Challenge of bile salt solution and epi-fluorescent microscopic observation	89
4.3.5. Sequential challenge of SGF and SIF.....	94
4.3.6. <i>In vitro</i> release of the microencapsulated <i>L. reuteri</i> DPC16 in simulated GI fluids	96
4.4. Discussion	98
Chapter 5. Evaluation of the storage stability of freeze-dried probiotic bacteria in the probiotic delivery system, and the inhibitory effect on food-borne pathogens	103
5.1. Introduction	103

5.2. Materials and methods	105
5.2.1. Strains and culturing conditions	105
5.2.2. Immobilization of the model strains in the probiotic delivery system	105
5.2.3. Production and freeze-drying	106
5.2.4. Accelerated storage test	106
5.2.5. Kinetics parameters of thermal inactivation	107
5.2.6. Inhibition of the food-borne pathogens by the probiotic delivery system in a co-culture model	108
5.2.7. <i>In vitro</i> reuterin production by <i>L. reuteri</i> DPC16 immobilized in the probiotic delivery system in a glycerol-water-fermentation system	109
5.2.8. Statistical analysis	110
5.3. Results	110
5.3.1. Post-freeze-drying survival of the model strains in free and microencapsulated forms with or without the presence of skim milk powder	110
5.3.2. Thermal death of the model strains in free and microencapsulated forms with or without the presence of skim milk powder	112
5.3.3. Determination of the inactivation kinetics and prediction of the stability at 4 °C and 20 °C	117
5.3.4. Inhibition of the food-borne pathogens by the probiotic delivery system	121
5.3.5. <i>In vitro</i> reuterin production by <i>L. reuteri</i> DPC16 immobilized in the probiotic delivery system	124
5.4. Discussion	127
Chapter 6. Evaluation of mucoadhesive coatings of chitosan and thiolated chitosan for the probiotic microcapsules	131
6.1. Introduction	131
6.2. Materials and methods	134
6.2.1. Materials	134
6.2.2. Preparation of the probiotic microcapsules	134

6.2.3. Preparation of FITC-conjugated chitosan and flow cytometric (FCM) analysis of the FITC-chitosan coating on the microcapsules	135
6.2.4. Zeta-potential of chitosan-coated probiotic microcapsules	136
6.2.5. Synthesis of thiolated chitosan and its characterization	136
6.2.6. Rheological synergism	137
6.2.7. <i>Ex vivo</i> tensile test	138
6.2.8. <i>In vitro</i> mucoadhesion of the probiotic microcapsules to the mucin-secreting HT-29-MTX colonic epithelial culture	140
6.2.9. Statistical analysis	141
6.3. Results	142
6.3.1. Adsorption of chitosan on alginate microcapsules	142
6.3.2. Synthesis of thiolated chitosan and confirmation of the presence of thiol groups	145
6.3.3. Evaluation of the bio-/muco-adhesion of chitosan and thiolated chitosan..	146
6.3.3.1. Viscosity synergism of polymers and mucin	146
6.3.3.2. Mucoadhesion of various alginate-gel surfaces assayed by <i>ex vivo</i> tensile test using freshly excised porcine tissue strip model	151
6.3.3.3. Adhesion of the chitosan and the thiolated chitosan coated probiotic microcapsules to mucin-secreting HT-29-MTX colonic epithelial monolayer.	154
6.4. Discussion	156
Chapter 7. General discussion and future directions	160
7.1. General discussion and conclusions	160
7.2. Future directions.....	163
Bibliography	165
Publications and presentations	193

List of Figures

- Figure 2.1** A simplified state diagram shows the glass transition curve which relates the glass transition temperature and moisture content. 12
- Figure 2.2** The thickness of adherent (dark grey) and non-adherent (light grey) mucus layers in the GI tract of rat..... 37
- Figure 2.3** The illustrative mucoadhesion process (theories and bondings) as it happens along the time. 41
- Figure 3.1** Dot plots of the FCM-enumerated *L. acidophilus* DPC201 exposed to the simulated GI challenges in the absence and presence of the protectants. (a) Fresh culture, positive control; (b) heat-killed DPC201, negative control; (c) DPC201 exposed to SGF pH 1.2 for 2 h; (d) DPC201 exposed to SGF pH 1.2 for 2 h in the presence of 20 mM sucrose; (e) DPC201 exposed to bsSIF (0.4% bile salts) for 2 h; (f) DPC201 exposed to bsSIF (0.4% bile salts) for 2 h in the presence of 2% lecithin vesicle; (g) DPC201 exposed to bsSIF (0.8% bile salts) for 2 h; (h) DPC201 exposed to bsSIF (0.8% bile salts) for 2 h in the presence of 2% lecithin vesicle..... 61
- Figure 3.2** Summary of the FCM-enumerated viability of six probiotic strains which were exposed to SGF for 2 h either with the absence or the presence of 20 mM sucrose..... 62
- Figure 3.3** The summary of the FCM-enumerated viability of six probiotic strains which were exposed to bsSIF for 2 h either with the absence or the presence of 2% (w/v) lecithin vesicle..... 64
- Figure 3.4** FCM-enumerated physiological heterogeneity of the *L. reuteri* DPC16 populations which were exposed to bsSIF challenge..... 68

- Figure 4.1** Survival of the four probiotic strains (log reduction of CFU count) in SGF, pH 1.2: (a) the non-encapsulated cells, (b) in the AlgC microcapsules, (c) in the FormE microcapsules, and (d) in the FormE microcapsules and SGF supplemented with 20 mM glucose..... 85
- Figure 4.2** Survival of the two probiotic strains *L. reuteri* DPC16 and *Bf. lactis* HN019 in SGF: (a) *L. reuteri* DPC16 fresh culture, (b) *L. reuteri* DPC16 in FormE microcapsules, (c) *Bf. lactis* HN019 fresh culture, and (d) *Bf. lactis* HN019 in FormE microcapsules. 88
- Figure 4.3** Survival of the four probiotic strains (log reduction of CFU count) challenged by bile salt solution with a concentration ranging from 0.0% to 1.2% (w/v): (a) the non-encapsulated cells, (b) in the AlgC microcapsules, (c) in the FormE-w/o-lv microcapsules and (d) in the FormE microcapsules..... 91
- Figure 4.4** Epi-fluorescent microscopy of the microencapsulated *L. reuteri* DPC16 stained by PI (red: dead) and cFDA (green: viable) after the 2-h treatment with (a) the AlgC microcapsules suspended in PBS buffer; (b) the AlgC microcapsules suspended in 0.4% bile salt solution; (c) the FormE microcapsules suspended in 0.4% bile salt solution; and (d) the FormE microcapsules suspended in 0.8% bile salt solution..... 93
- Figure 4.5** Survival of the four probiotic strains (log reduction of CFU count) subjected to a sequential challenge of SGF (with 20 mM glucose) and SIF. (a) The non-encapsulated probiotics or (b) the probiotics in the FormE microcapsules. The symbols represent the different probiotic strains as *P. acidilactici* DPC209 (◇), *L. plantarum* DPC206 (□), *L. reuteri* DPC16 (Δ) and *Bf. lactis* HN019 (●). 95
- Figure 4.6** *In vitro* release of *L. reuteri* DPC16 from the probiotic colonic delivery system. The samples were sequentially incubated in the simulated gastric fluid (SGF) pH 2.0 for 2 hours, in the simulated intestinal fluid (SIF) pH 6.8 for 4 hours, and in the simulated colonic fluid (SCF) pH 6.5 for 8 hours. 97
- Figure 5.1** Viability assessment of *L. reuteri* DPC16 by PI and cFDA dual staining after freeze-drying as (a) free form, (b) free form with the presence of skim milk

powder (SMP), (c) in the microcapsule-based delivery system, and (d) in the microcapsule-based delivery system with the presence of SMP.....	111
Figure 5.2 Thermal mortality curves of freeze-dried <i>L. reuteri</i> DPC16 (a) in free form, (b) in free form with the presence of skim milk powder (SMP), (c) in microencapsulated form, and (d) in microencapsulated form with the presence of skim milk powder at 25 °C, 35 °C and 55 °C, and their linear regressions (model fitting with R ² denoting the goodness-of-fit).	115
Figure 5.3 Thermal mortality curves of freeze-dried <i>L. plantarum</i> DPC206 (a) in free form, (b) in free form with the presence of skim milk powder (SMP), (c) in microencapsulated form, and (d) in microencapsulated form with the presence of skim milk powder at 25 °C, 35 °C and 55 °C, and their linear regressions (model fitting with R ² denoting the goodness-of-fit).	116
Figure 5.4 Arrhenius plot for the inactivation of the two model strains, i.e. (a) <i>L. reuteri</i> DPC16 and (b) <i>L. plantarum</i> DPC206, in different preparation forms: free form, free form with the presence of skim milk powder, microencapsulated form, and microencapsulated form with the presence of skim milk powder.....	119
Figure 5.5 Comparison between theoretical and actual measurement values of survival rate at 20 °C of freeze-dried (a) <i>L. reuteri</i> DPC16 and (b) <i>L. plantarum</i> DPC206.	120
Figure 5.6 Microscopy of newly grown <i>L. reuteri</i> DPC16 released from the chitosan-coated alginate microcapsules after 20h incubation at 37 °C in the modified MRS broth.....	124
Figure 5.7 Time-series of (a) the reuterin concentrations (mmol/L) and (b) the viable counts (log(CFU)/mL) in the glycerol-water system produced by the planktonic <i>L. reuteri</i> DPC16 (square), the alginate-microencapsulated <i>L. reuteri</i> DPC16 (triangle) and the chitosan-coated alginate-microencapsulated <i>L. reuteri</i> DPC16 (circle)..	126
Figure 6.1 The fluorescent microscopy (x100) of the Ca ²⁺ -alginate microcapsules coated by FITC-conjugated chitosan.....	142

Figure 6.2 Flow cytometric (FCM) analysis of FITC-conjugated chitosan adsorbed on the Ca-alginate microcapsules: (a) the fluorescent intensity of the FITC-chitosan coated microcapsules at different time point of coating treatment; (b) and (c) The histograms of the side scatter (SSC) and the forward scatter (FSC) readings of the samples; (d) the SSC vs. FSC plot of the microcapsules detected by FCM; and (e) average FITC-fluorescent intensities of the microcapsules that were exposed to various durations of coating treatment.	144
Figure 6.3 Zeta-potential of the chitosan or the thiolated chitosan coated microcapsules that were exposed to different duration of the coating treatments.	145
Figure 6.4 ATR-FTIR spectra of original chitosan, thiolated chitosan and 2-iminothilane (the thiolating agent).	146
Figure 6.5 Epi-fluorescent microscopy of the adhered microcapsules to HT29-MTX monolayer.	155

List of Tables

Table 2.1 Techniques used for encapsulating probiotic microorganisms. Modified from	19
Table 2.2 Frequently used fluorescent probes in combination with FCM for microbiology.	25
Table 2.3 Polysaccharide substrates for the colonic microbiota.	34
Table 2.4 Mucus layer thickness in the human GI tract.	38
Table 2.5 A group of thiomers and the improvement on measured mucoadhesion.	45
Table 2.6 Methods for measuring the mucoadhesion property of polymer.	48
Table 3.1 Percentages of cells of six LAB strains that formed or did not form colonies after being directly sorted on MRS agar plate.	66
Table 4.1 Releasing media for the sequential treatments of the probiotic microcapsules in the simulated GI environment.	81
Table 5.1 Post-freeze-drying survival (log CFU/g) of the model strains in free and microencapsulated forms with or without the presence of skim milk powder (SMP).	112
Table 5.2 Decimal thermal reduction of <i>L. reuteri</i> DPC16 in free and microencapsulated forms with or without the presence of skim milk powder for accelerated storage testing.	113
Table 5.3 Decimal thermal reduction of <i>L. plantarum</i> DPC206 in free and microencapsulated forms with or without the presence of skim milk powder for accelerated storage testing.	114

Table 5.4 Experimental and predicted D values and k values for the thermal reductions of <i>L. reuteri</i> DPC16 in free and microencapsulated forms with or without the presence of skim milk powder at various temperatures.	118
Table 5.5 Experimental and predicted D values and k values for the thermal reductions of <i>L. plantarum</i> DPC206 in free and microencapsulated forms with or without the presence of skim milk powder at various temperatures.	118
Table 5.6 Comparison of the inhibitory effect on two food-borne pathogens <i>E. coli</i> O157:H7 and <i>S. typhimurium</i> by planktonic and microencapsulated <i>L. reuteri</i> DPC16.	123
Table 6.1 Groups of the final concentrations (w/v) of the polymer (chitosan or thiolated chitosan) and mucin in the GI fluids for the study of mucoadhesion-based rheological synergism in blend system.	137
Table 6.2 Soaking treatments for the preparation of the four types of surfaces for the <i>ex vivo</i> tensile test.	139
Table 6.3 Viscosity of mucin (η_m) plus polymer (η_p), the blend system (η_i), the calculated viscosity of mucoadhesion (η_{ad}) and the calculated force of mucoadhesion (F).	148
Table 6.4 Power law index (n) and consistency index (K) of chitosan or thiolated chitosan at various concentrations in SGF or SIF with or without mucin, derived from the Ostwald-de Waele rheological model (mean \pm standard deviation, $n = 3$).	150
Table 6.5 The maximum detachment force and the total work to detach certain mucoadhesive surface from porcine GI tissue, as measured by a texture analyzer.	153
Table 6.6 Counts of <i>L. reuteri</i> DPC16 released from the adhered microcapsules with chitosan coating (A) or thiolated chitosan coating (B) to HT29-MTX monolayer.	154

Chapter 1. General introduction

1.1. General introduction

Probiotic bacteria are defined as live microorganisms which, when administered in adequate amounts, confer a beneficial physiological effect in the host [1]. More recently, probiotics have become a driving force in the design of functional foods, especially from dairy products. Scientific evidence is accumulating, supporting the use of probiotics to maintain human health, particularly against certain gastrointestinal (GI) disorders. Nowadays, most probiotic strains that have been intensively researched by academia and industry belong to the lactic acid bacteria (LAB), e.g. lactobacilli and bifidobacteria. Further to the original role of LAB in the dairy industry, the extended probiotic functions of selected LAB strains have opened up the new horizon of increased market potential for health products, which also turns into a new research focus in New Zealand [2].

Colonic delivery of viable probiotic bacteria is an essential prerequisite for many probiotic effects to initiate. However, stability of probiotic bacteria, i.e. the preservation of viable cells, is frequently challenged by various stress-factors during processing, storage, and post-consumption passage in the GI tract. Therefore, the development of effective delivery systems is consistently pursued for successful probiotic products with assured efficacy.

As a promising technology for the preservation of many types of probiotics, microencapsulation has made its contribution in many reported applications, and is thus recommended by many as a mandatory practice for achieving the promised health benefits. Microencapsulation has been defined as “the technology of packaging solid, liquid and gaseous materials in small capsules that release their contents at controlled rates over prolonged periods of time” [3]. Such technology is of significant interest to the pharmaceutical sector, but also has relevance for the food industry. It applies a physical barrier to protect bioactive components against any adverse environmental conditions. In regard to viable probiotics, it becomes more and more recognized that microencapsulation can have positive influence on stabilizing cells and bestow convenience to handling and storage of many probiotics on an industrial scale [4]. Some LAB strains have also been reported to profit from microencapsulation in matrices during dehydration and lyophilisation [5].

Many previously reported microencapsulation practices of probiotics were carried out with polysaccharide beads that have a size range of several millimetres. However, microcapsules at a reduced dimension (i.e. below 100 μm) offer a number of distinguishing features, which may make them a more efficient colonic delivery system for probiotic bacteria. Firstly, only particles less than 100 μm can avoid oral detection, thus providing an unaltered texture when incorporated in foods, such as yoghurt, ice-cream, and fermented drinks. Secondly, the reduced size may also allow a more efficient release of entrapped contents, in response to environmental releasing triggers, such as colonic-microflora-induced degradation of polysaccharide gels. Thirdly, the reduced size can mitigate inconsistencies in the performance of large probiotic beads caused by heterogeneous formations in wall matrix and uneven distribution of embedded bacteria. Fourthly, the increasing coating-to-core ratio can significantly alter

the physiochemical characteristics of microcapsules by highlighting the effects of applied coatings, e.g. the potential of mucoadhesive coating materials. Finally, microcapsules with reduced sizes are more prone to be lodged in surface folds and crevices of the lower GI tract, and subject to less forces of dislocation, thus supporting the prolonged GI retention of the system. Therefore, the value of such probiotic delivery systems is enormous. Hence, the current project will be dedicated to the development of such a colonic delivery system for probiotic bacteria based on the concept of sub-100- μm polysaccharide microcapsules.

1.2. The scope of the current project

In recent years, probiotic bacteria have attracted great attention for their promising uses as functional food ingredients and therapeutic agents. However, considerable difficulty lies in delivering this potential functionality to consumers. Microencapsulation has been reported in many studies to improve the survival of probiotic bacteria against various stresses. The principle is to apply polymer matrix and thus separate embedded cells from direct disturbance of harsh environments. Ca^{2+} -alginate hydrogel provides a successful example for this application.

Reducing the size of probiotic microcapsules (e.g. below 100 μm) can confer some extra advantages for the oral delivery of probiotic bacteria. However, the accordingly decreased protection by microcapsules inevitably questions the efficiency of such systems, particularly when they are subjected to the potent GI bio-barriers (e.g. gastric pH and bile). On the other hand, the conventional enumeration techniques based on proliferation (e.g. plate count) was suggested to be limited in providing in-depth evaluation of the stresses to probiotic bacteria. Flow cytometric (FCM) analysis was therefore considered to be a powerful supplement to the current research. In addition,

mucoadhesive properties of the delivery system are also worthy of careful investigation. The delivery system is expected to prolong retention time in the colon where release is triggered. Since the reduced size also opens the opportunity of increased amount (relative to per unit core content) of mucoadhesive coating, the use of novel mucoadhesive materials such as thiomers may be extended to improve the efficiency of colonic delivery of probiotics.

Therefore, the objectives of this study are summarised as follows:

1. Use FCM analysis to evaluate two hypothesized protectants for improved survival of probiotic bacteria against the GI stress factors
2. To prepare probiotic microcapsules with a narrow size distribution of 100 μm by a modified emulsion method; the microcapsules to provide a protective shield for probiotic cells against simulated GI challenges;
3. To evaluate the protection by the delivery system during lyophilisation and storage; to evaluate the probiotic function (e.g. antimicrobial effect against food-borne pathogens) after model probiotic strain is immobilized in the delivery system.
4. To evaluate the mucoadhesive property of the delivery system for prolonged colonic retention; to evaluate the potential use of thiomers as a mucoadhesive coating material.

The following experiments were conducted to test the hypothesis and fulfil the objectives. The results are detailed in the remainder of this study.

Chapter 2, the literature review, provides knowledge on probiotic bacteria, strategies for improving the survival of probiotic bacteria at various stages, advantageous FCM

analysis for evaluating protection to probiotic bacteria, colon delivery, and strategies for improved colonic retention.

Chapter 3 describes the use of flow cytometry for the evaluation of two hypothesized protectants metabolisable sugar and lecithin vesicle for the protection of probiotic LAB strains over the GI stress factors.

Chapter 4 describes the development of the probiotic delivery system based on sub-100 µm chitosan-coated Ca²⁺-alginate microcapsule and its performance against simulated GI challenges.

Chapter 5 evaluates the survival of probiotic strains in the probiotic delivery system during lyophilisation and storage. The probiotic inhibitory effect on food-borne pathogens after immobilization in the delivery system was also demonstrated on a model strain *L. reuteri* DPC16.

Chapter 6 evaluates the mucoadhesive property of the delivery system. Thiolated chitosan was also tested as the mucoadhesive coating for the probiotic delivery system for its improved mucoadhesion performance.

Finally, Chapter 7 concludes with a summary of experimental results and identifications of future utilization of developed models, modelling methods, and FCM.

Chapter 2. Literature review

This chapter is a review on probiotic bacteria, strategies for improving the survival of probiotic bacteria at various stages, advantageous FCM analysis for evaluating protection to probiotic bacteria, colonic delivery, and strategies for improved colonic retention.

2.1. Probiotics as functional food ingredients and therapeutic agents

2.1.1. Probiotics

Probiotics are attracting substantial attention as an important functional food ingredient owing to prophylactic and therapeutic effects on maintaining or restoring the physiological state of the human GI tract. Probiotics are “live microorganisms which when administered in adequate amounts confer a health benefit on the host” [1]. Many of the probiotics currently available for medical and commercial use are lactic acid bacteria (LAB), which predominantly come from the genera *Lactobacillus* and *Bifidobacterium*. They are also components of important intestinal microflora which contribute to the healthy human GI tract [6-7]. Evidence-based reports have claimed a variety of beneficial functions of probiotics over the years, which suggested that certain probiotics or combinations of probiotics can normalize the intestinal microflora, reinforce the mucosal barrier against invasion by potential pathogens, ameliorate lactose intolerance, relieve symptoms for several types of diarrhoea, provide adjuvant cure of irritable bowel syndrome (IBS) and inflammatory bowel disease (IBD), prevent colon

cancer, modulate immune function, potentially enhance calcium absorption, and reduce cholesterol level [8]. With more accumulation of knowledge, it is hence believed that the application and utilisation of these probiotics will be enriched.

2.1.2. Administering routes of probiotics

The applications of most probiotics are associated with their delivery to the human GI tract, which body region is their most popular habitat and site of function. Besides, most probiotic LAB are also largely incorporated as functional food ingredients, especially in dairy products (cheese, yoghurt, beverage and etc.). Therefore, oral consumption is always the most popular method for the intake of probiotics for household consumers.

It was also suggested that oral routes may not be essential for probiotic functions to take place, whereby alternative administering routes in some cases could exert the same effect [9]. As valuable supplements to oral administration, alternative administering routes of probiotics may also be practised for specific therapeutic purposes. Topical administration of probiotic strains selected from the skin microflora was innovatively demonstrated to stimulate innate immunity in a few cases [10-11] and was used to control the burn wound infection [12]. In another case, the parenteral administration of a probiotic strain *L. salivarius* 118 was proven to exert non-specific anti-inflammatory effects and attenuate the symptoms of colitis and arthritis in mice [9].

Nevertheless, these studies on unconventional administration of probiotics, however innovative, compose only a small fraction of the mainstream research. Current focus is still given to orally administered probiotics, owing to the incomparable ease of administration.

2.1.3. Mechanisms of probiosis

A number of mechanisms of probiosis have been postulated to elucidate the probiotic benefits.

- Many probiotics show markedly inhibitory effects against pathogens and reinforce the frontier protection of the GI tract.

Probiotics can compete for adhesion sites and nutrients, and therefore reduce the chance of the colonisation by pathogens. An extensively investigated strain - *Escherichia coli* strain Nissle 1917 (EcN) – sets an elegant example for this probiotic function. Studies revealed more than seven iron uptake systems are encoded in this strain's genome, which enable this strain to effectively compete for the limited iron resources with the pathogenic bacteria [13-14].

Some probiotic strains are also able to produce distinct antimicrobial substances. Class II bacteriocin Abp118 produced by *L. salivarius* strain UCC118 [15] and reuterin produced by *L. reuteri* species bacteria serve as typical examples.

Short chain fatty acids (SCFA) are also found to show inhibitory effects on certain pathogenic bacteria. Other antimicrobial mechanisms including anti-adhesive effects, anti-invasive effects and antitoxin effects are highlighted as well [16].

- Probiotics are capable to further ferment resistant carbohydrates or break down indigestible carbohydrates and produce SCFA.

The accumulation of acidic metabolites reduces the pH of the colon, which impedes proliferation of pathogenic bacteria, and also provides certain nutrition to colonocytes. It may even alter gene expression of epithelial cells owing to the production and accumulation of butyrates, for instance, the expression of interleukin (IL)-8 and

monocyte chemoattractant protein 1 (MCP 1). This mechanism is more related to the discussion of the next function.

- Probiotics can modulate hosts' immune system and probably promote homeostasis.

The main target cells for this modulation in GI tract are intestinal epithelial and gut-associated immune cells. Lomax and Calder [17] reviewed the human immune functions modulated by probiotics and summarised, including: (a) cytokines, IgA, IgE were regulated in a mixed pattern; (b) the NK cell activity was generally enhanced by most probiotics; (c) phagocytosis could be improved by lactobacilli but not clear for other probiotics; and (d) no obvious effects were observed on T cell activation. Similarly, Pagnini et al. [18] studied the multiple probiotic formulation VSL#3 for the prevention of intestinal inflammation and further concluded that probiotics promoted gut health through stimulation, rather than suppression, of the innate immune system.

In terms of most of the probiotic functions, the viability of probiotics obviously is a prerequisite to exert interactive protection and promotion of host's homeostasis. Therefore, how to ensure the delivery of viable probiotics at the function site is of paramount importance.

2.2. Solutions to the obstacles facing production, storage and *in vivo* delivery of probiotic products

2.2.1. Obstacles challenging the effectiveness of administering probiotics

2.2.1.1. During manufacture and processing

Probiotic cultures for food applications are usually supplied in frozen or dried form (either as freeze-dried or spray-dried powder). Production of probiotic products often involves incorporating probiotics in food-based media. Processing operations inevitably

expose these sensitive probiotic cells to a mixed range of harmful environments and conditions. Extremes such as heat, cold, osmotic and oxidative stress, can impact the viability of probiotics and thus affect their probiotic effects in the first place [19].

Heat stress occurs in thermal drying processes. For instance, during spray drying, probiotic cultures are suspended in a flow of hot air up to 200 °C. Fatty acids in the cell membrane are very susceptible to heat. Aggregation of proteins and dysfunction of ribosomes and RNAs also occur under such condition. Probiotics such as lactobacilli and bifidobacteria are commonly sensitive to a temperature above 50 °C. Strains with high thermal tolerance are rare, but this property would be an advantage in selecting successful probiotic strains [20-21].

Cold challenge during processing and storage, on the other hand, can reduce membrane fluidity. It also affects the level of DNA supercoiling, increases the rate of DNA strand breakage and rigidifies the secondary structures of DNA and RNA [22]. At low temperatures, vital activities such as energy metabolism, enzyme activity, protein-folding and ribosome functions are reduced. This lethargic state leaves probiotic bacteria less active in adapting to other stresses [23]. In addition, the cellular membrane can be compromised under freezing condition, either by the hyperosmotic stress caused by concentrated gases and solutes or by the intracellular formation of ice crystals [24].

Oxidative stress is presented to probiotic bacteria at various stages of production [25]. Reactive oxygen species (ROS) can be generated from partial reduction of oxygen and affect probiotic viability. Radicals such as superoxide anion radical (O_2^-) and hydroxyl radical (OH) can react with proteins, lipids and DNA to cause lethal damage [26]. Oxidation of cysteine in the active site of enzymes can also occur [27].

2.2.1.2. During storage

Dried concentrated probiotic cultures are considered the most convenient form for incorporation into foods [28]. However, the premature rehydration of dried probiotics is the major impedance in delivering the label-claimed number of viable probiotic cells for most probiotic products by the time of consumption. It emphasizes that the storage condition such as the storage temperature and the relative humidity can significantly influence the dried probiotic cultures. Although the real mechanism is still not fully clear, the selected protectants such as trehalose or sucrose for lyophilisation were found to replace most of the cell water as compatible osmolytes during drying. This is believed to transform the cytoplasm into a metastable glassy (amorphous solid) state [29-30], in which materials exhibit very high viscosity and show extreme retardation of diffusive molecular motions [31]. The glass transition temperature (T_g) is commonly used to differ the glassy state from the rubbery (amorphous liquid) state. Above T_g , the viscosity drops significantly. The mobility of the system, thus the susceptibility of dried cell, increases accordingly. T_g in relation to temperature and water content is depicted in Figure 2.1. The preservation in such highly viscous state can alleviate deleterious changes in the structure and chemical composition by immobilisation of cellular constituents and thus diffusion inhibition. Higl et al. [32] hence concluded that, although the control of T_g cannot account for all goods for bacterial stability during storage, rapid loss of product stability is often found above T_g .

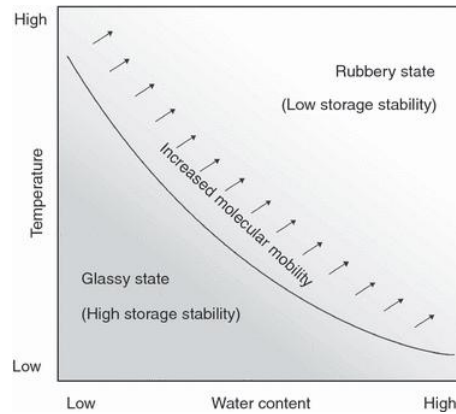


Figure 2.1 A simplified state diagram shows the glass transition curve which relates the glass transition temperature and moisture content. Molecular mobility and deleterious reaction rates in the glassy state are extremely low, while they increase at the storage conditions above the curve (rubbery state) [32].

Another cause of damage during storage of dried probiotic cells is due to changes in the fatty acid profile (ratio of saturated to unsaturated fatty acids) of the membrane, wherein lipid oxidation plays an important role [33-35]. Lipid oxidation was reported to be responsible for some physical changes in membrane functions and structure [36-37]. It was assumed that the increased proportion of saturated fatty acids could decrease the membrane fluidity and cause severe membrane leakage during rehydration. Free radicals can also occur at the end of many biological oxidations, which appear to attack fatty acid moieties thus lowering the hydrophobicity due to the introduction of hydrophilic groups. The reduced hydrophobicity therefore weakens the interactions of fatty acids with membrane proteins required to maintain a proper function. In addition, free radicals may also directly impact DNA synthesis and herald catastrophic events leading to cell death.

2.2.1.3. Gastric acidity

The gastric pH of the stomach of a healthy human adult in the fasting state can reach as low as approximately 1.5. Therefore, the first challenge to ingested probiotics is to

survive through this acidic environment. Long time survival at such low pH is a rare case even for LAB strains which generally exhibit a good acid tolerance down to pH 4. Hood and Zottola [38] reported a total loss of *L. acidophilus* cultures following 45 min exposure to pH 2.0. By contrast, there was no significant reduction at pH 4.0 after 2 h. Other commonly used probiotic strains share a similar susceptibility to gastric acid. Among them, *Bifidobacterium* species are universally found to be more sensitive than *Lactobacillus* species [39].

From a microscopic prospective, a sudden reduction of environmental pH introduces an elevated chemiosmotic pressure and thus imposes a great burden on cell membrane. It also disturbs the functions of membrane-bound proteins. Meanwhile, accumulation of the influent proton directly exposes intracellular organelles to the acid challenge, which further damages the DNA through protonisation of bases and disruption of glycosyl bonds [19]. In addition, more oxidizing intermediates also frequently occur at lower pH.

2.2.1.4. Bile challenge in intestine

Bile acids are amphipathic molecules that are synthesized from cholesterol. They serve as an important type of detergent for digesting fats and absorbing fat-soluble vitamins. The physiological concentration of bile acids is within the range of 0.2 to 2% in the human small intestine in response to the amount of fat intake in the diet. At high concentrations, their potent antimicrobial property is primarily attributed to rapidly dissolving membrane lipids and causing dissociation of integral membrane proteins [40-41]. This nearly instantaneous solubilisation results in the leakage of cell contents, thus cell death. Low concentrations of bile acids do not give instant antimicrobial effect but also disrupt cell membrane integrity in subtle ways. Membrane permeability and fluidity are affected, including altered activity of critical membrane-bound enzymes and

increased transmembrane flux of divalent cations [40, 42]. Low levels of bile have also been shown to affect the physical chemical properties of cell surfaces, including hydrophobicity and zeta potential [43-44].

Binding of bile acids to membrane lipids correlates with their hydrophobicity [45-46]. Unconjugated bile acids are usually more effective than conjugated bile acids and can flip-flop passively across the lipid bilayer, thus entering the cell. The rate of flip-flop is dependent on both the number and the position of hydroxyl groups [47]. For instance, bovine bile, which contains trihydroxyconjugated bile salts, is less inhibitory than porcine bile, which contains dihydroxyconjugated bile salts [48]. During passage in the caecum and colon, conjugated bile acids can be transformed to deconjugated counterparts by the indigenous bacterial flora, which leads to increased inhibitory effects to the bacteria [49-50].

Bile acids which can diffuse across cell membrane further damage the cell from inside. They can affect DNA, secondary RNA structure formation and protein folding. Bile stress can also generate free radicals. In addition, acid stress via intracellular bile salt dissociation and iron or calcium chelation can occur.

2.2.1.5. Challenge at mucosal surfaces especially in the GI tract

Subsequent to the arrival of probiotics at the site of function, the colonisation still depends on a successful initial attachment to the mucosal surface. Pre-treatment with low pH and pepsin was found to reduce the adhesion of some probiotic strains to human intestinal mucus, indicating that the passage through the upper GI tract could impact the later colonisation of these microorganisms [51]. The adhesion process of probiotic strain to mucin was also suggested to be closely related to the functioning state of the cell-wall components, which could be susceptible to the bio-barriers in the human GI

tract [52]. Accordingly, probiotics that maintain good vigour and integrity at the site function can gain further advantages to initialise successful colonization and compete for a turf with local microflora.

2.2.2. Strategies for overcoming the obstacles

2.2.2.1. Strain selection

A number of operable criteria are applied by researchers to select microbial strains as candidate probiotics [6, 53]. They include:

- the “generally recognised as safe (GRAS)” standard;
- the origin preferred from human microflora;
- the capability of surviving physiological extreme conditions, in particular low pH, bile salt;
- low viability loss during food processing and storage;
- the capability of antimicrobial activity/antagonisms against pathogens;
- the capability of modulating host’s immune system and promoting homeostasis; and
- other features like synergism with prebiotics.

In terms of ease for incorporation into foods, Ross et al. [54] further detailed the physiological traits of probiotics as oxygen tolerance, acid tolerance, bile tolerance, heat tolerance, the ability to grow in milk and the ability to metabolize prebiotics.

It is noticed that current practices of probiotics selection are mainly based on the above propositions [55]. However, in terms of analytical methods, it has been suggested by some researchers that the introduction of advantageous techniques, such as flow cytometry, as a supplement to the traditional proliferation-based enumeration

techniques may improve efficiency of lab work and the accuracy of results [56-58]. This will be further discussed in Section 2.2.3.

In addition to the DNA techniques applied in taxonomic study, it is noteworthy that modern genomic studies on probiotics or candidates show a potential to revolutionize the process of probiotic strain selection. O'Sullivan et al. [59] lately presented such an exemplar study, in which they proposed 9 “barcode” genes to identify the niche origin (i.e., dairy, gut or multi-niche) of specific LAB strains. The relevance of their findings on probiotic strain selection to potential applications is obvious. Similar approaches on identification of shock-adaptation genes from certain probiotic strains are equivalently enlightening.

2.2.2.2. Stress responses

Cellular stress response has been exploited to improve the survival of probiotic bacteria. Brief exposure to sub-lethal condition such as mild acid, heat, bile salts, osmotic pressure, or dehydration can elicit strong intracellular responses at molecular level (e.g. gene expression, protein synthesis) and induce resistance to challenges of elevated level. This behaviour is termed stress response [60].

Recently, efforts have been directed to understanding the underlying mechanisms of the stress responses of lactobacilli, so as to improve their viability and stability during industrial production [54]. In a real application, acid adaptation was demonstrated to elicit the acid stress response of *L. acidophilus* species and increased their survival in yoghurt [61]. Kullen and Klaenhammer [62] revealed a large set of up-regulated genes of *L. acidophilus* which were involved in the acid stress response. In particular, up-regulation of genes in charge of the synthesis of the membrane-bound F₁F₀-ATPase was explicitly connected to the improved tolerance to the gastric pH.

Cross-resistance is common for stress response. Prasad et al. [63] observed that to sub-stress *L. rhamnosus* HN001 either with heat (50 °C) or salt (0.6 M NaCl) could significantly improve its survival of storage at 30 °C in the dehydrated state. The subsequent 2D gel electrophoresis revealed that the cells stressed by either method could share quite a number of up-regulated shock proteins in common.

Genetic manipulation was also studied for the potential use in improving the stability of probiotic products. For instance, by overproducing the heat shock protein GroESL in *L. paracasei* NFBC338, a 54-fold increase in thermotolerance over that of the unmodified control was reported [64-65]. This sheds lights on the possibility to extend the use of otherwise susceptible strains, although the safety and stability of such strains deserve concern as well.

2.2.2.3. Packaging and formulae

Putting probiotics research in an even bigger picture, every technical detail deserves to be exploited for the improvement of probiotics. Some studies presented us with a few innovative perspectives and enriched the mainstream topics. Miller et al. [66] questioned the current packaging systems which, although favoured by manufacturers, played a negative role in preventing viability loss during storage. They compared a package with improved gas-barrier property to a few market-available packages of probiotic products and concluded that getting rid of dissolved oxygen during storage could benefit the survival of probiotic bacteria. Another interesting study performed by Liu and Tsao [67] suggested great improvement of the survival of *L. bulgaricus*, *L. rhamnosus* and *L. reuteri* (up to 10⁶-fold) in fermented milk in the presence of yeast, although the mechanisms remained to be explored.

2.2.2.4. Microencapsulation

Encapsulation is the most widely applied technique in research and industrial practices to improve the survival of probiotics, owing to its universal efficacy and little influence to the embedded microorganisms. Within the context of the present work, the encapsulation material is expected to be a food grade agent [68-69]. The basic principle is that the probiotic bacteria are immobilized in such material and thus protected from the harsh conditions [70].

The strict requirement on preservation of viability and functionality of probiotic cells during preparations imposes substantial stringency on the choice of encapsulation techniques. Many of the previously discussed techniques, however productive or efficient in other pharmaceutical applications, are intrinsically incompatible with probiotics production for either presenting harsh processing conditions or involving toxic chemicals. Considerations are particularly emphasized for the microencapsulation of probiotics for production purpose [71-74], including:

- Easily available and cheap encapsulation materials;
- Easily performed techniques to generate appropriate particle size;
- Encapsulation materials having desired the mechanical strength;
- Encapsulation giving appropriate release of the cells at the target site;
- Encapsulation withstanding the adverse environment *in vivo* and protecting the cells;
- Biocompatible and biodegradable encapsulation materials with the food product;
- Safety: non-toxic to both the embedded cells and consumers.

Brief descriptions of the current microencapsulation techniques for encapsulating probiotic microorganisms are given in Table 2.1. It is easily noticed that, despite the

diverse operations, the principle is all about the embedment of probiotics in a hydrogel. Similar to the wide application in pharmaceutical area, hydrogel microencapsulation can protect the sensitive active pharmaceutical ingredient (in this case, viable probiotic bacteria) against deterioration or adverse environmental conditions. It also allows entrapping probiotics in protective polymer that controls the release under specific conditions [75-76]. The advantages are obvious: (1) once encapsulated in matrix, the cells are easier to handle than in suspension; (2) the number of cells in microcapsules can be quantified, allowing the dosage to be readily controlled; (3) cryo- and osmo-protectants can be incorporated into the matrix, which can enhance the survival of cells during processing and storage; and (4) once the matrix microcapsules have been dried, a further surface coating can be applied to alter the aesthetic and sensory properties or to confer extra protection on the cells [77].

Table 2.1 Techniques used for encapsulating probiotic microorganisms.
Modified from [78-79]

Encapsulation techniques	Description	Comment
Spray-drying	The probiotic cells are suspended in a melt or polymer solution. The solution is then atomized and dried in a flow chamber. The probiotic cells then become trapped in the dried particle. The product in dry form is collected at last.	(1) the setup is widely used and available in industry (2) the heat and unflavoured dehydration process can injure and kill cells
Emulsion-gelling/coating-drying	Cells are suspended in an aqueous solution together with gelable polymer. The solution is mixed and dispersed in an immiscible organic phase as	(1) the beads are in perfect spherical shape; (2) the setup can be easily scaled-up;

droplets. A gelling agent is then added or the gelling condition is triggered (depending on the gelling mechanisms).

The obtained beads are then coated, hardened and dried.

The gelling mechanisms can be either: ionotropic (e.g. Ca^{2+} -alginate, Ca^{2+} -pectin) thermotropic (e.g. agarose, agar) enzyme-induced (e.g. rennet-milk protein)

The drying options include freeze-drying, spray-drying, laminar drying, etc.

(3) the beads have a wide size distribution.

Extrusion-gelling/coating-drying	<p>Cell-containing, cross-linkable polymer solutions are extruded through a small tube or needle, permitting the droplet formed to fall freely into a hardening bath where they are cross-linked by the addition of an appropriate reagent depending on the gelling mechanism. The gelling mechanisms can be either: ionotropic (e.g. Ca^{2+}-alginate, Ca^{2+}-pectin) thermotropic (e.g. agarose, agar)</p>	<p>(1) the beads have uniform size; (2) the setup is not suitable for industrial scale up; (2) the beads tend to be of teardrop-shape</p>
Microfluidic-gelling/coating-drying	<p>This technique takes advantage of precise control of capillary-driven break-up of a liquid stream formed by 2 immiscible fluids. It represents a mini-scale of extrusion technique in terms of micro-channels in the device. The gelling mechanisms can be either: ionotropic (e.g. Ca^{2+}-alginate, Ca^{2+}-</p>	<p>(1) very-small-sized beads can be obtained; (2) the beads are in good spherical shape; (3) the shearing force in hydrodynamic focusing could be harmful to cells; (4) the microfluidic device</p>

pectin) thermotropic (e.g. agarose, agar) is prone to block and fail and impossible to fix.

Layer-by-layer	By this technique, thin shells can be obtained by alternate deposition of layers of oppositely-charged poly-electrolyte molecules.	This technique is better applied in a cell surface-engineering scenario. The tedious operation and the very-thin shell formed on the surface of cells make it unsuitable for probiotics delivery.
----------------	--	---

A number of materials have been extensively investigated for microencapsulation of probiotic bacteria. The most commonly used materials include alginate [80-81], chitosan [82-83], hydroxypropyl methylcellulose, gelatin [84], Eudragit S [85] and resistant starch. Inefficient protection and unsuccessful delivery in the GI tract were associated with the drawback of using only one encapsulating material. Therefore, combinations of multiple materials in a system or addition of responsive coatings gain more attractions by current researchers, which can create more versatile applications in microencapsulation of probiotics [75, 83-84].

By contrast to probiotic microcapsules (beads) conventionally prepared by many researchers in lab at sizes of millimetres, probiotic microcapsules in probiotic products for household consumers are preferred to be prepared at reduced size owing to the following advantages:

- The presence of probiotic microcapsules at reduced size does not alter the mouth-feel of products (e.g. yoghurt), whereas large microcapsules can be detected by mouth and perceived as gritty [86].
- Probiotic microcapsules of reduced size are more prone to be lodged in the surface folds and crevasses on mucous membranes [87]. They may therefore be subjected only to minor dislodging stress.
- The smaller the particle, the greater the surface-area-to-volume ratio, and therefore the greater chance for mucoadhesive materials to be applied and take effect [87].
- Small probiotic polysaccharide microcapsules are more efficiently released by prolonged releasing mechanisms such as microbiota in human colon.
- However, reduced size also causes decreased protection by wall polymer matrix over stress factor such as the bio-barriers in the human GI tract, which consequently requires the presence of appropriate protectants in encapsulation formula [88].

2.2.3. Advantageous fluorescent-probe-based flow cytometric methods for probiotics research

The limit of the conventional enumeration technique based on microbial proliferation, also known as the standard culture technique (SCT), has been emphasized by some microbiological researchers [56, 58]. Arguments were based on the time- and labour-consuming operations, the relatively high variance in replicate results and above all facts that such techniques only enumerate the cultivability of bacteria rather than the viability. Increasing evidences have confirmed that stressed bacteria can enter into a “viable but non-cultivable” (VBNC) state. The transient loss of the capability of proliferation may therefore bias the SCT results. Particularly in the case of probiotics, viable count may underestimate the required amount of probiotics to elicit the beneficial effect, whereas the microorganisms are still able to exert probiotic functions.

Flow cytometry (FCM) was invented to enumerate, examine and sort microscopic particles on single-unit basis. It allows simultaneous multiparametric analysis of the physiological status of individual cell. Subpopulations are distinguished based on the combination of results indicated by various fluorescent markers. Since FCM analysis is commonly performed on a large number of individual bacterium, the result will naturally bear an increased statistical precision. When both SCT and FCM were validated against propidium monoazide (PMA)-qPCR technique [89] and another modified culture technique [90], FCM was confirmed as a rapid and accurate complement to SCT and provided more insightful information of bacterial samples.

2.2.3.1. Various fluorescent probes feature a physical/chemical multiparametric observation by FCM

FCM has a long history of application in the medical analysis of mammalian cells, which gradually matured into a powerful high-throughput technology [91]. Since FCM became more sensitive and available, probes routinely worked on eukaryotes were extended to bacteria.

Propidium iodide (PI) is a charged molecule that can intercalate between DNA (or RNA) bases with little sequence preference. Its fluorescence enhances up to 30 folds once bound to nucleic acids. Because strongly charged PI is impermeable to an intact cell, it selectively stains bacteria with a compromised membrane. Since integrity of cell membrane plays a pivotal role in maintaining proper cellular functions, highly PI stained bacteria are commonly deemed dead in many applications. Stains of similar function but with increased fluorescence enhancement and narrower spectrum were also available, e.g. SYTOX[®] series. The idea that PI selectively stains dead bacteria originates from past research on eukaryotes. It was also reported to give accurate

detection in a few studies of bacteria. However, arguments on the limit of PI were also heard. Shi et al. [92] claimed that, during early exponential growth, up to 40% examined bacteria could be stained by PI, whereas the number dropped to less than 5% when they grew to early stationary phase. This may cause a problem in environmental samples, in which bacteria at different growth phases are present. However, this particular concern is less relevant in the area of probiotic bacteria research. In fact, most probiotic bacteria are cultured to a stationary phase before further processing or administering, simply because at this stage they are more resistant to stress. Research of probiotic strains is hence commonly carried out on cultures of stationary phase. In addition, multiple probes are routinely applied in FCM to counteract the inadequacy of single probes.

Esterified fluorochromes are another popular type of viability probe for bacteria. They remain non-fluorescent until they are cleaved by intracellular esterases, and then release a fluorescent product [93]. For instance, carboxyfluorescein diacetate (cFDA) is such a plausible probe for intracellular enzyme activity. It is not charged, and can freely enter into the cytoplasm. Only bacteria with a normal activity of intracellular esterase can cleave cFDA and release fluorescent carboxyfluorescein (cF). cF is membrane-impermeant and thus confined to the cytoplasm, rendering stained bacteria with green fluorescence. Consequently, the positive observation indicates two folds of meanings: (i) marked substrate cleavage via proper function of cytoplasmic enzymes and (ii) fluorescein retention by an integral membrane [93-94]. Additionally, some bacteria under an energized state may actively pump out cF by certain membrane associated efflux mechanisms [94]. Bunthof and Bloemen [56] took advantage of this behaviour to study the energy status of the examined bacteria by tracing the loss of intracellular fluorescein over the time. On the other hand, derivatives with improved cellular

retention were also developed for the purpose of cell tracing. For example, chloromethylfluorescein di-acetate (CMFDA) has a chloromethyl moiety that covalently links the cleaved fluorescein to intracellular molecules [93]. In many practical applications, esterified fluorochromes such as cFDA, cFDA-AM and cFDA-SE are applied jointly with PI. The combination increases the credibility in determining the viability of bacteria. Sub-populations with distinguished physiological state are discerned. Successful applications of these fluorescent probes were reported for some probiotic LAB [56-57].

Some other reported useful probes are listed in Table 2.2. which were modified from [95].

Table 2.2 Frequently used fluorescent probes in combination with FCM for microbiology [95].

Fluorochrome substrates	Description	Reference
Cell Tracer		
Carboxyfluorescein diacetate succinimidyl ester (cFDA/SE)	cleaved by intracellular esterase and reduced to cF/SE	
Green fluorescent protein (Gfp)		[96]
Metabolic activity		
5-cyano-2,3 ditolyl tetrazolium chloride (CTC)	reduced by dehydrogenases to CTC-formazan; relative toxicity of intracellular accumulation	[97]
Calcein-AM		[98]

ChemChrome V6 (CV6; Chemunex)	with enhanced uptake of fluorogenic substrates and reduced extrusion by active pumps	[99]
-------------------------------	--	------

Membrane potential (vary from 100 to 200 mV in viable bacteria)

Carbocyanines, DioCn(3), Rhodamine (Rh123)	cationic dyes which accumulate inside polarized cells	[100]
--	---	-------

bis-(1,3-dibarbituric acid)-trimethine oxonol (DiBAC4(3); BOX)	oxonols, anionic and lipophilic accumulate inside non-viable cells. It is used to detect depolarized cells of numerous species usually in combination with SYTO or PI	[101]
--	---	-------

Membrane integrity

SYTOX, cyanines (TO-PRO, TOTO series)	nucleic acid binding and emitting fluorescence in cells with compromised membrane	
---------------------------------------	---	--

DNA content measurement

1,5-bis{[2-(di-methylamino) ethyl]amino}-4,8-dihydroxyanthracene-9,10-dione (DRAQ5)	permeable to cells and specifically intercalating between adenine and thymine bases.	[102]
---	--	-------

2.2.3.2. FCM is a powerful tool for probiotic strain selection (studies based on pH and bile salt tolerance)

Tolerance to low pH and high concentration of bile salts is generally accepted as an important criterion for probiotic strain selection. Since the cell membrane is the initial site of challenge in both cases, a probe like PI that instantly evaluates the status of

membrane become very helpful. Amor et al. [57] evaluated the viability via FCM and cell sorting of two *Bifidobacterium* strains challenged by bile salts. The results confirmed that the cFDA/PI staining was capable of revealing the physiological complexity within the population of the bile-salt-stressed strains. In another example, Bunthof et al. [73] applied cFDA/TOTO-1 staining to a number of LAB strains either used as probiotics or dairy starters which underwent acid or bile salt challenges. The results also proved that FCM analysis served as a more reliable and versatile assay technique than SCT. They explicitly pointed out that this type of FCM application could be used for screening LAB strains for potential probiotic use in terms of their tolerance against bile, acid or other various conditions. Following the suggestion, we designed a similar protocol and evaluated the acid and bile-salt tolerance of the probiotic *L. reuteri* DPC16 [103]. The FCM result was used to compare with other strains reported in other literatures. The outstanding tolerance of DPC16 was hence evident.

2.2.3.3. FCM is a valuable tool in evaluation of stress on probiotic cells during process and storage

In the past decade, FCM has been gaining popularity among researchers in LAB and probiotic related food industry where the time-critical quality control techniques and accurate enumeration methods are highly demanded. Increasing cases of FCM applications are proving that probiotics research can benefit from including FCM approach.

Rault et al. [104] used FCM to assess the viability of four cheese starter strains of *L. delbrueckii* that had been exposed to freezing challenge during storage. cFDA and PI were combined for this purpose. Three distinct subpopulations were successfully identified as viable (cF+/PI-), injured (cF+/PI+) and dead (cF-/PI-) cells. Diverse

tolerance of the four strains was clearly characterized by the shift of composing proportions among these three subpopulations. The percentage of viable subpopulation was reported to be comparable with the plate count results. Considering the largely reduced time- and labour- consumption, the authors concluded FCM as a convenient and rapid tool to evaluate the viability of LAB.

In another case, using a similar FCM setup, Ananta et al. [105] studied spray drying in the production of skim milk-based preparations containing *L. rhammosus* GG ATCC53103. Based on the FCM results, they profiled the impact of the composition of carrier matrix and the temperature of spray outlet on the final survival rate of this strain. The FCM results also indicated that cell death was caused mainly by the damage to cell membranes. The degree of membrane disintegration was correlated to the increase of the outlet temperature.

Muller et al. [106] applied FCM to study the resuscitation of the dried cultures (*Bf. longum* NCC3001 and *L. johnsonii* La1), which was a critical step in reactivating probiotic bacteria before use or consumption. A multivariate design of experiment (DoE) approach was used to model the PI-probed cell-membrane integrity. The obtained response surface model suggested that pH had a significant influence on the reactivation of the two strains. Their research also demonstrated that FCM could be recruited as an important part of the high throughput routine for modelling and optimising parameters of processing.

2.3. Strategies for colon-specific delivery

Orally-consumed probiotic bacteria need to reach the lower GI tract in order to exert their probiotic function. In particular, it is preferred that they be delivered alive to the colon. Successful delivery systems are therefore expected to recruit mechanisms to

target this region, while preventing immature release which exposes probiotics to bio-barriers too early in the preceding compartments of the GI tract.

2.3.1. Physiology of colon and the benefits of colon delivery

As the most distal segment of human digestive tract, the colon has little digestive function but mainly serves the purposes of lubricating waste products, absorbing fluids and salts, and storing waste products until excretion.

The colon is around 1.5-m long with a surface area of 0.3 m², which contrasts sharply with the small intestinal surface area of ~120 m² [107]. This lower surface area results from the lack of villi on the colonic mucosa. A primary physiological feature of the colon is absorption of water. Early researchers reported that the fluid volume in the caecum, ascending colon, and proximal transverse colon measured in humans (postmortem) was, on average, 83 mL (ranging from 7 to 430 mL) [108]. After the mid-transverse colon, a short transition area of 1 to 2 cm long was observed to control the efficient water absorption and transform the colonic contents into hard, dry pellets. More recently, free fluid in the GI tract was quantified using magnetic resonance imaging [109]. The free fluid in the large intestines was present as dispersed fluid pockets of 2 mL. The total volume of the free fluid showed individual variability but had an average of 12 mL, which was insignificantly different between in fasting state or after a meal. In addition, the free fluid was found to be markedly lower than in stomach or small intestines. Ingested model tablets were also found to have the least possibility to contact the free fluid pockets in the colon compared to all other compartments in the GI tract.

Another distinct environmental factor is the microbiota in the colon. Each gram of material in the colon can contain bacteria of approximately 10¹¹-10¹² colony forming

units (CFU), which belong to as many as 3000 different species [110]. The microbiota can ferment the constantly arriving undigested food material (polysaccharides and proteins) to produce energy. A variety of polysaccharides, including those that are indigestible by human pancreatic enzymes, are vigorously digested by the colonic bacteria. Consequently, the fermentation activity and products have a high impact on the conditions of the colonic lumen, such as the viscosity, pH, and redox potential [111].

The human colon has a slightly acid to neutral pH. However, the colonic transit is the most variable part. Compared to the relatively consistent transit time of the small intestine, the general transit time of the colon falls widely within the range of 6 – 48 h described by Coupe et al [112] while reports on values in excess of 70 h are not rare [113]. It may be even more complicated if taking pathology into account. Decreased colon transit time is commonly observed in patients with ulcerative colitis. In addition, asymmetric distribution of materials also aggravate under pathological conditions, which significantly reduces the exposure to therapeutic agents.

A number of colon-specific delivery mechanisms have been proposed, and explored by using those physiological conditions of the colon.

2.3.2. pH-controlled colonic delivery system

The significant increase of the physiological GI pH from stomach to small intestine has long been exploited to deliver therapeutic agents to small intestines. Particular polymers containing carboxylic acid groups were found to dissociate poorly under acidic condition of the stomach, but ionise and dissolve preferably at the neutral pH of the proximal small intestines. Coating with these pH-sensitive polymers prevents core

agents from dissolution in the stomach. This rationale of pH-controlled delivery was naturally extended to colon-specific delivery.

However, contrary to the general belief of constant pH increase along the GI tract, profiling *in vivo* objects proved that a sharp drop in pH occurred at the transition from ileum to caecum and the average pH of colon was in fact noticeably lower than small intestine [114]. Investigations on pathological cases further demonstrated that extremely low colon pH could occur in patients who suffered from inflammatory bowel diseases [115-116]. Although natural or synthetic pH-sensitive polymers are still evaluated for colon-specific delivery, the system which uses pH as the sole trigger appears inefficient. However, enteric coating is still a universal practice to guarantee the intact passage through stomach and mitigate the challenges of acid and gastric enzymes.

2.3.3. Time-controlled colonic delivery system

Time-controlled colonic delivery systems utilize a pre-determined delayed release. Strategies in practice include rupturable polymeric coatings, erodible polymeric coatings, diffusive polymeric coatings, capsule systems with release-controlling polymeric plugs, and osmotic systems [117].

However, location of initial drug release is still hard to predict due to the variety of transit time in the GI tract. Contrary to the relatively consistent transit time in small intestines, the retention time in stomach, however, falls in a wide range. It justifies why time-controlled colon delivery system is often coupled with pH-controlled element to circumvent the drawback of unpredictable retention time in stomach. Moreover, as aforementioned, an accelerated transit time through different regions of colon can occur in patients with inflammatory bowel diseases. It also questions the accuracy of the time-dependent colonic delivery systems [118].

2.3.4. Pressure-controlled colonic delivery system

The relatively strong peristaltic motion in colon is utilized by pressure-controlled colon delivery systems. For example, the well-described pressure-controlled colonic delivery system - PCDC - consists of a capsular shaped suppository coated with insoluble ethyl-cellulose [119]. In the upper GI tract where environmental fluid is abundant (as either in stomach or in small intestine), the system was not directly subject to luminal pressure. In the meantime, the ethyl-cellulose coating prevented the liquefied suppository core from premature release. When it reaches the colon, a large volume of ambient water is absorbed. It increases the viscosity of luminal content. As a result, the increased intestinal pressure finally breaks the ethyl-cellulose coating by colonic peristalsis, and the loaded content is subsequently released.

However, this releasing mechanism crucially depends on the occurrence of raised pressure, which follows the circadian rhythm at its maximum frequency after wakeup or meals, or during defecation [113]. Therefore, administration of such pressure-controlled colonic delivery system should be well managed to obtain the desired release in place.

2.3.5. Microbiota-controlled polysaccharide colonic delivery system

More recently, microbiota-triggered colonic release has attracted much attention during the latest development of colon-specific delivery.

The huge and complex microbial community of the colonic microbiota produces a versatile capability of catabolising various carbohydrates. Members of the gut microbiota share a great number of distinctive gene clusters related to carbohydrate catabolism. In a large-scale comparative metagenomic analysis, Kurokawa et al. [84] screened faecal samples from 13 healthy Japanese of various ages. 647 novel gene families specific to human intestinal microbiomes were distinguished from the

microbial communities of other natural niches. These gut microbiome-enriched genes were further grouped as clusters of orthologous groups (COGs) and classified into 20 functional categories for either adult/child or infant. 24% of the COGs in the adult/child subjects were identified as under the functional category of carbohydrate metabolism while the number was even higher in the infant subjects. More than 14 families of glycosyl hydrolases enriched in adults are involved in the depolymerisation of plant-derived dietary polysaccharides and host-tissue derived proteoglycans or glycoconjugates. In contrast, most genes for fatty acid metabolism were selectively suppressed, indicating that the colonic microbiota preferred polysaccharides and peptides for energy production and the biosynthesis of cellular components.

The human gut microbiota has very efficient machinery for polysaccharides utilization. Several stages consist of the hydrolysis process. Initially, a handler protein binds to an ambient sugar molecule with certain specificity. It then subjects the molecule to outer membrane polysaccharide lyases by which small pieces of oligosaccharide are cut off. The oligosaccharide pieces are then passed to adjacent porins to be internalised following intracellular degradation and utilization. For example, a remarkable flexibility of *Bacteroides thetaiotaomicron* was observed, for it could opportunistically deploy the different subsets of 209 paralogs of SusC (porin) and SusD (handler), and 226 predicted glycoside hydrolases, plus 15 polysaccharide lyases. The findings explained its prodigious capacity of digesting various dietary fibres and host mucus glycans, and the rapid adaptation to the host's diet [120-121]. This distinct catabolism of polysaccharides supported the assumption that the indigenous microbiota could be exploited to release entrapped content from polysaccharide matrix. Natural polysaccharides which are indigestible by the host but fermentable by the gut microbiota have thus been widely involved in studies of colon delivery [122].

A variety of polysaccharides which were evaluated for the degradation by the colonic microbiota and proved to have the potential to be used for colonic release are listed in Table 2.3.

Table 2.3 Polysaccharide substrates for the colonic microbiota [123].

Polysaccharide	References
Amylose	[124-125]
Amylopectin	[124-125]
Arabinogalactan	[124]
Arabinoxylan	[126]
Carageenan	[127]
Chitosan	[128]
Chondroitin	[124]
Dextran	[129]
Gum Arabic	[124-125, 130]
Gum ghatti	[124-125]
Gum locust bean	[124-125]
Gum tragacanth	[124-125]
Hyaluronate	[125]
Inulin	[131]
Laminarin	[124, 132]
Pectin	[125, 127, 133]
Polygalacturonate	[124, 133]

Psyllium hydrocolloid	[133]
Ulvan	[134]
Xyloglucan	[135]
Xylo-oligosaccharides	[136]

2.4. Prolonged colonic retention by mucoadhesion

2.4.1. Physiological role of colonic mucus

Most epithelial surfaces are coated with a type of viscous and heterogeneous biological product – mucus. It serves a wide range of purposes, such as lubrication for minimizing shearing stresses, maintenance of a hydrated epithelium layer, protection barrier against harmful substances and permeable interface for the exchange of materials. In the digestive tract, mucus is synthesized and secreted by the specialized goblet cells which are present on the whole organ that are exposed to the external environment. Large granules storing mucus are located near the apical side of the goblet cells and subsequently released by either exocytosis or exfoliation of the whole cell.

Mucus consists mainly of water (up to 95% weight), mucin (up to 4% weight), inorganic salts (about 1% weight), lipids (1~2% weight), DNA (approximately 0.02%) and cellular debris. The randomly interwoven network of mucin sustains the three-dimensional structure of mucus whilst all other soluble constituents are involved in determining the viscosity and helping maintain an unstirred environment inside [137]. The dynamic composition is associated to the viscoelastic properties of mucus. At the macroscopic level, unlike classic solids and liquids, mucus is a non-Newtonian thixotropic gel, which behaves like an elastic solid or a viscous liquid in response to low or high shear respectively.

The mucin content plays a vital role in the interaction between mucus and microflora. Mucins can be generally separated into two families: (1) the membrane-associated mucin which ranges from 100 to 500 nm in length and (2) the secreted mucin (either gel-forming or non-gel-forming) which is up to several microns long. Two layers of mucus were thus observed (a cell-adherent layer and a non-adherent layer) especially in the gastrointestinal and the cervicovaginal tracts [138]. Recently, Johansson et al. [139] reported that these two layers had similar protein compositions in mice colon. They also observed that the cell-adherent layer in physiological state was devoid of bacteria whilst, in contrast, the non-adherent outer layer was heavily colonised by bacteria. The *in vivo* study by Autma et al. [138] on the mucus thickness of rats confirmed increased depth of both types of mucus layers in the lower GI tract, particularly in the colon (Figure 2.2). It was partly attributed to the prevalent occurrence of goblet cells, and the elevated recovering rate and the reduced turnover of mucus in this region. Despite the lack of in-depth knowledge on the human GI tract, the mucus of human large intestines has been widely reported to be markedly thicker than small intestines. Some reported measurements of mucus thickness of the different regions of the human GI tract are summarised in Table 2.4. This distinct characteristic of colonic mucus opens a new horizon for taking advantage of mucoadhesion to achieve a prolonged retention of the colonic delivery systems.

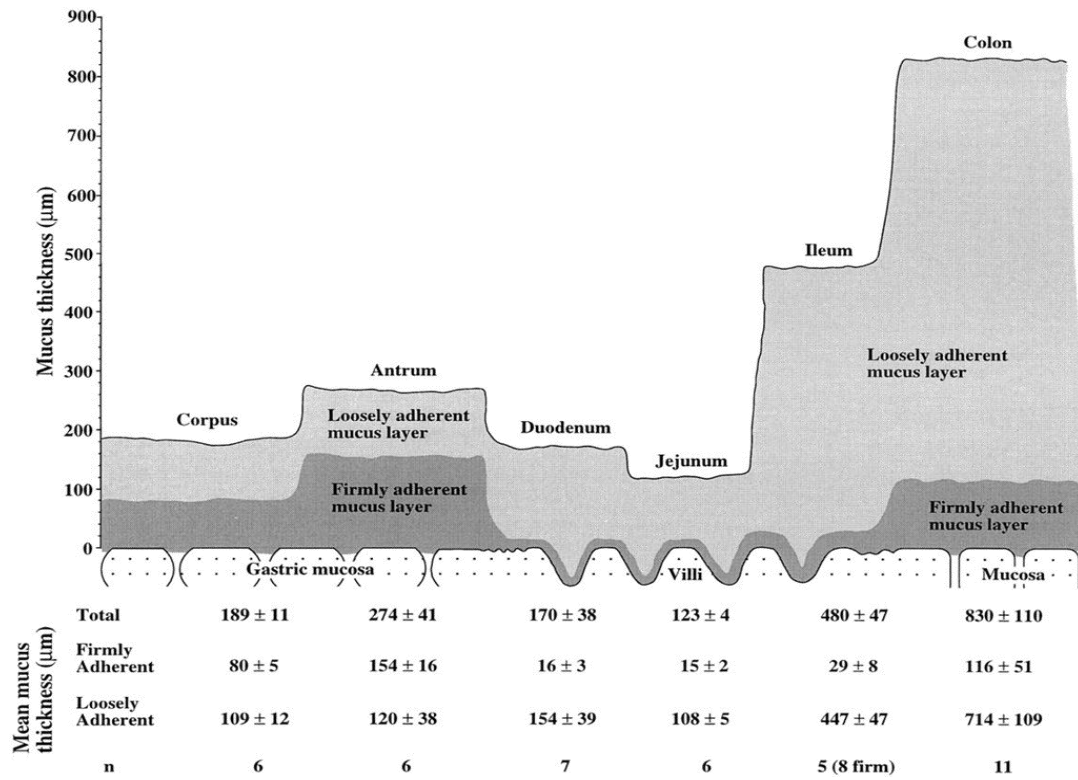


Figure 2.2 The thickness of adherent (dark grey) and non-adherent (light grey) mucus layers in the GI tract of rat [138].

Table 2.4 Mucus layer thickness in the human GI tract [140].

Region in the human GI tract	Thickness (μm)	References
Oesophagus	Absent	[141]
	95 \pm 12	[142]
Gastric antrum	144 \pm 52	[143-144]
Duodenum	16 \pm 5	[143-144]
Proximal colon	107 \pm 48	[145]
Distal colon	134 \pm 68	[145]
Sigmoid colon	66 \pm 47	[143-144]
Rectum	155 \pm 54	[145]

2.4.2. Mucoadhesion and its advantages

Mucoadhesion is defined as a phenomenon of attachment of natural or synthetic polymer to a mucosal surface [87].

The advantages of mucoadhesive delivery system have been suggested as follows:

- As a result of adhesion and intimate contact, the formulation stays longer at the delivery site which can improve the bioavailability. Therefore, therapeutic agents after incorporation into dosage forms can be applied at lower concentrations;
- The use of specific mucoadhesive materials allows the potential benefit of selectively targeting biological mucus-rich regions;
- Increased retention time in combination with controlled release may justify less frequent administration;
- Dose-related side effects may be reduced due to the localisation of therapeutic agents at disease site, and cost reduction may also be achieved.

The mucoadhesion process is considered to consist of several distinct steps [87]. First, wetting and swelling of polymer allows intimate contact with mucus surface; then loose polymer chains physically interpenetrate the mucus layer and entangle with the mucin chains; finally, the formation of chemical bonds occurs. Based on the study of mucoadhesion in the rat GI tract, Rubinstein and Tirosh [146] suggested that the colon and caecum exerted superior effects of mucoadhesion compared to stomach and jejunum.

2.4.3. Theories of mucoadhesion

To explain mucoadhesion, a number of general theories have been adapted from the investigation of mucoadhesion [87, 147-149].

The wetting theory. Wetting describes how a liquid (or a low viscosity drop) spreads across the contact interface in terms of adhesive forces between this liquid and solid. Cohesive forces within the mucoadhesive tend to determine the swelling and spreading behaviour on the mucus layer.

The electronic theory. This theory presumes that the electron transfer may occur at the immediate contact surface between the mucus and the molecular chains of the mucoadhesive polymers. This phenomenon comes from the divergent electronic structure of each material and creates a jacket layer of electrical charges at the interface. The attraction forces are consequently created.

The adsorption theory. This type of adhesion is commonly associated to the physical interaction among macromolecules by secondary bonds (e.g. van der Waals forces, hydrophobic interaction and hydrogen bond). Nevertheless, it also refers to primary bonds due to chemisorption as a result of ionic, covalent and metallic bonding. The

attractive interactions are remarkably stronger than the force referred by the electronic theory.

The diffusion theory. Concentration gradients mainly drive the interpenetration of polymers chains across adhesive interface. The depth of diffusion and the extent of physical entanglement with mucin are assumed to be related to the diffusion coefficient, the molecular weight, the cross-linking density, the chain flexibility and its spatial conformation. In addition, diffusion increases with the time of contact.

The mechanical theory. Mechanical interlocking of adhesives according to the irregular feature of rough surface has also been proposed as a mechanism [150]. However, it was also suggested that the according surface treatment merely provided an increased contact area of the substrates available for improved wetting characteristics [151]. The energy dissipated at the interface during joint failure may also be increased.

The actual phenomenon of mucoadhesion is a result of interactions of all the proposed theories. Figure 2.3 summarizes the aforementioned theories and illustrates the sequential occurrences of the distinct phases during the continuous mucoadhesion process [87].

A noteworthy fact is that the distal end of the GI tract does not provide an easily accessible mucosal surface. It means that the mucoadhesive formula cannot be directly placed onto the mucosa. The possible blockage of the GI tract also undermines the application of large-sized formulations. In contrast, the design of micro- and nano-formulations owing to a reduced size and a greatly enhanced surface-to-volume ratio could prolong the retention in folds and protrusions of intestines, and meanwhile provide a superior opportunity for the application of adhesive material.

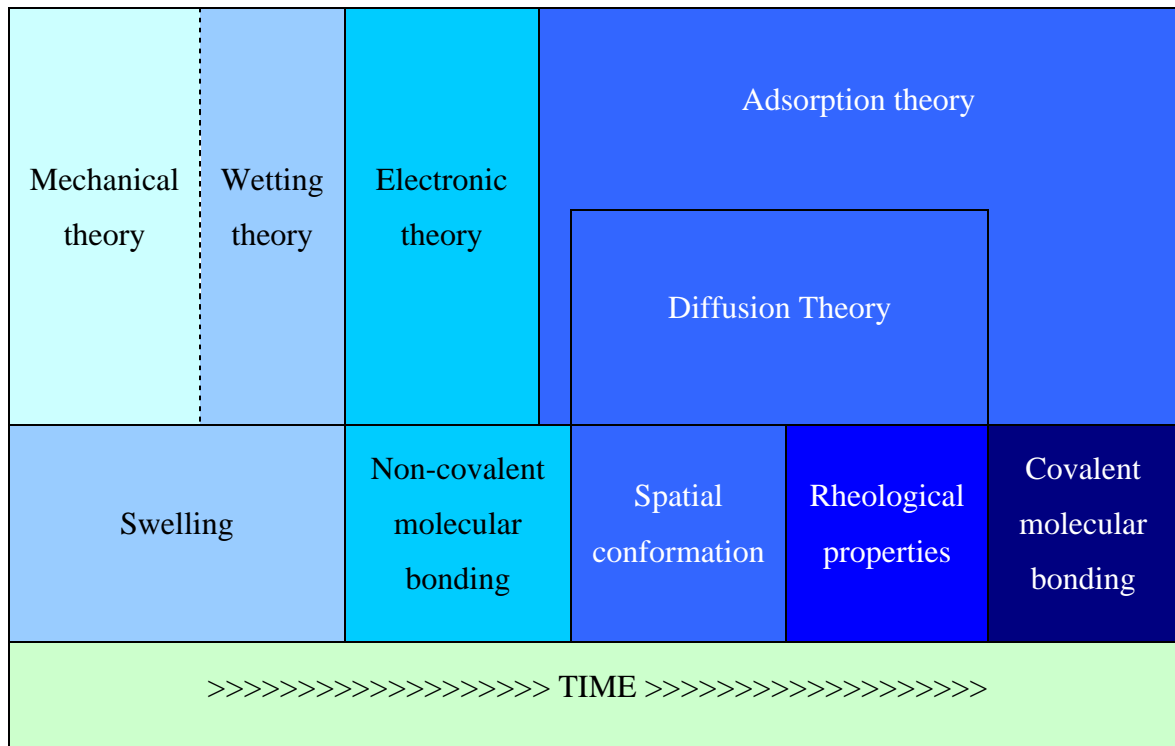


Figure 2.3 The illustrative mucoadhesion process (theories and bondings) as it happens along the time. Summarized and adapted from [87].

2.4.4. Conventional mucoadhesive polymers

Mucoadhesive polymers feature a wide physicochemical range depending on particular application purposes, for example, soluble/ insoluble, non-biodegradable/biodegradable, hydrogel, thermoplastic, homopolymer/copolymer, natural polymer/synthetic polymers [152]. In this review, my focus will be on biodegradable natural polymers which are “generally recognised as safe” (GRAS) and suitable for delivering probiotic bacteria to the colon. Natural dietary polysaccharides, such as alginate, pectin and chitin-derived chitosan, are all adhesive to human GI mucus owing to their prevalent linear long chains and polar groups (hydroxyl, carboxyl or amide groups) in the molecules. They can interact with the mucin network via either secondary chemical bonds (hydrogen bond, electronic bond or van force), or physical entanglement. Natural dietary polysaccharides are also preferred by probiotics researchers for biocompatibility and biodegradability.

Because these materials are extensively used in encapsulating probiotic bacteria, they usually confer some mucoadhesiveness to the final system. Here follow two examples:

Anionic Pectins. Pectin is an anionic polysaccharide with rich carboxylic groups. Pectin has a very complex structure which contains α -D-galacturonic acid with 1-4 linkage. The degree of (methyl-)esterification (DE) of galacturonic acid in the backbone is usually used to classify pectin type. DE also determines the performance of mucoadhesion. Schmidgall and Hensel [96] reported that rhamnogalacturonans with a low DE and linear oligogalacturonides derived from pectin showed a significant bioadhesion to colonic mucus membranes while high DE pectins with neutral backbones were ineffective. Similarly, Thirawong et al. [153] also reported the comparatively much stronger adhesion of pectins to colonic tissue than all other regions of the GI tract. However, they claimed that the strength of mucoadhesion of pectin was more related to molecular weight instead of the previously assumed DE.

Cationic Chitosan. Chitosan is a natural polycationic hydrophilic polymer produced by deacetylation of polysaccharide chitin. Good biocompatibility and biodegradability together with wide availability of chitosan promote its increasing importance in industrial application. Strong mucoadhesive properties were observed for chitosan due to the formation of hydrogen and ionic bonds between positively charged amino groups of chitosan and negatively charge sialic acid residues of mucin glycoprotein. The linear chitosan molecule also provides chain flexibility for interpenetration. However, chitosan is a weak base and has a pK_a value around 6.5. Therefore, it is insoluble at neutral and basic environments, which make it unsuitable as the major absorption enhancer in a colonic delivery system. However, due to the rich active amino groups exposed on chitosan molecule, it is flexible to be modified to obtain novel polymers with altered

physiochemical property. For example, chitosan solubility can be achieved by trimethylating its primary amino groups.

2.4.5. Novel strategies for enhanced mucoadhesion

Those aforementioned natural polysaccharides together with some synthesized mucoadhesive polymers (e.g. polyacrylic acid), are categorised as the first-generation mucoadhesive systems [87]. They provide delivery system with some “off-the-shelf” mucoadhesiveness [87]. In order to extend the performance, novel strategies have been explored, which address the question in terms of (i) cell-specific recognition (lectins), (ii) enhanced adhesion by forming covalent bond (thiomers), and (iii) environment-sensitive mucoadhesion (pH-sensitive mucoadhesive polymers).

2.4.5.1. Lectins

Lectins belong to a class of proteins of non-immune origin that bind glycans reversibly and non-covalently without inducing any change. Plants, animals and microorganisms recruit lectins to fulfil a wide range of defensive or pathogenic biological recognition functions. Promising applications of lectin-based systems do not only rely on targeted specific attachment, but they also allow efficient delivery of the macromolecules of therapeutic agents via active cell-mediated drug vesicular transport following lectin recognition. Positive applications particularly in the GI tract have been reported, for example, the targeting gut associated lymphoid tissue (GALT) for immunisation by the lectins specifically attaching to M-cells, or in another example *E. coli* K99 fimbriae lectin used to target the corticosteroid 6-methyl-prednisolone to areas in the colon affected by Crohn’s disease.

However, concerns regarding lectin toxicity, immunogenicity and adverse effect of repeated lectin exposure undermine their wide application. Safety issues should be also

taken good care on lectin-induced antibodies which could otherwise impact the effect of subsequent administration of same lectin-based vehicles or on occasional lectin-induced systemic anaphylaxis.

2.4.5.2. Thiomers

Thiomers are a new generation of mucoadhesive polymeric drug carriers [154]. The concept of thiomers targets on the insufficiency of mucoadhesion by relatively weak non-covalent bonds between polymers and mucins, which may affect effective retention of delivery system. Thiomers display reactive thiol groups on their side chains. Therefore, thiol exchange reactions and/or oxidation processes can form covalent disulfide bonds that link polymer molecules to cysteine-rich subdomains of mucus glycoproteins. It is worth mentioning that cysteine-rich subdomains are prevalent in almost all secreted gel-forming mucins manifesting as C-/CK-domains at the C end of mucin polymer [155], which justifies the concept of thiomers. Thiomers have been demonstrated *in vitro* to markedly prolong the adhesion performance, and thus the retention period [156]. An *in vivo* example of this gastroretentive property was also reported [157-159].

Since the advent of the concept of thiolated polymers, many first-generation mucoadhesive polymers have been derivatised for the desired mucoadhesiveness. Some examples and the according enhancements in mucoadhesiveness are given in Table 2.5. Thiomers were proved to provide a more endurable bonding with mucin regardless of the changes of ionic strength and environmental pH.

Table 2.5 A group of thiomers and the improvement on measured mucoadhesion [160].

Polymer	Enhancement of mucoadhesive bonding strength
Chitosan-iminothiolane	250-fold improvement
Poly(acrylic acid)-cysteine	100-fold improvement
Poly(acrylic acid)-homocysteine	Approx. 20-fold improvement
Chitosan-thioglycolic acid	10-fold improvement
Chitosan-thioethylamidine	9-fold improvement
Alginate-cysteine	4-fold improvement
Poly(methacrylic acid)-cysteine	Noticeable improvement
Sodium carboxymethylcellulose-cysteine	Noticeable improvement

As the modified polymers, concerns toward thiomers' cytotoxicity deserve to be well addressed, especially in the food or pharmaceutical applications. Evidence of bio-safety is accumulating for various thiomers [161-162]. For instance, Guggi et al. reported that chitosan-TBA (thiolated with 2-iminothiolane) showed a comparable toxicity profile to the corresponding unmodified chitosan, which should not compromise its use as a pharmaceutical excipient [163].

2.4.5.3. pH-responsive mucoadhesive polymers

The pH responsive polymers, such as acrylic-based polymers, can be widely seen in enteric formula where gastric (low pH) release is unexpected. The mucoadhesive properties of these pH-responsive polymers can be further improved by grafting

adhesive promoters such as poly(ethylene glycol) (PEG) onto their backbone. The so-designed copolymers were classified as complexation hydrogels [164]. Such polymers therefore acquire both pH-responsive and enhanced mucoadhesive behaviours. When the environmental pH is substantially lower than the pK_a of the copolymer, an interpolymer complexation forms between electron deficient moieties, such as the carboxylic acid groups found along the backbone of polyacids, and moieties containing regions of high electron density, such as the ether groups comprising poly(ethylene glycol)(PEG). Once the environmental pH approaches the pK_a of the copolymer, deprotonation occurs causing the network to decomplex and swell. When such polymer system comes into contact with the mucus, the concentration gradient across the interface causes the PEG chains to diffuse out of the network and penetrate into the mucus layer. However, as the surface coverage of PEG tethers increases, the repulsion between the tethers among themselves can also increase, thus provoking the displacement of some of the tethers inside the hydrogel. As a consequence, the tethers available for the interaction with the mucus decreased, resulting in a lower polymer-mucus interaction [165-167]. It therefore requires necessary optimisations for this type of system.

Other strategies to elicit a specific recognition to certain cells or surface molecules on mucosa include amino acid sequences and antibodies. However, they are more related to the treatments of certain pathological conditions and may not be suitable for generally administering probiotics in the GI tract, thus are not covered by this review.

2.4.6. Methods for mucoadhesion analysis

2.4.6.1. *In vitro* methods

In vitro methods and related techniques for measuring the mucoadhesive property of polymer are summarized in Table 2.6. The methods developed particularly for measuring mucoadhesion performance of polymer-based microsphere were basically altered from those methods, with recruiting some precise machinery. They include: the electrobalance-based method [168] and the novel electromagnetic force transducer (EMFT) method [148]. In addition, scanning electronic microscopy (SEM), electron microscopy and scanning tunnelling microscopy (STM) are also frequently applied to study the surface morphology of polymer-based microspheres, because the smooth texture of the microsphere surface is believed to lead to weak mucoadhesive properties, while the coarser surface texture improves the adhesion through stronger mechanical interactions.

Table 2.6 Methods for measuring the mucoadhesion property of polymer, modified from [169].

Description of method	Comment
<i>By measuring the detaching performance</i>	
<p>A polymer-coated plate was raised from mucus gel. The detaching force to remove the plate was measured by a microbalance. Different polymers were ranked according to the microbalance readings.</p>	<p>This method:</p> <ul style="list-style-type: none"> (1) was easy to set up; (2) did not consider the possible dissolution of polymer; (3) lacked the involvement of a biological tissue.
<p>A textural analyzer was used to measure the tensile force when detaching two pieces of freshly excised animal (porcine) intestinal tissue (up and down) with a compressed polymer disc in the middle.</p>	<ul style="list-style-type: none"> (1) Results could be influenced by variables as contact force, contact time and the removing speed of probe while a longer contact and higher probe speed were found to give a greater sensitivity; (2) This method could be altered to emulate shearing stress.
<p>A number of compressed polymer discs were attached to freshly excised porcine intestinal tissue which had previously been spanned onto a stainless steel cylinder. The cylinder was then placed in a dissolution apparatus and rotated at a predetermined speed. Records were made at a fixed time interval until all the discs were either disintegrated or detached from the mucosal surface.</p>	<p>This method allowed the measurement of mucoadhesion under the application of a shearing stress.</p>
<i>By rheology measurement of mucoadhesion</i>	

The binary blend of candidate polymer and mucus was compared to either the similarly concentrated monocomponent mucus or the polymer according to rheological sum.

- (1) This method could examine the synergistic interaction between the polymer and mucus from the bond forming perspective;
- (2) The synergistic interaction was found to be polymer-concentration dependant;
- (3) The replacement of fresh mucus with rehydrated mucin could affect the measurement especially to ion-sensitive polyacrylic acids depending on the preparation of the mucin.

Fluorescent-probe-based methods

The lipid bilayer of cultured human conjunctiva cells was labelled with fluorescent probe pyrene. The adhesion of polymers to these cells caused a change in the intensity of fluorescence due to surface compression when compared to control cells. The degree of change was assumed to be proportional to the amount of polymer binding.

Findings suggested that highly charged carboxylated anions exhibit the best properties for bioadhesion.

Fluorochrome-labelled polymers were delivered onto animal mucosal tissue. A washing solution was applied at a fixed rate to mimic bio-fluid flow. The eluted material was measured by fluorometer.

Other methods

This measurement was via the BIACORE instrumentation based on the principle underlying an optical phenomenon called Surface Plasmon Resonance (SPR). SPR response is sensitive to the solute concentration on the sensor chip.

This instrument setup allowed the real-time measurement and label-free detection of polymer mucin binding.

2.4.6.2. *In vivo* methods

In vivo mucoadhesive studies are less frequently reported than *in vitro* tests due to cost, time constraints and, more importantly, ethical considerations [169]. Therefore, novel non-invasive techniques are sought to overcome those drawbacks.

γ -scintigraphy is a technique whereby the transit of a dosage form through its intended site of delivery can be non-invasively imaged *in vivo* via judicious introduction of appropriate short lived gamma emitting radioisotope. For example, Anande et al. [170] reported using this technique that Eudragit S100 coated gelatine capsule retarded the release of Con-A conjugated microsphere at low pH and released microspheres slowly at pH 7.4 in the colon.

In another interesting case [171], an oral delivery system based on thiomers matrix coated by pH-responsive polymer was subject to test. The internal dry form protected by pH-responsive polymer through stomach was imaged by matrix-entrapped gadolinium complex (Gd-DTPA), which does not show positive magnetic resonance signal until it is hydrated and ionised.

These techniques provided good examples of the non-invasive technique, which help to extend the knowledge on how the delivery system may respond to *in vivo* environment.

Chapter 3. Flow cytometric assessment of protectants for enhanced survival of probiotic lactic acid bacteria through human gastro-intestinal environment

This chapter describes the use of flow cytometry for the evaluation of two hypothesized protectants (i.e., metabolisable sugar and lecithin vesicles), for the protection of probiotic LAB strains over the GI stress factors.

3.1. Introduction

Lactic acid bacteria (LAB) such as lactobacilli and bifidobacteria are commonly used as dietary supplements for their favoured probiotic attributes and are administered orally for obvious convenience. Because the benefits were more pronounced under the functional status, probiotic bacteria are favoured to be delivered to the distal area of the human gastro-intestinal (GI) tract in a live state [16, 172]. However, the stress factors in the GI tract inevitably affect the cellular functions of probiotic bacteria [51, 173-174]. Their physiological conditions including the integrity of cellular membrane, intracellular pH, functional enzymes, etc., are constantly challenged by the stress factors such as gastric acidity, bile acids and other digestive enzymes. In particular, the acidity of gastric juice as low as pH 1.5 under a fasting state can rapidly inactivate LAB, exhausting them in retaining a constant cytoplasmic pH [175]. It was also reported that strains of LAB, even if they commonly exhibited good intrinsic tolerance to pH 4, suffered increased sensitivity at pH values below 3 [176-177]. In the attempt to enhance

the survival in acidic environments, metabolisable sugars were tested on some probiotic LAB and improved their transient endurance [178-179]. The protection was further attributed to the membrane-bound F_1F_0 -ATPases which could actively pump out overabundant protons under the energized state [174, 179-181]. In regard to another major stress factor, bile acids (or their salts) are potent bio-surfactants especially in the unconjugated form. They exhibit a substantial anti-microbial effect by disturbing the cell membrane integrity, lowering the intracellular pH and interfering with normal cellular metabolism [173]. The minimum inhibitory concentrations (MIC) were reported to be 3 to 13 mM for cholic acid (CA) and 0.3 to 0.8 mM for deoxycholic acid (DCA) individually for a variety of LAB [182]. My previously published work also confirmed this bactericidal effect, whereby 2-h exposure to 0.4% (wt/vol) of mixed CA and DCA (50:50, equal weight) induced around two-log drop in CFU count among all the four examined probiotic strains [88].

In most previous studies on probiotic LAB, proliferation-based techniques (e.g. plate count) were widely employed as the standard method for viability enumeration. However, the drawbacks of these have been highlighted by some probiotics researchers in recent years [56, 183]. It is argued that, in many cases, the proposed probiotic mechanisms are dependent on metabolic activity rather than cell replication [184]. Additionally, a good re-growth in the laboratory may not always represent a comparable proliferation capacity in the intestine [183]. It has also been confirmed that stressed probiotic bacteria can enter into a viable-but-not-culturable (VBNC) state, in which bacteria fail to grow on nutrient agar but still possess some properties typical of viable cells [183, 185]. The arguments complicate the story of the viability enumeration. It is reasonable to justify that proliferation-based methods provide only a limited view of the

physiological status of cells. Therefore, alternative techniques are desired for revealing viability in terms of physiological status and functionality rather than cultivability.

Flow cytometry (FCM) in combination with fluorescent labelling is a rapid technique for single-cell-oriented multi-parametric assessment. A variety of fluorescent probes have been applied to examine different physiological parameters including cell membrane integrity, intracellular enzyme activity, cellular vitality, cytoplasmic pH and membrane potential [186]. Among the numerous choices, propidium iodide (PI) and carboxyfluorescein di-acetate (cFDA) are the most widely used combination. FCM analysis combined with cF/PI dual staining was successfully applied to discriminate the physiological heterogeneity in some *Bifidobacterium* and *Lactobacillus* species which were exposed to a variety of biological and environmental stress factors such as acid, bile salts, freezing, lyophilisation, heat, ultrasound and high pressure [56-57, 89, 103-104, 187-189]. In some studies, the correlation between the probe-indicated viability and the cultivability for the cells from heterogeneous subpopulations was also explored by FCM-based single-cell sorting technique [57, 190].

In the current investigation, FCM analysis was applied to profile the physiological status of six probiotic LAB strains which were challenged by the simulated human GI stressors. Improved protection provided by the selected protectants was expected to be reflected in altered patterns of FCM-enumerated physiological heterogeneity. Single-cell-sorting technique was also utilized to compare the FCM-enumerated viability with the proliferation-based cultivability.

3.2. Materials and methods

3.2.1. Materials

Bile salts (mixture of 50% sodium cholate and 50% sodium deoxycholate) were procured from Sigma-Aldrich (Australia). The fluorescent probes, PI and cFDA, were procured from Invitrogen Inc (U.S.). Egg yolk lecithin (>98% phosphatidylcholine) was donated by GMP Pharmaceuticals NZ (New Zealand). The simulated gastric fluid (SGF) and the simulated intestinal fluid (SIF) were prepared following U.S. Pharmacopeia 29 (USP29):

- The SGF test solution was prepared by dissolving 2.0 g of NaCl and 3.2 g of purified pepsin in 7.0 mL of HCl and sufficient water to make 1000 mL (either with or without 20 mM glucose supplement). This test solution had a pH of about 1.2;
- The SIF was prepared by firstly dissolving 6.8 g of KH_2PO_4 in 250 mL of water, mixing, and adding 77 mL of 0.2 N NaOH and 500mL of water, then adding 10 g pancreatin, mixing and adjusting the resulting solution with either 0.2 N NaOH or 0.2 N HCl to a pH of 6.8, and finally diluting with water to 1000 mL. Bile salts at different concentrations were prepared based on the SIF by dissolving according weight of bile salts powder.

The preparation of lecithin vesicles followed the method of Hope *et al.* [191]. Briefly, egg yolk lecithin (average mol wt 760.09 g/mol) was dried under nitrogen, dissolved in warm *tert*-butanol, frozen at -80 °C, and lyophilised overnight. It was then suspended in Tris-buffered saline, vortexed vigorously for 20 min, followed by five freeze and thaw cycles using liquid nitrogen, and extruded under nitrogen through the paired 0.1- μm polycarbonate filters. The extruded vesicles were stored under nitrogen at 4 °C and used

within a week. Vesicles formed this way had a uniform surface available for surface interactions.

3.2.2. Strains and culturing conditions

Probiotic strains including *Lactobacillus acidophilus* DPC201 (BRNZ#001DU), *Lactobacillus plantarum* DPC206 (BRNZ#006DU), *Pediococcus acidilactici* DPC209 (BRNZ#009DU), *Lactobacillus reuteri* DPC16 (NZRM 4294), *Lactobacillus rhamnosus* HN001 (BRNZ#001FP) and *Bifidobacterium lactis* HN019 (BRNZ#002FP) were obtained from Bioactives Research New Zealand (BRNZ, New Zealand) culture collection, delivered as frozen. These strains were revived anaerobically in deMan-Rogosa-Sharpe (Difco, USA) broth supplemented with 0.5 g/L cysteine (MRSc) for 36 h at 37 °C. The culture was again purified via single colony purification by sterile streaking. The identification of each purified strain culture was confirmed at species level by API 50 CHL system and API Rapid ID 32A system (bioMérieux, Inc., Australia). Prior to experimenting, each strain was anaerobically propagated twice in MRSc broth at 37 °C to the early stationary phase. Enumeration was performed by the drop plating technique on MRS agar plate. The inoculated plates were incubated in an anaerobic system at 37 °C for 24 hours.

3.2.3. Simulated gastric fluid and sucrose supplement

For each strain, 5 mL fresh culture was harvested by centrifugation at $4,000 \times g$ for 5 min, re-suspended in 5 ml SGF and agitated (120 rpm) at 37 °C for 2 hours. By the end of this duration, 1 ml samples were withdrawn from the SGF solution. The pH was neutralized with 0.1 M NaOH. The probiotics in each sample were centrifuged and re-suspended in 2 mL 1x PBS pH 7.4 prior to fluorescent staining and FCM analyses. The energy supply for probiotics to survive low pH was studied following the same process

except that the SGF was supplemented with 20 mM sucrose. Freshly harvested bacteria of each strain served as positive control while heat-killed bacteria (85 °C, 45 min) served as negative control. Both control groups followed identical harvest and wash process as treated groups.

3.2.4. Simulated intestinal fluid and lecithin vesicle supplement

Bile salts were weighed and dissolved in the SIF to make bile-salt-SIF solutions (bsSIF) at concentration 0.4 and 0.8 g/100mL. For each strain, 5 mL fresh culture was harvested by centrifugation at $4,000 \times g$ for 5 min, re-suspended in 5 ml bsSIF solution and agitated (120 rpm) at 37 °C for 2 hours. By the end of this duration, 1 ml samples were withdrawn from the bsSIF solution. The probiotics in each sample were centrifuged and re-suspended in 2 mL 1x PBS pH 7.4 prior to fluorescent staining and FCM analyses. The protection provided by lecithin vesicle for probiotics to survive bile salt challenge was studied following the same process except that the bsSIF was supplemented with 2% (w/v) lecithin vesicles. Freshly harvested bacteria of each strain served as positive control while heat-killed bacteria (85 °C, 45 min) served as negative control. Both control groups followed identical harvest and wash process as treated groups.

3.2.5. Time course study of bile salts challenge to *L. reuteri* DPC16 at serial concentrations

L. reuteri DPC16 strain was exemplified to demonstrate the time course challenge on probiotics induced by bile salts at different concentrations. The treatment followed the same procedure as described in Section 3.2.4. Two time points (0.5 and 1.5 h) were selected for viability enumeration and bsSIF solutions were prepared at 0.05%, 0.1%, 0.2%, 0.4%, 0.8% and 1.2% (w/v, g/100mL).

3.2.6. Fluorescence labelling and FCM analysis

FCM analysis followed the same method described in my previously published study [103]. Briefly, cFDA was prepared as a 10-mM stock solution in anhydrous DMSO and was further diluted in DMSO to 1-mM working solution before use. Each treated bacteria concentrate was suspended and diluted using an anaerobic PBS (pH 7.0; containing 1 mM DTT) to approximately 10^7 CFU/mL. Ten microlitre of cFDA working solution was added into 990 μ L bacteria suspension, mixed well and incubated in the dark at 37 °C for 10 min. Afterwards, the bacteria were spun down and washed once using the anaerobic PBS (pH 7.0) to remove excess of cFDA. The cF-stained bacteria were re-suspended in 980 μ L of anaerobic PBS (pH 7.0). PI was supplied by the manufacturer as a 1-mg/mL solution in distilled water and was used as the working solution. Twenty microlitre of PI solution was added in the cF-stained bacteria suspension and mixed well. The dual stained bacteria suspension was further incubated in the ice-bath for 15 min prior to FCM analysis.

FCM analysis was performed with the BD LSR II Flow Cytometer (BD Biosciences, New Zealand). The cytometer was adjusted at low flow rate to count 100,000 fluorescent events. The measurements acquired for each bacterium included the forward scatter (FSC), the side scatter (SSC), the green (FL1) and the red fluorescence (FL3) channels. The cF-stained bacteria were detected at 530 nm. The PI-stained bacteria were detected at 635 nm. Both were excited by a laser beam with a wavelength at 488 nm. All signal channels were recorded on logarithmic scale. The data were collected by BD FACSDiva program and were stored in the standard “.fcs” format.

The raw data were analyzed with FlowJo program (v7.6.1, Tree Star, Inc. USA) in the post-run mode. A polygon gate was created on dot plot of FSC vs. SCC to discriminate bacteria population. On dot plot of FL1 (cF) vs. FL3 (PI), four quadrants were divided

by cross-line gating. The four quadrants were defined clockwise starting from the top-left one as Q1, Q2, Q3 and Q4. Three heterogeneous subpopulations were observed as: Q1 (cF+/PI-): the intact (healthy) sub-population, Q2 (cF+/PI+): the stressed sub-population and Q3 (cF-/PI+): the damaged sub-population.

3.2.7. Cell sorting

Cell sorting followed the method described by Papadimitriou *et al.* [190] with few modifications. The EPICS Elite Flow Cytometer (Beckman-Coulter, UK) ran under the compatible workstation software ver. 4.5. The instrumental settings involved the 15 mW air-cooled argon ion laser (488nm), the confocal beamshaper (15 x 60 µm spot-size) and the 76 µm sort sense flow cell operating at 15 psi sheath pressure with a droplet frequency at 38 kHz. Bacteria were discriminated by their FSC/SCC signals and were sorted based on the region of interest with cF (FL1) only, cF and PI (FL1 and FL3) or PI (FL3) only fluorescence. Discriminator was created as a noise background <50 events/s on a filtered sheath sample. Sorting rate was set at <300 cells/s. Coincidence abort and triple drop deflection were activated. The probiotic bacteria of each strain were challenged by either SGF or bsSIF in the presence of corresponding protectant. They were labelled with the probes and analyzed by FCM. Twenty cells from each subpopulation were sorted on an MRS agar plate for proliferation evaluation.

3.2.8. Statistical analysis

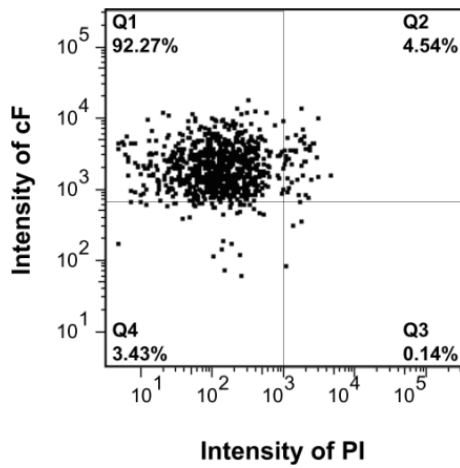
Results were generated from five independent experiments, each performed in duplicate. $P = 0.05$ was selected as the significance level unless otherwise specified. The type of statistics was stated separately for every result being presented and/or discussed.

3.3. Results

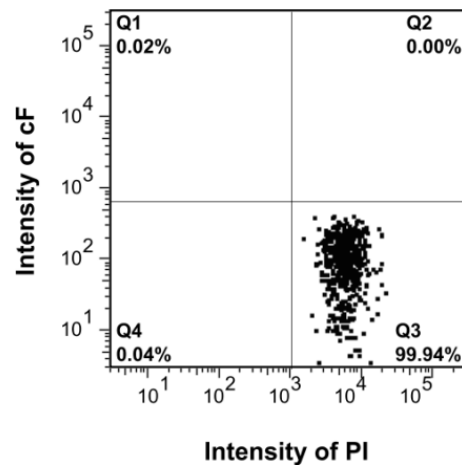
3.3.1. SGF challenge and sucrose supplement

FCM analysis clearly distinguished the physiological heterogeneity of the challenged bacteria population. Taking *L. acidophilus* DPC201 for instance, Figure 3.1 shows the acquired FCM dot plots (FL1 vs. FL3) of this strain that had been exposed to simulated GI challenges either in the presence or the absence of the protectants. The *x*- and the *y*-axes in this plot represent the intracellular PI and cF fluorescent intensities in logarithmic scales, respectively. The plot space was divided into four quadrants in terms of the combinations of PI and cF intensities at low (-) or high (+) level. The four quadrants corresponded to the four subpopulations including intact (healthy) subpopulation (Q1: cF+/PI-), stressed (injured) subpopulation (Q2: cF+/PI+), damaged subpopulation (Q3: cF-/PI+), and artifacts (Q4). In Figure 3.1(a), the fresh *L. acidophilus* DPC201 culture (the positive control) mainly fell into the category of intact cell (Q1 quadrant) while Figure 3.1(b) shows that the heat-killed *L. acidophilus* DPC201 mainly fell into the category of damaged cell (Q3 quadrant). Both plots matched the characteristic of the respective control samples. After being challenged with SGF, *L. acidophilus* DPC201 in the absence of sucrose (Figure 3.1(c)) was found to suffer a huge loss of cell membrane integrity and enzyme activity. Nearly 97% of the cells appeared to be severely damaged and shifted to Q3 quadrant, making the plot quite comparable to the one of the heat-killed sample. In contrast, the presence of 20 mM sucrose in SGF (Figure 3.1(d)) substantially enhanced the survival of *L. acidophilus* DPC201. More than one tenth bacteria (Q1: 12.27%) were kept intact. In comparison, a nearly complete loss of the intact cells was observed in the non-supplemented sample. The number of bacteria in Q2 (consisting of injured but not severely damaged bacteria) also expanded more than 10 folds. The number of damaged bacteria was reduced by

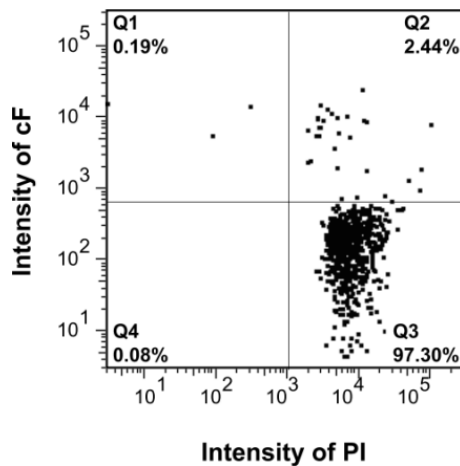
more than half. For each strain, the composition of subpopulations was collected from the cF/PI dot plots and summarized in Figure 3.2. It is clearly shown that the supportive effect of sucrose is universal among all the six probiotic strains. Considering the particular enhancement for each strain, the highest yield of intact bacteria was observed in *L. rhamnosus* HN001 (Q1: 23.2%) while the lowest was seen in *L. plantarum* DPC206 (Q1: 12.3%).



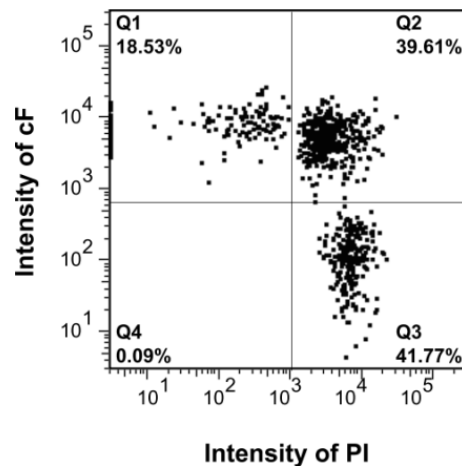
(a)



(b)



(c)



(d)

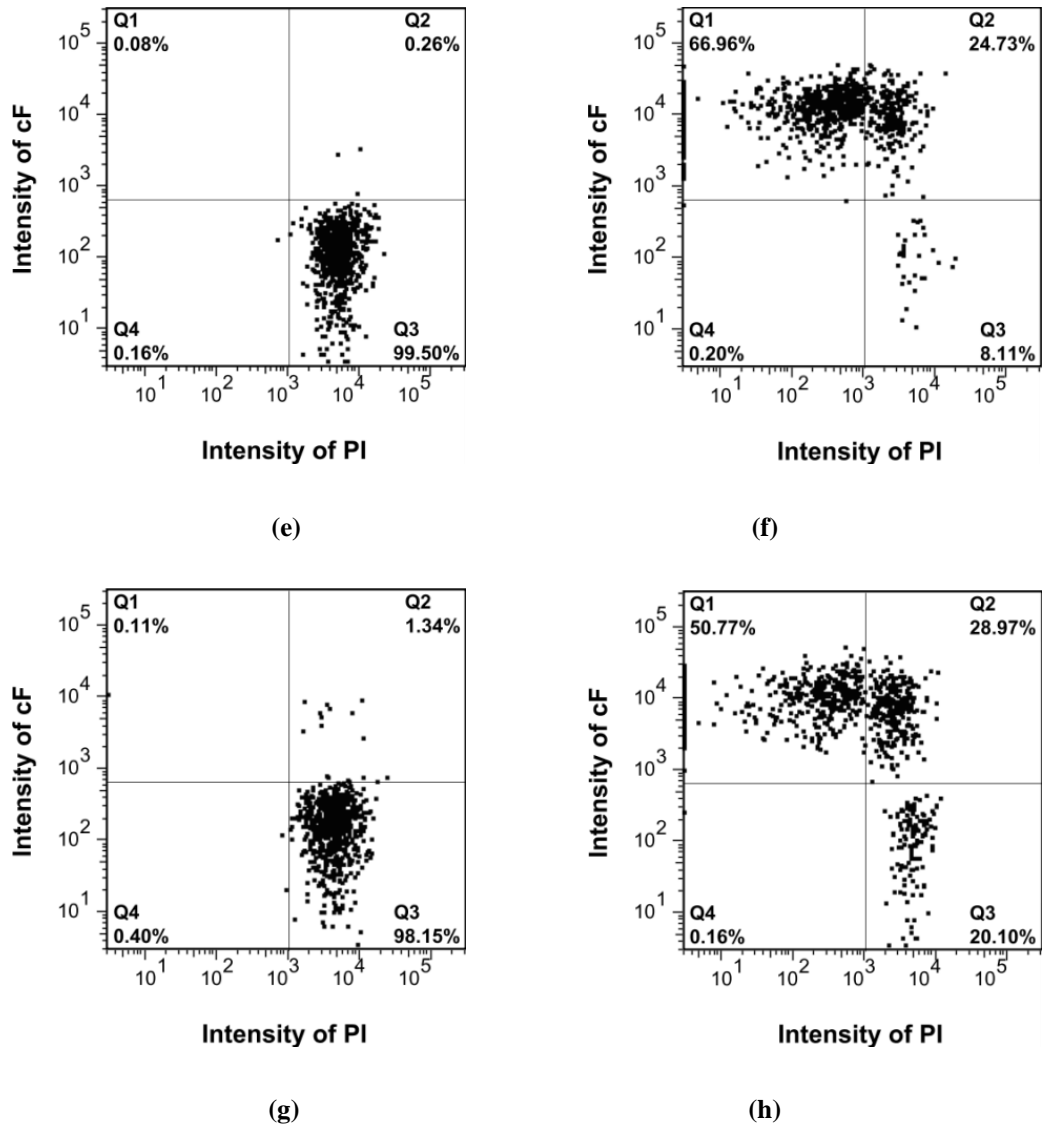
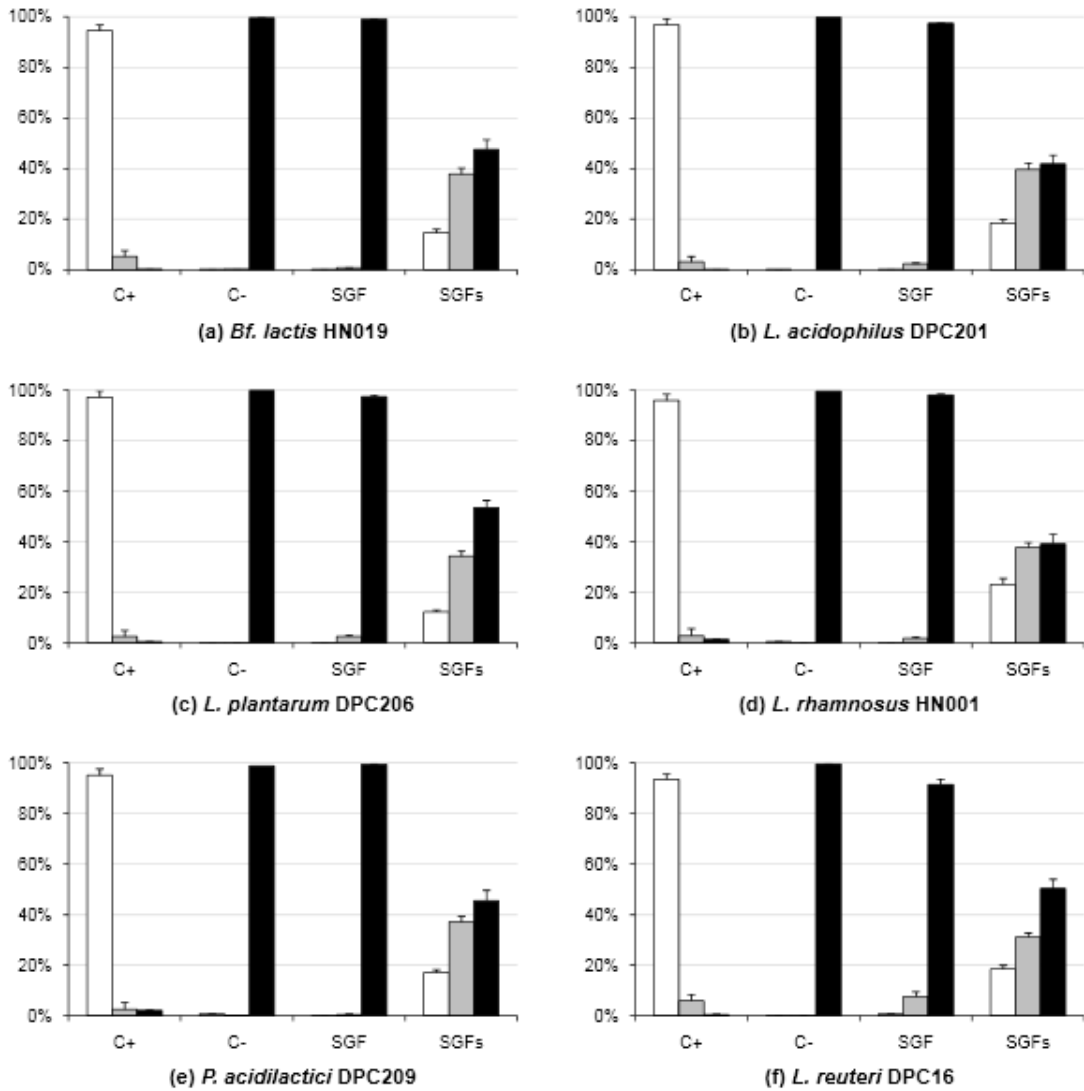


Figure 3.1 Dot plots of the FCM-enumerated *L. acidophilus* DPC201 exposed to the simulated GI challenges in the absence and presence of the protectants. (a) Fresh culture, positive control; (b) heat-killed DPC201, negative control; (c) DPC201 exposed to SGF pH 1.2 for 2 h; (d) DPC201 exposed to SGF pH 1.2 for 2 h in the presence of 20 mM sucrose; (e) DPC201 exposed to bsSIF (0.4% bile salts) for 2 h; (f) DPC201 exposed to bsSIF (0.4% bile salts) for 2 h in the presence of 2% lecithin vesicle; (g) DPC201 exposed to bsSIF (0.8% bile salts) for 2 h; (h) DPC201 exposed to bsSIF (0.8% bile salts) for 2 h in the presence of 2% lecithin vesicle. The y-axis indicates the logarithmic fluorescence intensity of cF (FL1). The x-axis indicates the logarithmic fluorescence intensity of PI (FL3). Four quadrants (sub-populations) are defined as Q1(cF+/PI-, healthy), Q2(cF+/PI+, stressed), Q3(cF-/PI+, dead), and Q4(cF-/PI-, artefacts).



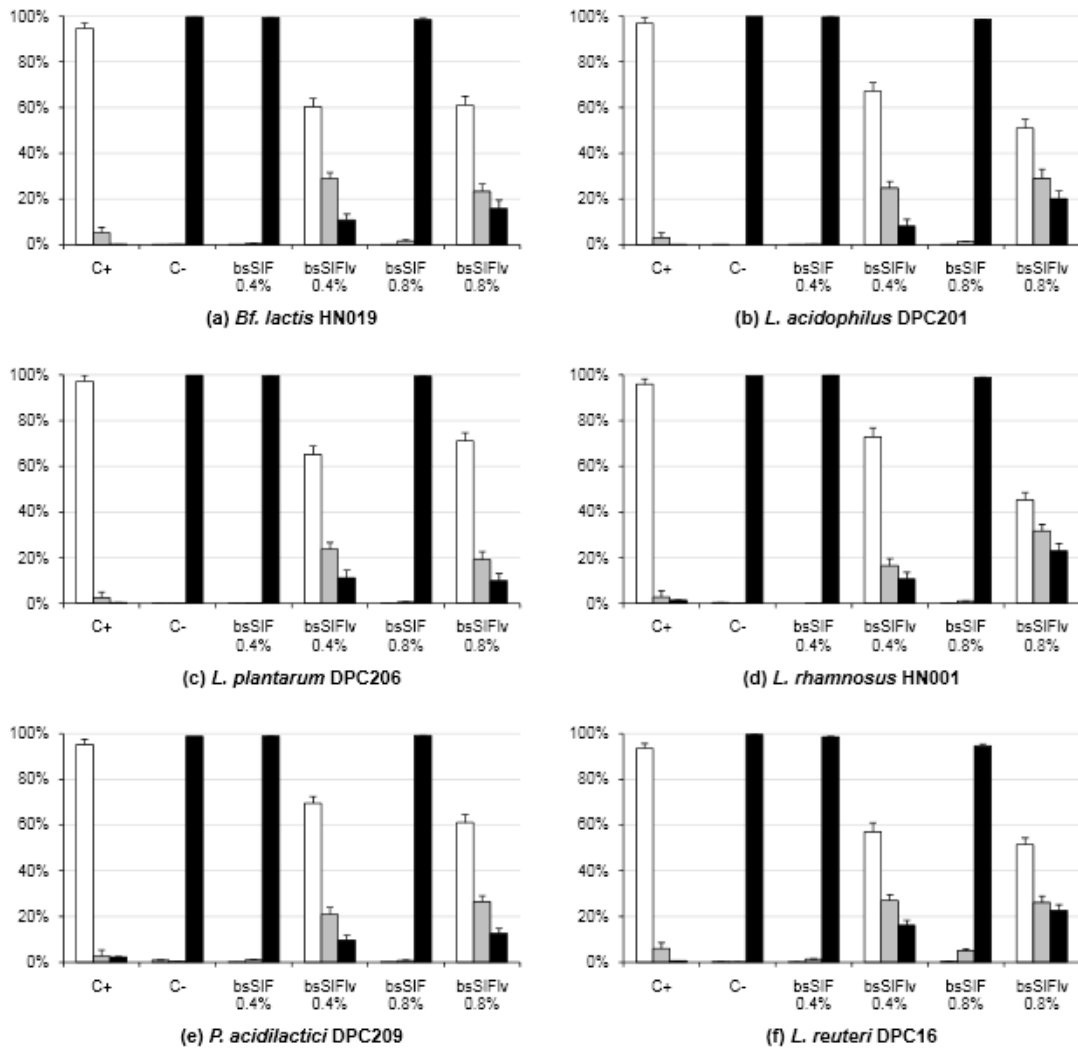
Notes:

1. C+ denotes the positive control (fresh culture).
2. C- denotes the negative control (heat-killed culture).
3. SGF denotes the treatment of the simulated gastric fluid treatment (pH 1.2).
4. SGFs denotes the SGF supplemented with 20 mM sucrose.

Figure 3.2 Summary of the FCM-enumerated viability of six probiotic strains which were exposed to SGF for 2 h either with the absence or the presence of 20 mM sucrose. The three subpopulations are indicated by the colours as intact: □, stressed: ■, and damaged: ■. The y-axis indicates cell number of the subpopulations in percentage. The y-axis error bars indicate the 95% confident interval. Data was acquired from five individual experiments, each performed in duplicates.

3.3.2. Bile-salt SIF challenge and lecithin vesicle supplement

The presence of lecithin vesicle conferred a substantial protection on the LAB strains which were exposed to lethal concentrations of bile acids in SIF. FCM analysis successfully revealed this improvement by showing the significant changes among the heterogeneous subpopulations. Still taking *L. acidophilus* DPC201 for instance, Figure 3.1(e)-(h) show the acquired FCM dot plots (FL1 vs. FL3) for this strain which was challenged by bsSIF either in the presence or the absence of lecithin vesicles. It is obvious in Figure 3.1(e) and Figure 3.1 (g) that after a 2-h challenge, bile acids at either concentration almost depleted the intact bacteria (Q1 quadrant), resulting in less than 0.2% integral cells in the whole bacterial population. Similarly, only a small number of the bacteria fell in the category of stressed subpopulations, as defined by the Q2 quadrant. In contrast, most of the cells (>98%) appeared to be damaged (Q3 quadrant) and resembled the heat-killed sample. This indicates a high potency of bile salts to disrupt bacterial cell membrane and interfere with the functionality of cytoplasmic enzymes in the light that both probes indicate the worst status. Comparatively, the supplement of lecithin vesicle to bsSIF substantially mitigated the harmful impact of the bile salts. The number of intact DPC201 rose from almost none to 67% in the case of bile-salt concentration at 0.4% (w/v) and to 50% in the case of 0.8%. The protection was further demonstrated to be universal among all the six examined strains. More than a half of the challenged cells benefited from the protection, remaining intact, whilst the number of damaged bacteria was reduced to below 20%. For each strain, the composition of the subpopulations was collected from the FCM data and illustrated in Figure 3.3.



Notes:

1. C+ denotes the positive control (fresh culture). C- denotes the negative control (heat-killed culture).
2. bsSIF 0.4% denotes the treatment with the simulated intestinal fluid in the presence of 0.4% (w/v) bile acids. bsSIF 0.8% denotes the treatment with the simulated intestinal fluid in the presence of 0.8% (w/v) bile acids.
3. bsSIFlv denotes the bsSIF supplemented with 2% (w/v) lecithin vesicle.

Figure 3.3 The summary of the FCM-enumerated viability of six probiotic strains which were exposed to bsSIF for 2 h either with the absence or the presence of 2% (w/v) lecithin vesicle. The three sub-populations are indicated by the colours as intact: □, stressed: ■, and damaged: ■. The y-axis indicates cell number of the subpopulations in percentage. The y-axis error bars indicate the 95% confident intervals. Data were acquired from five individual experiments, each performed with duplicate.

In addition, there was another unexpected observation on the interaction between the bacteria and bile salts at different concentrations. The 0.8% (w/v) bsSIF was found to induce slightly less damaged cells (one-tailed paired Student *t*-test, $P = 0.044$) and result in more stressed cells (one-tailed paired Student *t*-test, $P = 0.043$) than the 0.4% (w/v) bsSIF. This phenomenon was further demonstrated on *L. reuteri* DPC16 in the following Section 3.3.4.

3.3.3. Cell sorting

In order to verify the FCM-analysed improvement in viability, single-cell sorting was performed, which evaluated each subpopulation based on their proliferation capacities. The results are listed in Table 3.1. The intact subpopulations among all the strains through different treatments were proved to consist of most cultivatable cells, showing no less than 90% growth on agar plate. In contrast, no growth was observed in all the samples from damaged subpopulations. Growth of the stressed (injured) cells exhibited some complexities, whereby the percentages of the colony-forming cells ranged from 35% for *Bf. lactis* HN019 challenged by 0.8% bsSIF to 72% for *L. reuteri* DPC16 challenged by SGF.

Table 3.1 Percentages of cells of six LAB strains that formed or did not form colonies after being directly sorted on MRS agar plate. The cells were exposed to various treatments in simulated GI challenges in the presence of the selected protectants. The criterion of cell sorting was based on the cF/PI dual-staining results analyzed by FCM. Results were acquired from five independent experiments and presented as mean \pm 95% confident interval.

Treatment	Strain	Intact cells Q1: cF+/PI-			Stressed cells Q2: cF+/PI+		Damaged cells Q3: cF-/PI+	
Fresh culture	<i>Bf. lactis</i> HN019	93%	\pm	1.9%	NT	NT		
	<i>L. acidophilus</i> DPC201	94%	\pm	2.3%				
	<i>L. plantarum</i> DPC206	95%	\pm	2.0%				
	<i>L. rhamnosus</i> HN001	94%	\pm	1.4%				
	<i>P.acidilactici</i> DPC209	95%	\pm	2.2%				
	<i>L. reuteri</i> DPC16	96%	\pm	2.3%				
SGF challenge in the presence of 20 mM sucrose	<i>Bf. Lactis</i> HN019	90%	\pm	3.1%	51%	\pm	2.6%	NG
	<i>L. acidophilus</i> DPC201	93%	\pm	1.7%	61%	\pm	2.6%	NG
	<i>L. plantarum</i> DPC206	95%	\pm	3.1%	66%	\pm	2.6%	NG
	<i>L. rhamnosus</i> HN001	93%	\pm	2.6%	61%	\pm	1.4%	NG
	<i>P.acidilactici</i> DPC209	91%	\pm	4.0%	65%	\pm	2.2%	NG
	<i>L. reuteri</i> DPC16	96%	\pm	2.8%	72%	\pm	1.7%	NG
SIF (0.4% bile salts) challenge in the presence of 2% lecithin vesicles	<i>Bf. Lactis</i> HN019	88%	\pm	2.8%	36%	\pm	2.6%	NG
	<i>L. acidophilus</i> DPC201	92%	\pm	2.8%	58%	\pm	3.5%	NG
	<i>L. plantarum</i> DPC206	92%	\pm	2.8%	61%	\pm	4.6%	NG
	<i>L. rhamnosus</i> HN001	91%	\pm	3.4%	59%	\pm	1.4%	NG
	<i>P.acidilactici</i> DPC209	90%	\pm	4.4%	63%	\pm	1.7%	NG
	<i>L. reuteri</i> DPC16	95%	\pm	3.1%	71%	\pm	2.6%	NG
SIF (0.8% bile salts) challenge in the presence of 2% lecithin vesicles	<i>Bf. Lactis</i> HN019	87%	\pm	3.5%	35%	\pm	2.2%	NG
	<i>L. acidophilus</i> DPC201	91%	\pm	4.0%	59%	\pm	1.4%	NG
	<i>L. plantarum</i> DPC206	92%	\pm	3.5%	61%	\pm	3.4%	NG
	<i>L. rhamnosus</i> HN001	89%	\pm	4.6%	58%	\pm	2.8%	NG
	<i>P.acidilactici</i> DPC209	90%	\pm	3.1%	62%	\pm	3.5%	NG
	<i>L. reuteri</i> DPC16	94%	\pm	3.4%	70%	\pm	4.9%	NG

Notes:

1. NT denotes that no test was performed due to the low percentage of this subpopulation.
2. NG denotes that no growth on nutrient agar plate was detected for this subpopulation.

3.3.4. Time course study of bile salts challenge to DPC16 at serial concentrations

In the previous bsSIF challenge test, we observed that 0.8% (w/v) bsSIF unexpectedly induced slightly less damage to the LAB strains in comparison to 0.4% bsSIF. This phenomenon was further demonstrated on the strain *L. reuteri* DPC16 at a wider range of bile-salt concentrations using FCM analysis. The results are summarized in Figure 3.4. It was observed that the presence of bile salts at concentration around 0.1% to 0.2% started to inflict noticeable damage on *L. reuteri* DPC16. However, this damaging effect did not uni-directionally increase with the elevated bile-salt concentrations. It peaked when the bile-salt concentration reached around 0.4% (w/v). In the case that the bsSIF challenge was as brief as 0.5 h, the number of intact cells showed a slight increase at higher bile-salt concentrations. Similarly, the stressed subpopulations substantially expanded at the bile-salt concentrations above 0.4%, accompanying the reduction of damaged cells. This phenomenon was still visible in the 1.5 h samples although only to a much reduced extent.

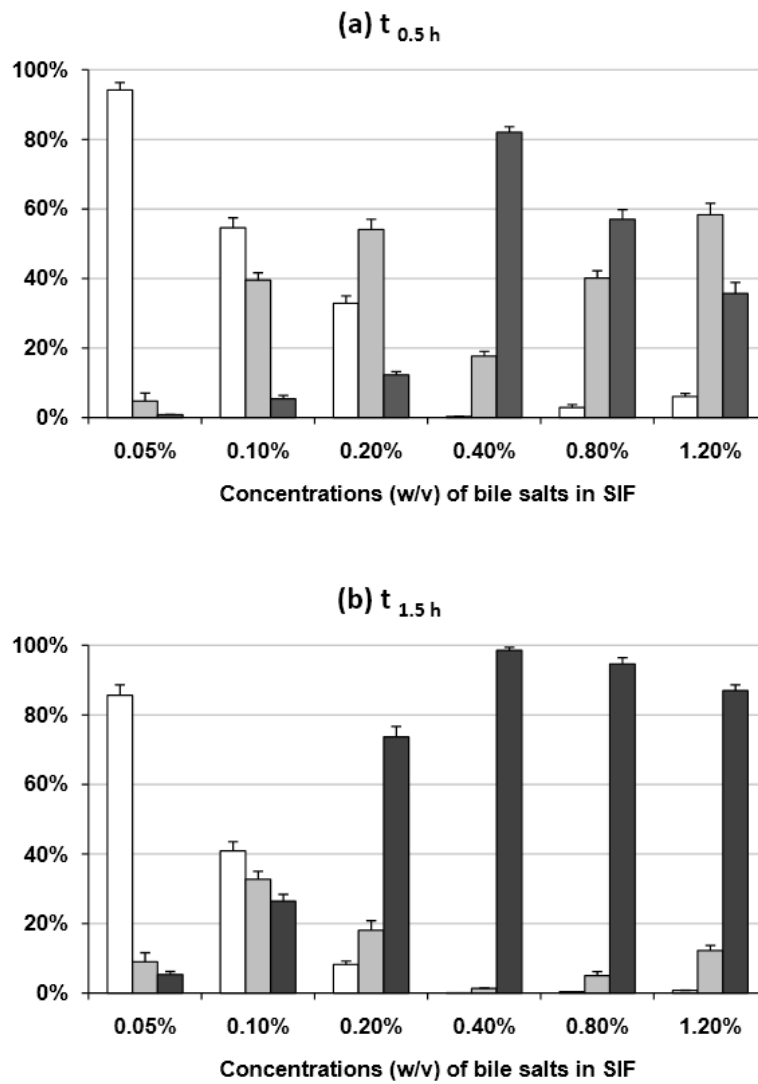


Figure 3.4 FCM-enumerated physiological heterogeneity of the *L. reuteri* DPC16 populations which were exposed to bsSIF challenge. Bile-salt concentrations in SIF ranged from 0.05% to 1.2% (w/v). The three sub-populations are indicated by the colours as intact: □, stressed: ■, and damaged: ■. Two time points: (a) 0.5 h and (b) 1.5 h were selected for the enumeration. The y-axis error bars indicate the 95% confident interval.

3.4. Discussion

In this study, FCM assessment combined with cF/PI dual staining was successfully applied to evaluate the protective effects of sucrose and lecithin vesicles on six early-stationary-phase probiotic strains of LAB. The use of multiple physiological probes provided a superior discrimination of physiological heterogeneity within the bacteria population, and overcame the deficiency of single probe. Some studies reported that the viability count based on the cF-stained bacteria tended to give an overestimated result as compared to plate count [57, 192]. The discrepancy is attributed to the existence of viable-but-not-culturable (VBNC) cells which are injured and fail to grow on nutrient agar but still preserve good enzyme (esterase) activity and hence get stained by cF. This type of VBNC cells was observed in the current study in all examined strains. In particular, VBNC cells occurred in a large quantity in the stressed subpopulations (stained by both cF and PI) as evaluated by cell sorting. It may suggest that the process of proliferation involves sensitive mechanisms which are easily compromised by certain environmental stressors. The existence of VBNC cells of some LAB strains was investigated and was suggested to be very common among probiotics [183, 185], which makes enumeration complicated. The other probe used in my study PI was considered as a sensitive probe for cell membrane integrity. False positive results of this probe, however, were reported on some environmental strains during the early exponential growth, possibly because fast cell size growth affected the cell membrane integrity [92]. The experiment settings of my current study avoided this potential problem by growing the bacteria to early stationary phase when cell membrane was fully developed and underwent only limited structural change. The measured integrity loss was subsequently considered to be caused mainly by environmental stress factors. The use of early-stationary-phase probiotic bacteria has another advantage. Stationary-phase probiotic

culture was found to be inherently resistant to a variety of stressors, which would benefit following processes such as encapsulation and spray-drying [60, 76, 193]. The resistance was considered to rise from the stress response elicited by starvation and sub-lethal acidity of the spent media [194-195].

The intrinsic tolerance to acidic environments can facilitate the passage of probiotics through the host's stomach. However, the availability of an energy source proved to be equivocally important in order to maintain the function for the acid tolerance. The current study showed that the presence of sucrose coincided with the significantly enhanced preservation of favourable physiological conditions among all the six strains. It agreed with the reports about the supportive role of metabolisable sugars for the acid tolerance of bacteria [179, 196]. The protection is fulfilled by energizing the membrane-bound F_1F_0 -ATPase proton pump [180, 196], which consequently maintains a near-neutral cytoplasmic pH for bacteria. Because the esterase activity of LAB strains was commonly found to be optimal at pH 6 to 7 and severely inhibited below pH 4 [197-199], the normal functionality of intracellular enzymes as revealed by cF staining may have provided evidence for the undisturbed internal pH under the stress of acidity. In addition, the results may have some useful indications for the effective administration of oral probiotics. The probiotics are better to be administered with food or soon after a meal when the gastric pH is elevated, a supportive food matrix is present and the transient time is shortened.

Bile acids, one of the major components of bile, are strong biological membrane disruptors due to their amphiphilic characteristic, particularly in unconjugated form. All the six probiotic strains in the study suffered a huge loss of the cell membrane integrity in the presence of bile salts, as evaluated by permeation of PI. The two bile-salt concentrations used in the study represent critical ranges around (as of 0.4%) and above

(as of 0.8%) the critical micelle concentration (CMC) of the mixture of sodium cholate and sodium deoxycholate. It also covered the highest biological presence of bile salts in human bile which is up to 14 mM. Interestingly, the bile salt concentration (0.4%) near the CMC was found to induce slightly more damage to the examined bacteria than the higher concentration (0.8%). The underlying mechanisms of this unexpected increase in survival are unclear. However we propose that it may be due to the occurrence of secondary aggregates of bile salt micelles. It has been reported that, at concentrations above CMC, the average aggregation number of primary bile-acid micelles increases, creating an expanded spatial formation of various irregular shapes [200-202]. Complex secondary aggregates are spontaneously assembled from these expanded primary micelles due to increased hydrophobic effect and hydrogen-bonding [202]. We propose that the secondary aggregates are less toxic than the bile acid monomer or its simple micelles. The reduction in toxicity is assumed to arise from the increased stability of this type of aggregation, which impedes the free contact of monomer and small micelles with the membrane of bacteria. Further investigation, however, may be needed to explore this hypothesis, which is beyond the scope of the current study.

The responsible role of lecithin vesicle for the protection of probiotic bacteria over bile salt challenge was affirmed by FCM assessment in this study. Probiotic bacteria, especially for commercial use, are generally judged and selected by their tolerance to bile salts. However, to the best of my knowledge, no particular protectant was ever investigated to mitigate the toxic effect of bile salts for the purpose of delivering viable probiotic bacteria. In the current study, the protection was evaluated in terms of the preservation of cell membrane integrity and cytoplasmic enzyme activity, both of which are the direct targets of bile-salt stress. The substantial increase of intact (cF+/PI-) bacteria in the presence of lecithin vesicles provided evidence that lecithin vesicle

effectively protected the cellular membrane from the disturbance of bile salts. Similar to the formation of secondary aggregates of bile-salt micelles above the CMC, the presence of lecithin vesicles promotes the formation of a type of hybrid (lecithin and bile acids) micelles [203-204]. Because bile-salts monomers and simple micelles are most potent in terms of disrupting biological bi-layers, their concentration, also termed the inter-mixed micellar/vesicular concentration (IMC) [205], influences the damaging effect of bile salts. The formation of the hybrid micelles is considered to reduce the bile salt IMC and therefore produce the protective effect.

In conclusion, sucrose and lecithin vesicles were assessed for the protective effects on six probiotic LAB strains which were exposed to stressful GI-simulated environments. FCM analysis disclosed significant improvements of survival in the presence of the protectants among all the examined probiotic bacteria in terms of their physiological conditions. Cell sorting of the FCM-discriminated bacteria subpopulations further confirmed a comparable enumeration between the proliferation-based cultivability and the probe-indicated viability in the samples of the intact and the damaged subpopulations. It also revealed the complexities of the stressed (injured) subpopulation. Thus, FCM analysis proved to be a useful analytical tool for probiotics research.

Chapter 4. Development of the probiotic colonic delivery system based on microencapsulation with protectants

This chapter describes the development of a probiotic delivery system (i.e., probiotic bacteria being immobilized in sub-100 μm chitosan-coated Ca^{2+} -alginate microcapsule supplemented with the selected GI protectants) and its performance in protection against simulated GI challenges. The colonic release of the immobilized probiotic bacteria from the delivery system was also assessed in the simulated GI environments.

4.1. Introduction

Probiotics are able to confer prophylactic and, in some cases, therapeutic benefits to the host, once these bacteria reach and start functioning at the distal regions of the host's digestive tract. Many *in vitro* studies confirm their positive contributions in regulating the host homeostasis [16, 172], while animal and clinical trials sometimes present less consistent results [206-209]. Such *in vitro/in vivo* inconsistency is partly attributed to the fact that the colonisation and the function of probiotics always encounter great challenges from the defensive factors within human body. Among these barriers, the most stringent are extreme acidity in stomach, surfactant bile acids in intestinal fluids and assorted digestive enzymes along the gastrointestinal (GI) tract [51, 173-174, 210].

The gastric pH of stomach of healthy human adult in fasting state is approximately 1.5, which can elevate to between 3.0 and 5.0 during feeding. Long-time survival in such an acidic environment is rare for the majority of ingested bacteria [181]. Initially, damage

occurs as an unrestrainable influx of protons. The presence of excessive protons finally leads to the disintegration of the cellular membrane, disturbing normal metabolism and reproduction processes. Although some probiotics, e.g. strains belonging to lactic acid bacteria (LAB), exhibit a good acid tolerance down to pH 4, intrinsic resistance to gastric acid is still a relatively rare probiotic property [211]. Some studies have revealed that the resistant bacteria recruit a number of strategies to survive low pH including proton pumps, the protection or repair of macromolecules, cell membrane adaptation, the production of alkali, and the alteration of metabolic pathways [174]. Among those diverse mechanisms, F_1F_0 -ATPase is a universal proton pump widely reported for LAB to generate a physiological proton motive force (PMF) at the expense of ATP [196, 212-213]. The important role of F_1F_0 -ATPase played in the survival of probiotic strains is attracting attention among researchers of the related acid-tolerance studies [180]. Some cross-resistance cases have also been reported [214]. The value of supplying probiotics with metabolisable sugars was therefore emphasized in order to achieve an enhanced survival during passage through the stomach [179].

In human intestines, bile acids contribute to digestion by emulsifying and solubilising fats. The surfactant character of bile acids also enables them to interact with bacterial membrane lipids, thereby conferring a potent antimicrobial property on bile. Due to the less durable structure of their membrane, Gram-positive bacteria (to which most LAB belong) are more sensitive to the bactericidal effect of bile than Gram-negative bacteria [173]. Even within the group of LAB commensals, the diversity concerning bile tolerance is often observed, thus imposing a strict criterion on the selection of successful probiotic strains. In the light of the protective role of lecithin vesicle for preventing bile salt injury to biliary and GI epithelia [215-216], we have applied the flow cytometric analysis to evaluate its potential use for improving the survival of

probiotic bacteria against bile-salt challenge in the previous chapter. In this chapter, the novel application of lecithin vesicles is further investigated in a formula of probiotic microencapsulation.

Orally administered probiotics commonly suffer significant loss of viability and impaired probiotic functions following sequential exposures to the detrimental conditions in the host's GI tract. Therefore, probiotics have to be consumed in large amounts and in a consecutive manner to achieve their successful transient colonisation in the host's gut. To improve efficacy, strategies have been sought to reduce viability loss during the passage in the GI tract. Immobilization in a polysaccharide matrix under mild preparation conditions as a cell-preservation method has been widely applied to tackle this practical issue. Many studies have extensively reviewed this type of technique in regard to encapsulation method and mechanism, property of wall materials, storage stability, etc [77, 217]. The general principle is to establish physical protections to prevent probiotic cells from direct exposure to injurious conditions. Since the emergence of the practice of encapsulating probiotics, a large number of studies have been carried out based on probiotic microcapsules with a size range of millimetres. However, due to the advantages of reduced size, as reviewed in Chapter 2 Section 2.2.2.4, the trend for smaller-sized capsules of less than 100 μm is developing over time. Surprisingly, the reduced size was also reported to weaken the protection provided by the wall matrix that served the role to curb the permeation of stressful factors [218-220]. It was even suggested that the Ca^{2+} -alginate microcapsules, if prepared at a size range of sub-100 μm , showed no noticeable effect in preserving the viability of probiotics against the stresses in the GI tract [219, 221].

Although microcapsules with reduced sizes have been questioned for their ability to protect encapsulated probiotics, we hypothesized that an appropriately designed formula,

which is supplemented with the selected protectants as evaluated in the previous chapter, might overcome the problem. The aims of the study described in this chapter were to assess the protective effect of sub-100 μm microcapsules for the survival of encapsulated probiotics in the simulated GI environments, and to develop and to evaluate the probiotic colonic delivery system based on the sub-100 μm microcapsules reinforced with the selected protectants (*i.e.* metabolisable sugar and lecithin vesicles), which were proposed to promote the survivability of probiotics in the GI tract.

4.2. Materials and methods

4.2.1. Materials

Sodium alginate, chitosan (low molecular weight), maltodextrin, ultrafine calcium carbonate and bile salts (mixture of 50% sodium cholate and 50% sodium deoxycholate) were procured from Sigma-Aldrich (Australia). The fluorescent stains propidium iodide (PI) and carboxyfluorescein di-acetate (cFDA) were procured from Invitrogen Inc (U.S.A). Egg yolk lecithin (>98% phosphatidylcholine) was donated by GMP Pharmaceuticals NZ. The wall material for microencapsulation was prepared according to the encapsulant formula, hereafter termed “FormE”, comprised of 2% (w/v) sodium alginate, 50mM sucrose, 0.5% (w/v) yeast extract, 0.5% (w/v) soluble starch and 20 mM egg yolk lecithin (in the form of unilamellar vesicle; see below for the preparation method). The simulated gastric fluid (SGF), the simulated intestinal fluid (SIF) and lecithin vesicles were prepared following the methods described in the previous chapter.

4.2.2. Strains and culturing conditions

Probiotic strains including *Lactobacillus plantarum* DPC206, *Pediococcus acidilactici* DPC209, *Lactobacillus reuteri* DPC16 and *Bifidobacterium lactis* HN019 were obtained from Bioactives Research New Zealand (BRNZ, New Zealand) culture collection (under accession numbers 006DU, 009DU, 016DP and 002FP respectively), delivered as frozen. These strains were revived anaerobically in deMan-Rogosa-Sharpe (MRS, Difco, USA) broth supplemented with 0.5 g/L cysteine for 36 h at 37 °C. For the microencapsulation preparation, a fresh culture at stationary phase was propagated twice in MRS broth at 37 °C each time for 20 hours. Enumeration was performed by the drop plating technique on MRS agar plate. The inoculated plates were incubated in an anaerobic incubator at 37 °C for 24 hours.

4.2.3. Preparation of microcapsules

The microcapsules entrapping probiotics were prepared through emulsification/internal gelation method primarily adapted from the practice by Larisch et al. [222], with some modifications. Briefly, 10 mL fresh culture of each strain was centrifuged at 5,000 g for 5 min and pellets were washed twice by re-suspending in an equal volume of PBS buffer (pH 7.4). The washed pellets were re-suspended in 10 mL FormE. Ultrafine calcium carbonate powder was added in each suspension at 5% (w/v). After thoroughly vortexing, the mixture was dispersed into 40 mL canola oil (25% internal phase ratio, v/v) containing 2% (w/v) lecithin as the emulsifier by stirring at 800 rpm on a magnetic stirrer. After 15 min emulsification, 10 mL of canola oil containing glacial acetic acid (acid/Ca molar ratio of 3.5) was introduced drop wise into the emulsion. The stirring speed was reduced to 400 rpm and remained for 30 min to allow calcium carbonate to solubilise. Microcapsules were recovered in a separatory funnel (Pyrex[®] 125 mL, Corning Inc., USA) from oil phase by using an acetate buffer supplemented with 15

mM sucrose at pH 5.8, and washed once with this buffer to remove oil residues. Afterwards, the microcapsules were suspended in 40 mL chitosan-coating solution and stored in 4 °C for 3 h to allow adsorption of chitosan polymers. Microcapsules prepared by the same method but using 2% (w/v) alginate alone or using the FormE recipe without lecithin vesicles (for the following bile salt challenge assay) were also prepared for comparison and hereafter termed “AlgC” and “FormE-w/o-lv” respectively.

4.2.4. Particle size analysis

The size distribution of microspheres both before and after coating by chitosan was determined in washing media by laser diffractometry using a Malvern Mastersizer 2000 particle analyser, with a size range from 0.1 to 1000 µm. Measurements were made in triplicate for each batch. Particle size is expressed as volume mean diameter (µm) ± standard deviation.

4.2.5. Challenge of simulated gastric fluid

For each strain, approximately 500 µL (net volume) of wet microcapsules were transferred to PBS buffer, and incubated at 37 °C for 15 min. The microcapsules were then centrifuged at $3,000 \times g$ for 5 min and re-suspended in 5 mL SGF at 37 °C for 2 hours. At interval 0, 1 and 2 hours, 1 mL samples were withdrawn from the SGF solution. The sample pH was neutralized with 0.1 M NaOH. The microcapsules in the sample were spun down and re-suspended in 5 mL 0.2 M sodium citrate solution, in preparation for releasing the entrapped probiotic bacteria and subsequent plating.

4.2.6. Inactivation of the F₁F₀-ATPases of *L. reuteri* DPC16 and *Bf. lactis* HN019 in microcapsules

Two strains were recruited to study the role of F₁F₀-ATPase in acid resistance of encapsulated probiotics. The samples were prepared following Corcoran's method [179] with some modifications. Approximately 500 µL wet FormE microcapsules for each examined strain were suspended in 5 mL 0.25× Ringer's solution, and incubated for 1 h at 37 °C. *N, N'*-Dicyclohexylcarbodiimide (DCCD) (1.4 mM, Sigma, Australia), prepared as an ethanol stock containing 288.86 mg/ml, was added to each sample (250 µg/mL, final concentration) 20 min prior to harvesting by centrifugation. The microcapsule samples were then assayed for the survival in SGF either in the presence or in the absence of 20 mM glucose as described above. The samples in PBS buffer were used as the controls. The fresh culture of each strain was prepared and treated the same way for comparison.

4.2.7. Challenge of bile salt solution

The AlgC, FormE-w/o-lv and FormE microcapsules for each strain were prepared for this study. 1.5 mL wet microcapsules were equivalently distributed in 5 vials each containing 2 mL 0.1% (w/v) peptone with additive bile salts giving a final concentration of 0.0%, 0.2%, 0.4%, 0.8% or 1.2% (w/v) respectively. The vials were kept at 37 °C for 2 hours. Afterwards, all the vials were centrifuged at 3,000 × *g* for 5 min. The supernatants containing bile salts were aspirated and the microcapsules re-suspended in 5 mL PBS buffer. This procedure was repeated to remove bile salt residues. Finally, the microcapsules were suspended in 0.2 M sodium citrate solution, ready for the release and the plating experiments.

4.2.8. Probiotics release from chitosan-coated alginate microcapsules and plate count

In order to release the probiotic bacteria, the treated microcapsules were suspended in 0.2 M sodium citrate and later subjected to an ultrasonic homogenizer at 20 kHz for 30 sec, with a 10-sec rest interval. The samples were kept on ice at all times to avoid heat. Disintegration of the microcapsules and release of bacteria were confirmed using a light microscopy.

4.2.9. Epifluorescent microscopy of bile salt challenged samples

Two fluorescent stains, PI and cFDA, were recruited to probe the membrane permeability and the intracellular enzyme activity respectively, which in combination visualised the viability of probiotics in microcapsules. Approximately 50 μL wet microcapsules were first suspended in 1 ml PBS buffer. 5 μL cFDA working solution was pipetted in and vortexed well. The mixture was kept at 37 °C for 20 min before the microcapsules were harvested by centrifugation at $3,000 \times g$ for 5 min, washed once and re-suspended in PBS buffer. 10 μL PI working solution was added followed by 10-min incubation on ice. Following this, the samples were mounted on an epifluorescent microscope (Leica AF6000 E, Leica microsystems, USA) and photos were taken. The four microcapsule samples embedding *L. reuteri* DPC16 evaluated by this method were: (1) the FormE microcapsules; (2) the alginate microcapsules exposed to 0.4% (w/v) bile salts for 1 hour; (3) the FormE microcapsules exposed to 0.8% (w/v) bile salts for 1 hour; and (4) the FormE microcapsule exposed to 1.2% (w/v) bile salts for 1 hour.

4.2.10. Sequential challenge of SGF and SIF

Approximately 1 mL FormE microcapsules were first challenged by 9 mL SGF supplemented with 20 mM glucose following the method as described above. Viability was estimated at the intervals 0, 1 and 2 hours. Afterwards, the remaining 7 mL SGF

solution was neutralised with 0.1 M NaOH. The remaining FormE microcapsules were then spun down and re-suspended in SIF with volume adjusted to 7 ml. One millilitre of the sample was withdrawn from SIF solution at intervals 1, 3 and 6 hours, when viability was estimated.

4.2.11. *In vitro* release of the microencapsulated *L. reuteri* DPC16 in simulated GI fluids

In order to simulate the release of probiotic bacteria from the delivery system in the GI tract, *L. reuteri* DPC16 was recruited as the model strain and was prepared in the FormE microcapsules. The bacterial concentration was measured as $9.12 \pm 0.02 \log(\text{CFU})/\text{g}$ in the prepared probiotic microcapsules. To simulate the GI conditions, the following releasing media were used in subsequent manner, as listed in Table 4.1.

Table 4.1 Releasing media for the sequential treatments of the probiotic microcapsules in the simulated GI environment.

Treatment Duration	Medium	Corresponding segment in the GI tract
2 h	Simulated gastric fluid (SGF), pH 2.0, with pepsin	Stomach
4 h	Simulated intestinal fluid (SIF), pH 6.8, with pancreatin	Small intestines
8 h	Simulated colonic fluid (SCF), pH 6.5, with faecal enzymes extracted from human faeces	Colon

SGF and SIF were prepared following the descriptions in the previous section except that the pH of SGF was adjusted to 2.0. This elevated pH value reduced the chance of rapid inactivation of released *L. reuteri* DPC16, thus allowing successful enumeration.

The simulated colonic fluid (SCF) was prepared by supplementing faecal water supernatant (containing colonic microfloral enzyme systems for degradation of

polysaccharides) with 8 g/L glucose, 2 g/L yeast extract, 0.5 g/L cysteine and 0.05 g/L bile salts. For comparison, phosphate buffer (50 mM, pH 6.5) with the supplements was used as the modified SCF (mSCF) that lack the colonic microfloral enzyme systems.

The faecal water supernatant was prepared by the following method. Fresh faecal sample was collected from a healthy non-vegetarian, non-smoking male who had no history of GI disease and consumed normal balanced diet. The faecal sample was mixed in phosphate buffer (50 mM, pH 6.5) at a ratio of 1:5 (w/w) and homogenised in a stomacher. The colonic microfloral enzyme systems were isolated by a differential centrifugation technique [223]. First, the faecal solution was centrifuged at $500 \times g$ for 15 min to remove debris. Supernatants were then re-centrifuged at $15,000 \times g$ for another 30 min using an IEC Micromax microcentrifuge (Thermo Electron Corporation, USA) so as to obtain a clear supernatant containing extracellular enzymes, but free of faecal flora. All operations were carried out with controlled temperature around 0-4 °C. The faecal water supernatants were store at -20 °C until further use for preparing SCF.

To profile the releasing behaviour, 5 g probiotic microcapsules were sequentially suspended in the 20 mL of each simulated GI fluid according to Table 4.1. The reactor was kept in the dark at 37 °C with gentle agitation (20 rpm). Every hour, 100 µL of sample was removed from the reactor and the released probiotic bacteria were enumerated on MRS agar. To switch between the simulated GI fluids, first medium was removed after a predetermined time; probiotic microcapsules were gently spun down, washed, and then incubated in next medium.

The count of released bacteria at each time point was expressed as percentage of the total supplied bacteria.

4.2.12. Statistical analysis

All experiments were performed in triplicates. Comparisons between two groups were drawn with Student's independent *t* test. A *P* value of 0.05 or less was taken as significant.

4.3. Results

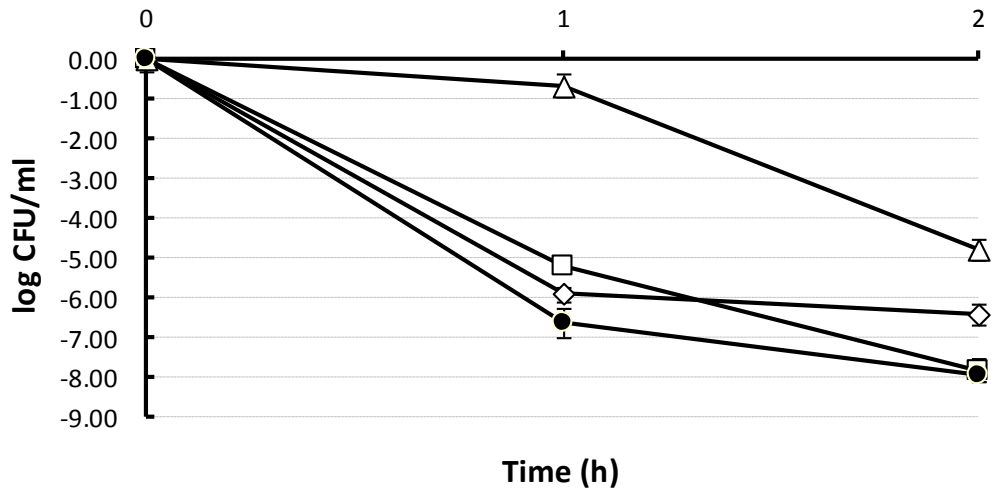
4.3.1. Microcapsule size analysis

The diameter values of the microcapsules were measured before and after coating with chitosan as $74.5 \pm 8.6 \mu\text{m}$ (mean \pm standard deviation) and $76.7 \pm 9.2 \mu\text{m}$, respectively. Therefore, the microcapsules for all the four probiotic strains were considered to be less than $100 \mu\text{m}$, whereas the coating of chitosan did not significantly increase the dimensions ($p > 0.05$).

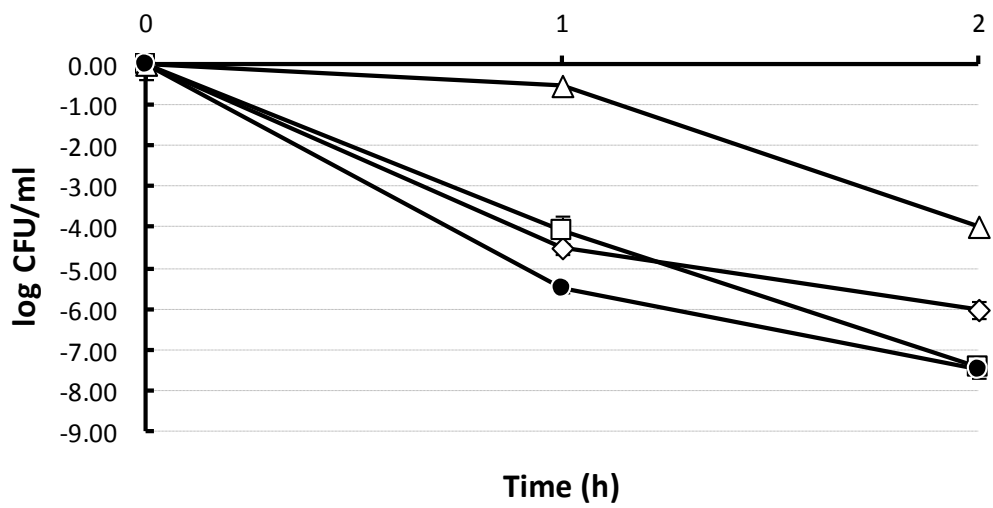
4.3.2. Challenge of simulated gastric fluid

The trends of viability loss of the different strains exposed to SGF are shown in Figure 4.1. Each probiotic strain suffered an accumulated reduction of viability to a different extent over time. The capability of acid resistance varied among the strains. *L. reuteri* DPC16 showed the highest survival and *Bf. lactis* HN09 the least. Encapsulating the probiotics in the AlgC matrix did not exert significantly higher protective effects on any of the four examined strains as compared to the planktonic ones ($p > 0.05$). However, once the extra nutrients (mainly the energy sources, e.g. sucrose) were presented in the matrix formulae, 2 to 3 log-units increase in the viable count could be yielded ($p < 0.01$). Moreover, when the metabolisable sugar (i.e. glucose) was available in SGF, even greater survival rates (up to 6 log increase) were detected among all the examined strains.

(a) Fresh culture



(b) AlgC microcapsules



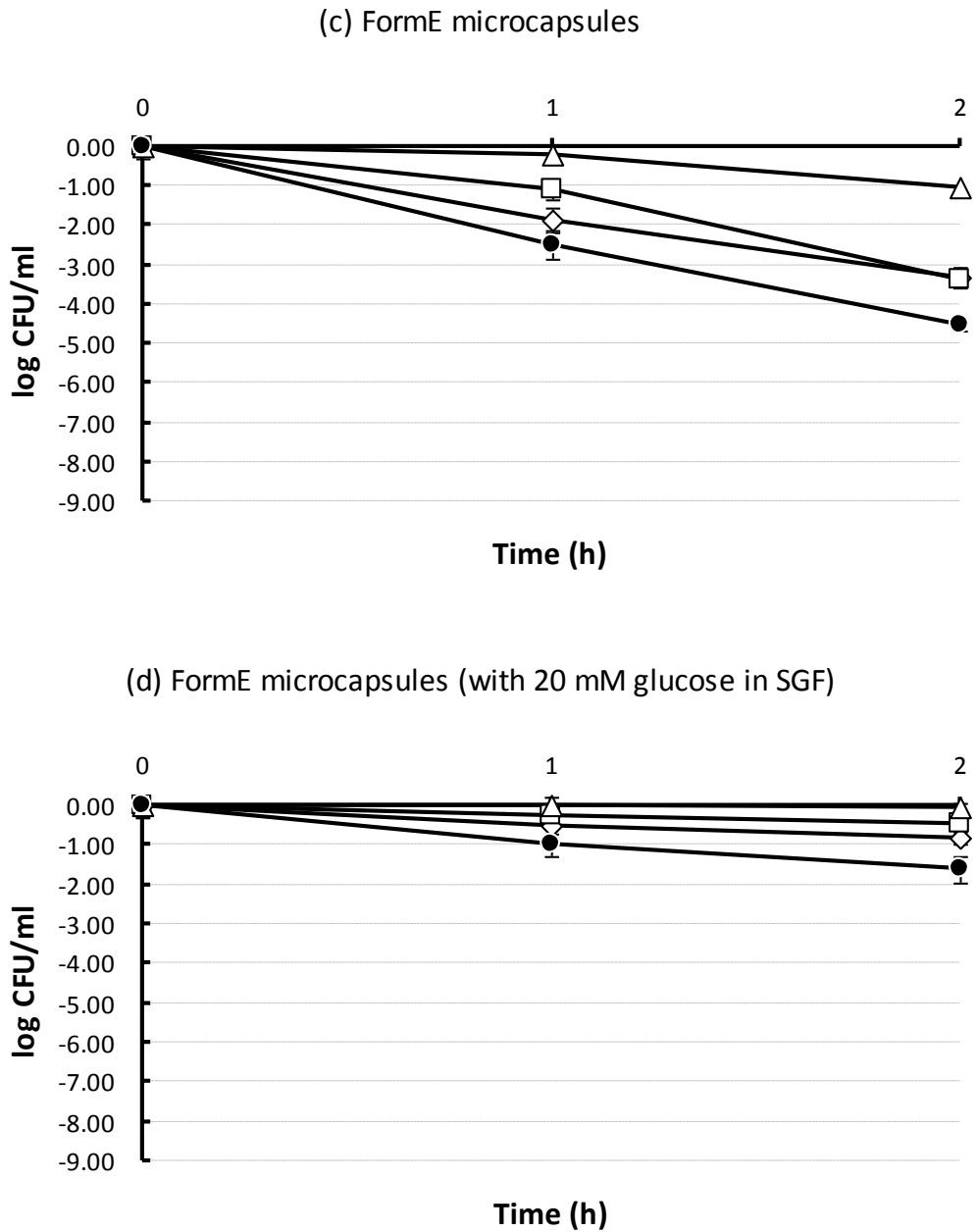
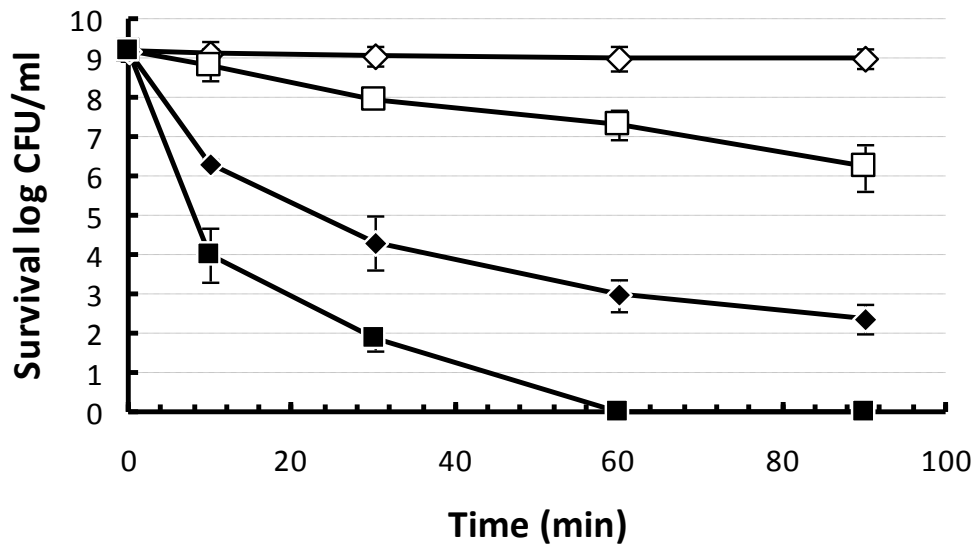


Figure 4.1 Survival of the four probiotic strains (log reduction of CFU count) in SGF, pH 1.2: (a) the non-encapsulated cells, (b) in the AlgC microcapsules, (c) in the FormE microcapsules, and (d) in the FormE microcapsules and SGF supplemented with 20 mM glucose. The symbols represent the different probiotic strains as *P. acidilactici* DPC209 (◇), *L. plantarum* DPC206 (□), *L. reuteri* DPC16 (Δ) and *Bf. lactis* HN019 (●). The data are the means of triplicate experiments, and the error bars indicate standard deviations.

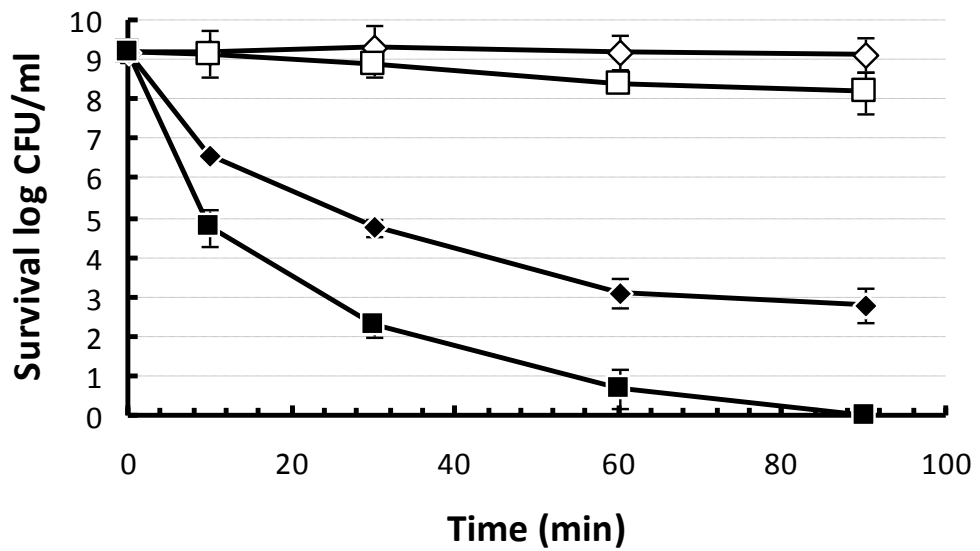
4.3.3. F₁F₀-ATPase inhibitor treatment

In order to evaluate the significance of the membrane-bound F₁F₀-ATPase complex for probiotics to survive acid stress in the scenario of microencapsulation, we added the inhibitory DCCD to the samples of two strains: *L. reuteri* DPC16 and *Bf. lactis* HN019, and studied their consequent survival patterns in SGF. As shown in Figure 4.2, the treatment with DCCD substantially impacted the survival of both strains either with or without the ambient presence of glucose. Although microencapsulating probiotics in polysaccharide matrix retarded the damage by low pH, the protective effect of the metabolisable sugars either in the microcapsules or in the environment was deprived by the addition of DCCD in that no viable bacteria were detected after 90 min incubation. However, the non-encapsulated bacteria of both strains were killed faster than the ones in the microcapsules.

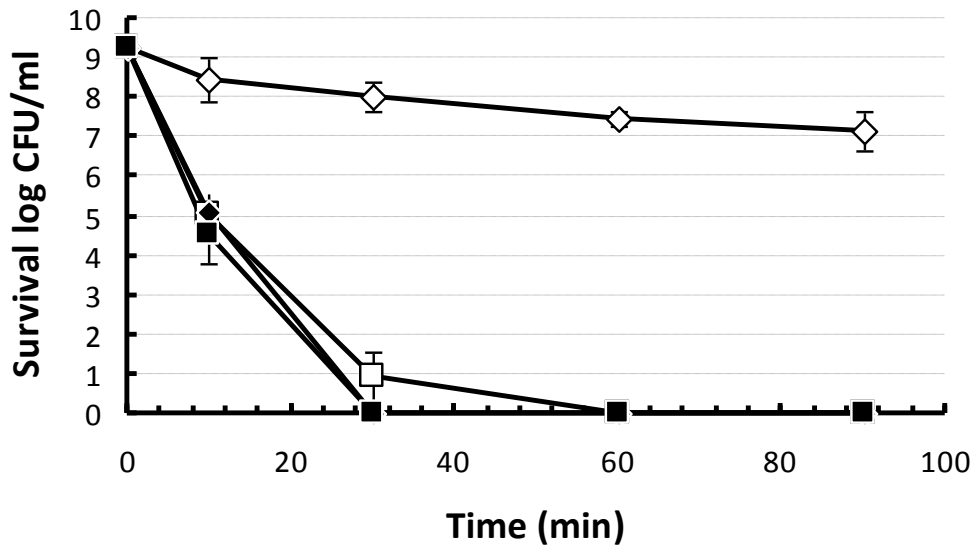
(a) *L. reuteri* DPC16 fresh culture



(b) *L. reuteri* DPC16 in FormE microcapsules



(c) *Bf. lactis* HN019 fresh culture



(d) *Bf. lactis* HN019 in FormE microcapsules

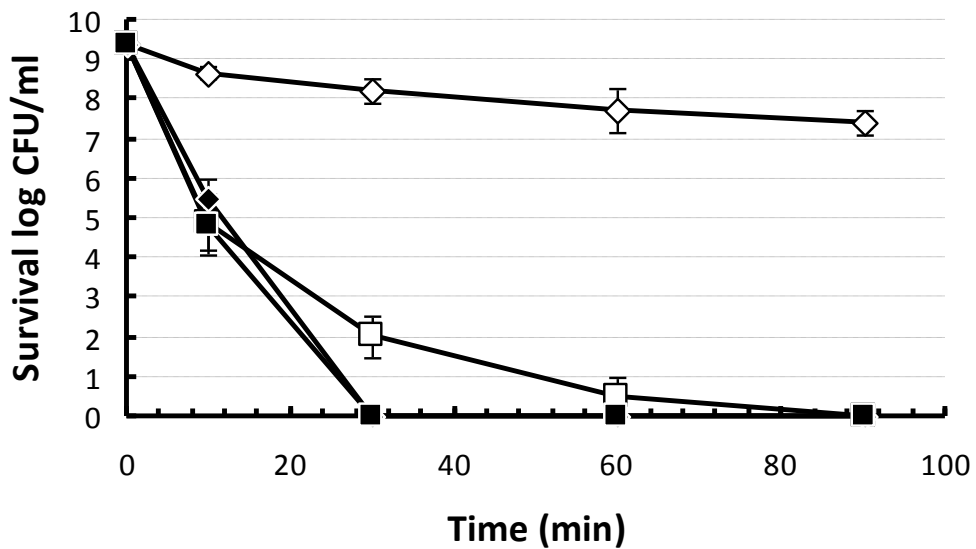


Figure 4.2 Survival of the two probiotic strains *L. reuteri* DPC16 and *Bf. lactis* HN019 in SGF: (a) *L. reuteri* DPC16 fresh culture, (b) *L. reuteri* DPC16 in FormE microcapsules, (c) *Bf. lactis* HN019 fresh culture, and (d) *Bf. lactis* HN019 in FormE microcapsules. The symbols represent the different treatment conditions of: no treatment with DCCD and in the SGF with 20 mM glucose (\diamond), prior treatment with DCCD and in the SGF with 20 mM glucose (\square), no treatment with DCCD and in the SGF without glucose (\blacklozenge) and prior treatment with DCCD and in the SGF without glucose (\blacksquare).

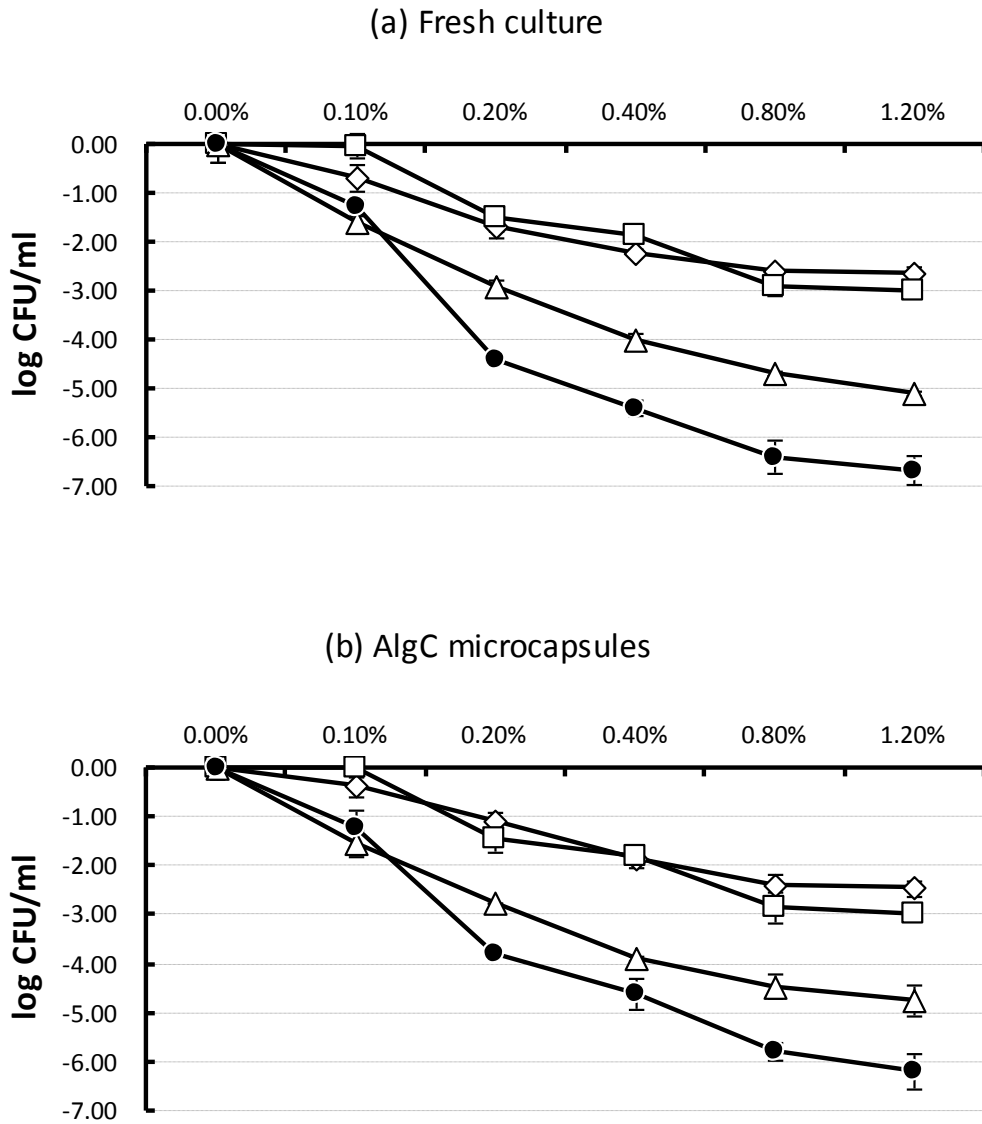
4.3.4. Challenge of bile salt solution and epi-fluorescent microscopic observation

All four examined probiotic strains appeared to be sensitive to bile salts at concentrations higher than 0.1% (w/v). The viability loss showed a bile-salt-concentration dependant pattern. The largest drop occurred at the bile salt concentrations from 0.2% to 0.4% (w/v). *Bf. lactis* HN019 suffered most loss from the bile salt challenge in that a more than 6 log drop in viable count was detected in the extreme case of concentrations above 0.8% (w/v). *L. reuteri* DPC16 only ranked third among the total four strains considering its performance of bile-salt tolerance.

In order to diminish the detrimental impact of bile salts to the probiotics, especially at high concentrations, lecithin vesicles as the protectant were embedded in the microcapsules. As shown in Figure 4.3(d), lecithin vesicles substantially increased the survival of the probiotics in the presence of bile salts, especially at concentrations above 0.2% ($p < 0.01$), as compared to the minor protection conferred by encapsulating probiotics in the AlgC microcapsules (Figure 4.3(c)). Except for the most sensitive strain HN019, the viability loss of all the other three strains could be limited to less than one log unit in the aforementioned 0.2%-0.4% (w/v) range. At extreme bile salt concentrations ($>0.8\%$), a 2-to-3 log increase of viability could be achieved by the FormE microcapsules as compared to the other samples either non-encapsulated or encapsulated without this particular protectant.

In order to rule out the protective effect of other components in the FormE composition against bile salt challenge, the FormE-w/o-lv microcapsules (following the FormE composition but without adding lecithin vesicles) were prepared. Their performance is illustrated in Figure 4.3(c). A slight protective effect was observed on *P. acidilactici* DPC209 and *Bf. lactis* HN019 by this FormE-w/o-lv microencapsulation at the elevated bile salt concentrations above 0.4% ($p < 0.05$), as compared to the non-encapsulated

samples. However, once the lecithin vesicles were present, significant increases in viable counts could be observed in all the four strains ($p < 0.05$). It therefore justified the key contribution of lecithin vesicles for the protection on the probiotics against bile salt challenges.



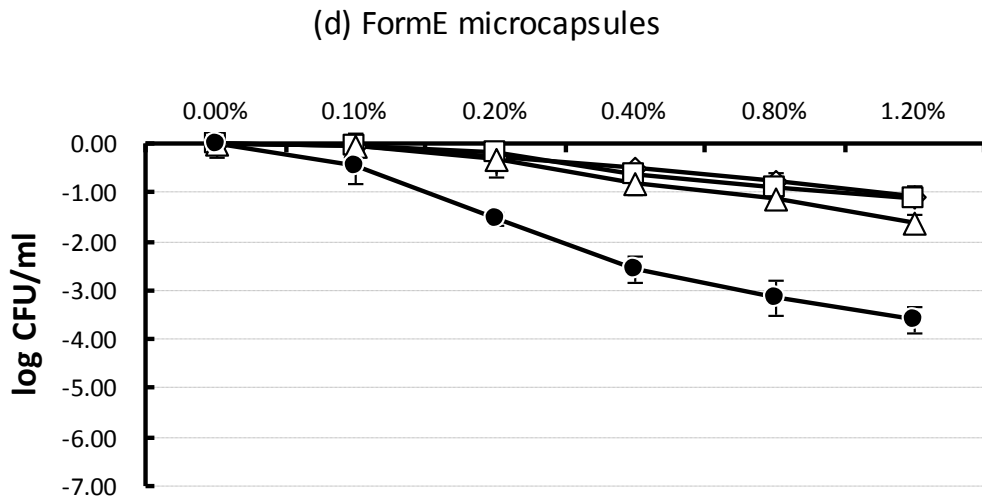
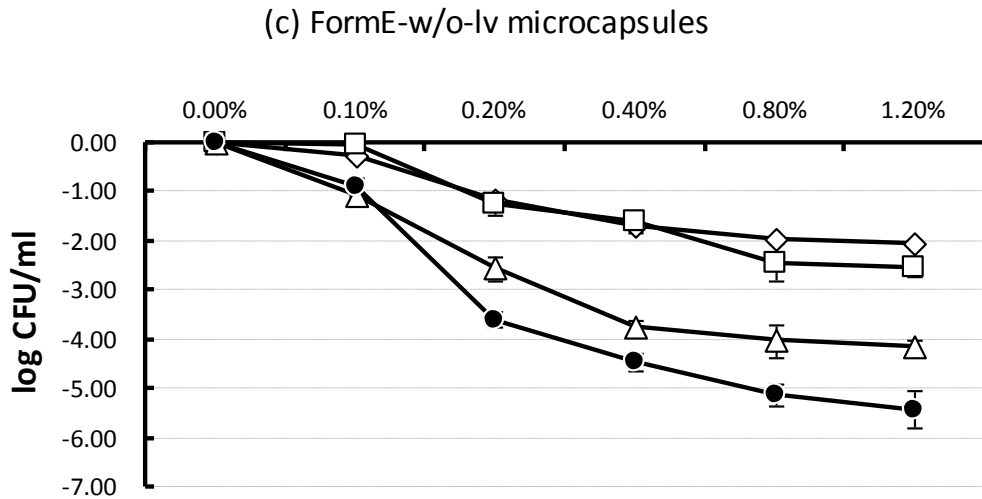


Figure 4.3 Survival of the four probiotic strains (log reduction of CFU count) challenged by bile salt solution with a concentration ranging from 0.0% to 1.2% (w/v): (a) the non-encapsulated cells, (b) in the AlgC microcapsules, (c) in the FormE-w/o-lv microcapsules and (d) in the FormE microcapsules. The symbols represent the different probiotic strains as *P. acidilactici* DPC209 (◇), *L. plantarum* DPC206 (□), *L. reuteri* DPC16 (△) and *Bf. lactis* HN019 (●). The data are the means of triplicate experiments, and the error bars indicate standard deviations.

Further to the above evaluation by plate count, the fluorescent microscopic technique in combination with two probes – PI and cFDA was also utilised to visually evaluate the health status of the bile-salt-stressed probiotics in the microcapsules. Figure 4.4 illustrates four *L. reuteri* DPC16 samples treated under different conditions. The coloured dots represent single probiotic DPC16 bacteria stained by PI and cFDA. Compared to the non-stressed sample (Figure 4.4(a)), the permeation of plasma membrane of single bacterium indicated by the red fluorescence of DNA-bound PI is clearly shown in the AlgC sample treated with 0.4% bile salts (Figure 4.4(b)). Also missing is the presence of the green fluorescence of carboxyfluorescein (cF), which indicates that the intracellular enzymes could not function adequately to release the cF from the probe cFDA. In the case of the FormE microcapsules treated with the same concentration of bile salts (Figure 4.4(c)), a marked portion of the viable DPC16 bacteria could be observed. Even at the elevated bile salt concentration of 0.8% (Figure 4.4(d)), the fluorescent staining results still revealed a discernible protection conferred by the FormE composition.

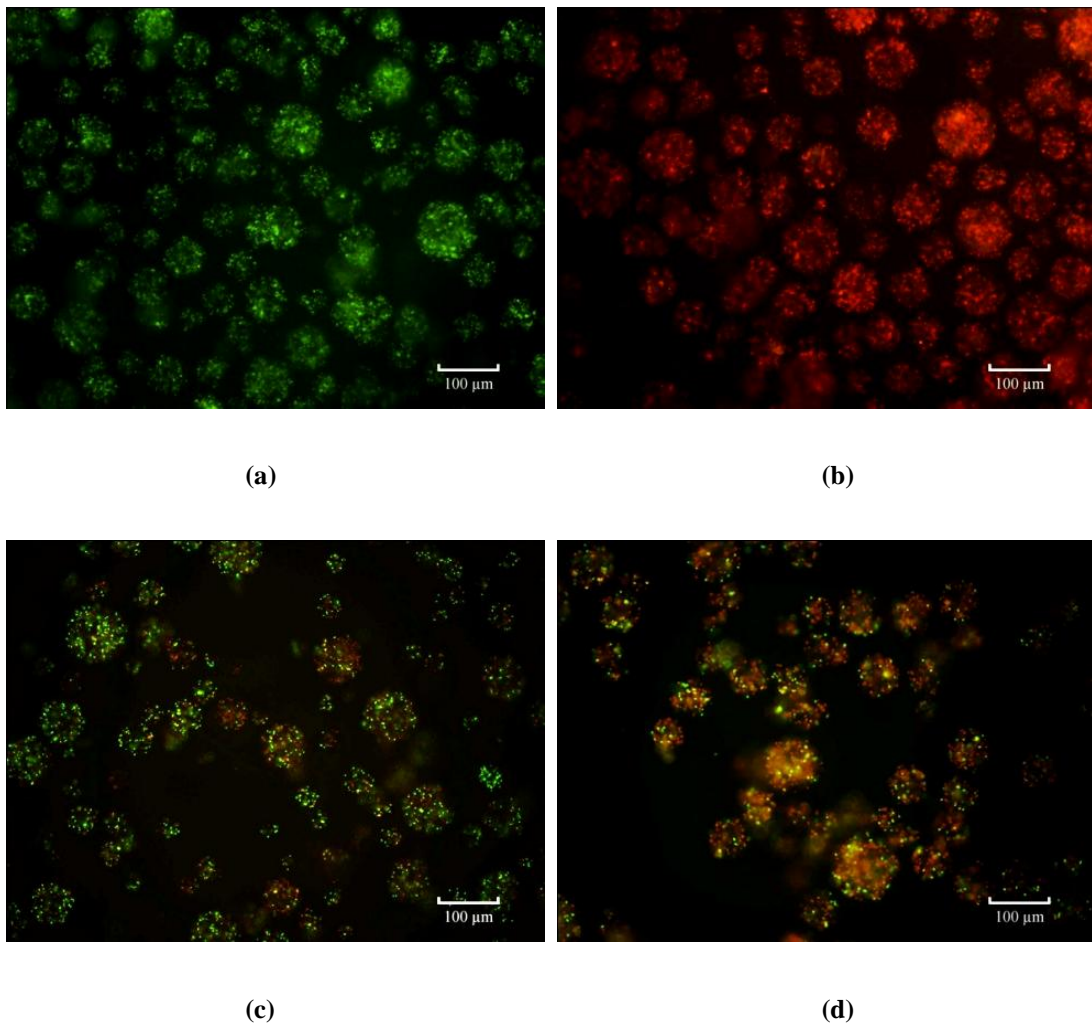


Figure 4.4 Epi-fluorescent microscopy of the microencapsulated *L. reuteri* DPC16 stained by PI (red: dead) and cFDA (green: viable) after the 2-h treatment with (a) the AlgC microcapsules suspended in PBS buffer; (b) the AlgC microcapsules suspended in 0.4% bile salt solution; (c) the FormE microcapsules suspended in 0.4% bile salt solution; and (d) the FormE microcapsules suspended in 0.8% bile salt solution. (The scale bars indicate a length of 100 μm .)

4.3.5. Sequential challenge of SGF and SIF

Survival of the four probiotic strains, either free or in the FormE microcapsules after 2 h in SGF, followed by 6 h incubation in SIF, is shown in Figure 4.5. When glucose was readily available to probiotics in SGF, three out of the four strains suffered only around 1 log drop in viable count, whereas the most vulnerable *Bf. lactis* HN019 fell by 2 log units. The microencapsulation did not show any further protection on the probiotics in SGF supplemented with 20 mM glucose ($p > 0.05$).

Nevertheless, divergence occurred between the free and the encapsulated probiotics after transferring them into SIF containing bile salts. Significantly higher viable counts were observed for all the four strains in the FormE microcapsules after the first hour in SIF when compared to those had no protection ($p < 0.05$). The probiotics in the FormE microcapsules suffered a slight drop after 1 h in SIF while the free probiotics lost their viability constantly, thus presenting an even larger difference by the end of 8 h incubation in SIF ($p < 0.01$). Overall, the microencapsulation with reinforced energy supply and lecithin vesicles markedly reduced the viability loss of the probiotics exposed to the simulated GI fluids.

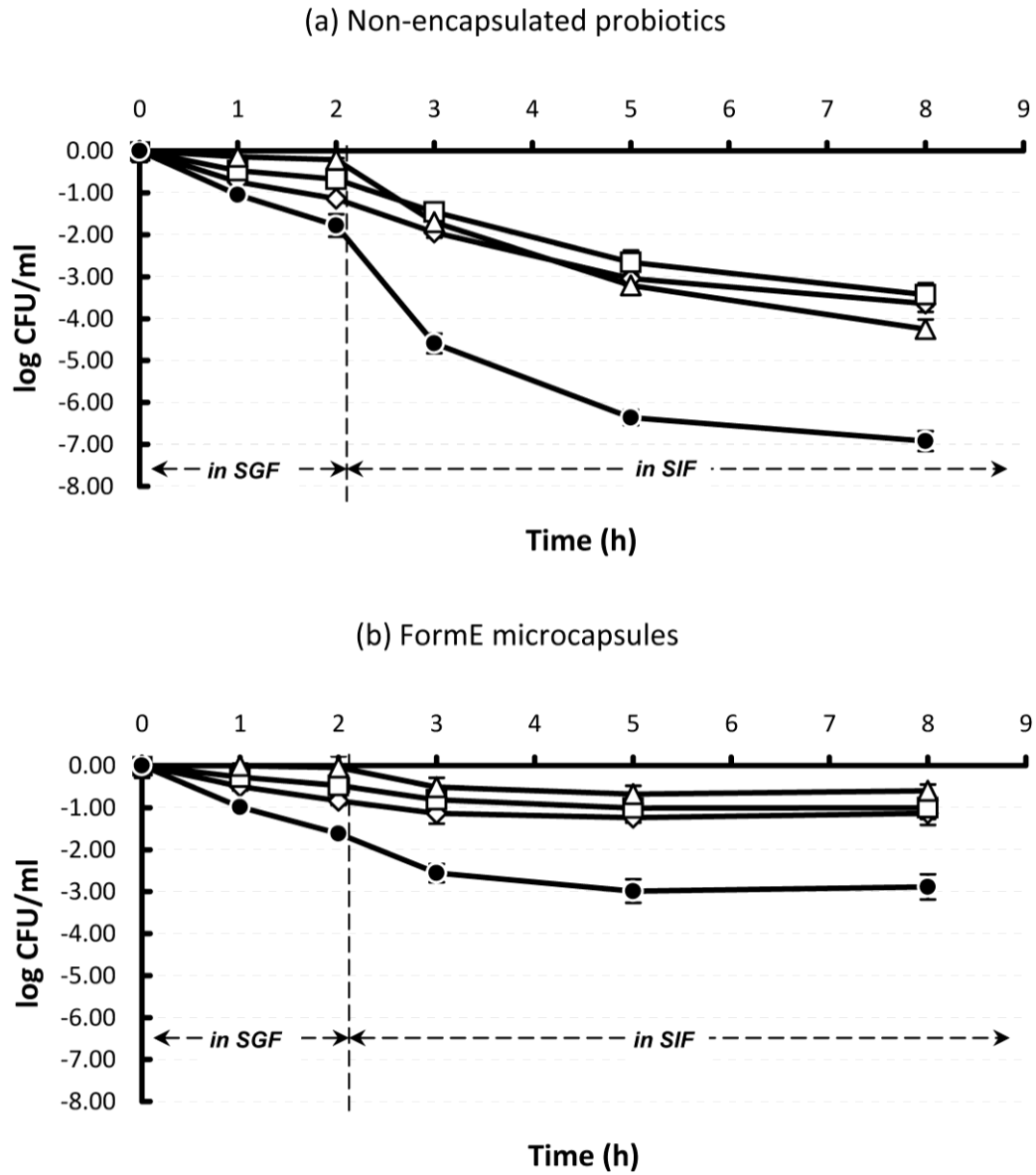


Figure 4.5 Survival of the four probiotic strains (log reduction of CFU count) subjected to a sequential challenge of SGF (with 20 mM glucose) and SIF. (a) The non-encapsulated probiotics or (b) the probiotics in the FormE microcapsules. The symbols represent the different probiotic strains as *P. acidilactici* DPC209 (◇), *L. plantarum* DPC206 (□), *L. reuteri* DPC16 (Δ) and *Bf. lactis* HN019 (●). The data are the means of triplicate experiments, and the error bars indicate standard deviations.

4.3.6. *In vitro* release of the microencapsulated *L. reuteri* DPC16 in simulated GI fluids

To evaluate the release of immobilized probiotic bacteria from the probiotic colonic delivery system, the microcapsules entrapping the model strain *L. reuteri* DPC16 were sequentially exposed to the simulated GI fluids. The exposure durations were controlled at 2 h, 4 h and 8 h for SGF, SIF and SCF, respectively, in order to mimic the *in vivo* transient periods in the corresponding segments of the GI tract. The hourly enumerations of the released *L. reuteri* DPC16 were plotted in Figure 4.6.

The results indicated that the release of immobilized bacteria from this delivery system was very limited in SGF and SIF. Only less than 5% of the immobilized *L. reuteri* DPC16 were enumerated in the medium after the consecutive exposures of 2-h in SGF and 4-h in SIF. The releasing of this stage was considered to be partly due to the non-specific degradation of the chitosan-alginate matrix by the digestive enzymes (i.e., pepsin and pancreatin) [224].

After the probiotic microcapsules were transferred into SCF containing colonic microfloral enzyme systems, a rapid release of the immobilized *L. reuteri* DPC16 occurred along with gradual disintegration of the microcapsules. The release continued before the end of the observation, by when more than 85% of the immobilized *L. reuteri* DPC16 were enumerated in the medium. In contrast, the mSCF treatment did not give such a rapid release. By the end of the examination, the slow release only achieved approximately 10% of the total immobilized bacteria. The difference was attributed to the absence of the colonic microfloral enzyme systems in mSCF.

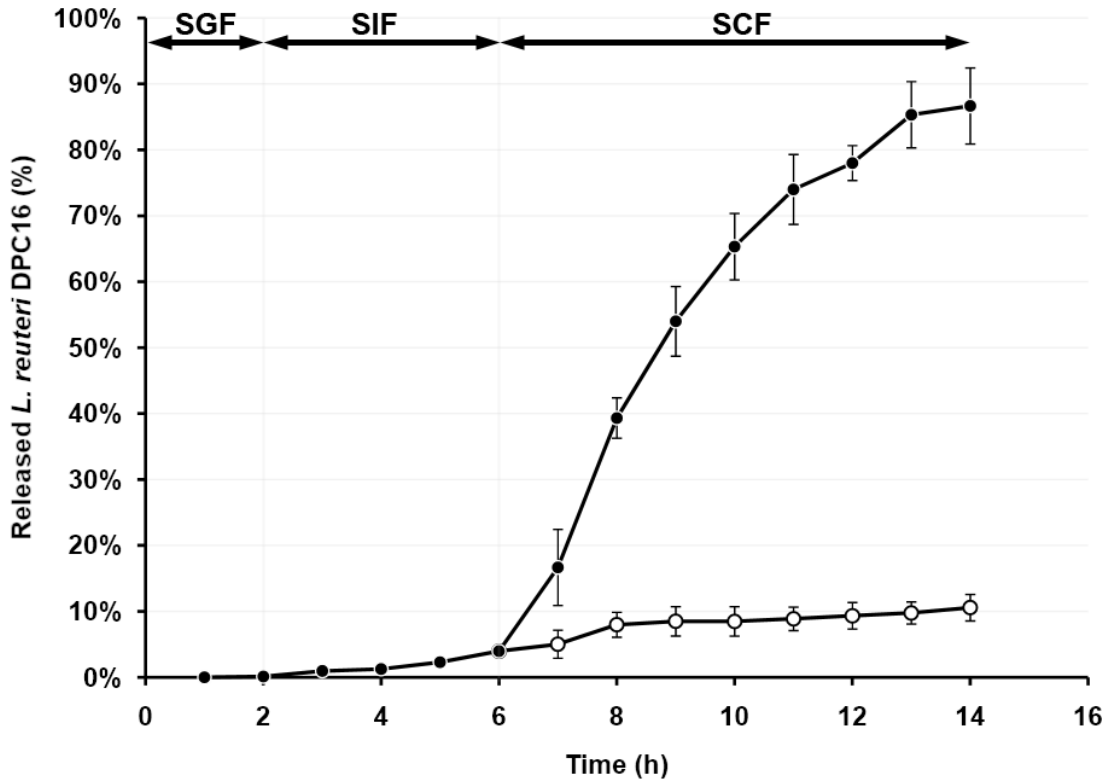


Figure 4.6 *In vitro* release of *L. reuteri* DPC16 from the probiotic colonic delivery system. The samples were sequentially incubated in the simulated gastric fluid (SGF) pH 2.0 for 2 hours, in the simulated intestinal fluid (SIF) pH 6.8 for 4 hours, and in the simulated colonic fluid (SCF) pH 6.5 for 8 hours. The symbol (●) represents the release from the colonic delivery system suspended in SCF containing the extracted colonic microfloral enzyme systems for degradation of polysaccharides, whereas the symbol (○) represents the release in the absence of the enzyme systems.

4.4. Discussion

Alginate-based microcapsules have been widely used as a vehicle for probiotics preservation and *in vivo* delivery. However, in the present study, only a minor protective effect was observed when the alginate microcapsules prepared at a size range of sub-100 μm were exposed to the challenges of simulated GI environments. By the end of the 2-h treatment, no significant differences could be observed between the non-encapsulated and the encapsulated samples ($p > 0.05$). This result agreed with the other studies which suggested that the microcapsule of larger size was more likely to retard the ingress of environmental stress factors [218, 225]. Nevertheless, it should not be ignored that there was a slight but noticeable protection conferred by microencapsulation at the early stage of the SGF challenge. Compared to the groups of free cells, three out of the four probiotic strains encapsulated in the ArgC microcapsules showed an average 1-log increase in viable count ($p < 0.05$) at the 1 h time point (except for *L. reuteri* DPC16), possibly due to the active exclusion of the macromolecules of pepsin by the chitosan-coated alginate matrix. However, unrestrained influx of excessive protons finally overwhelmed this positive effect over time.

Owing to the effect of macromolecules exclusion, the chitosan-alginate based microencapsulation has been widely applied to the enhanced gastric passage of acid-labile proteins. In a study on the intestinal delivery of egg yolk immunoglobulin (IgY), this type of polymer vehicle was reported to successfully protect the encapsulated proteins from the *in vitro* gastric peptic hydrolysis as a direct outcome of preventing direct contact of the IgY proteins and the digestive enzymes [226]. In addition, the authors also observed an effect of reduced acid damage achieved by this type of microcapsules. However, despite the positive comment on the acid protection of their microcapsules, a noteworthy difference between their preparation and ours was that

their capsules were made at a size of 1 mm. In contrast, ours were less than 100 μm . This distinct difference explained why the microcapsules in the present study showed a limited effect in retarding the permeation of protons.

Interestingly, the size of sub-100 μm conferred a distinct feature on the microcapsules. After being coated with chitosan, the microcapsules were found to be more resistant to erosion by SGF and SIF by retaining a much longer visual integrity. Visual evaluation further revealed a limited swelling in response to a wide change of environmental pH. This alteration was attributed to the increased occurrence of the adsorption of chitosan onto alginate cores, owing to the greatly expanded total surface area of the tiny microcapsules. A similar finding of the chitosan coating on the sub-100 μm microcapsules was reported by Silva et al. [227], which was utilized to produce a slow release of the protein agents in intestines. It is reasonable to believe that this feature may also be useful for the targeted delivery of probiotics to the colon. Additionally, another potential advantage of reduced size is that the enlarged total surface area can also be exploited to provide an improved chance of mucoadhesion, thereby achieving a prolonged retention in the consistently motile GI tract.

The energy-dependent mechanisms of acid tolerance among the LAB species are universally reported, which supports the addition of the metabolisable sugars in the microencapsulation formula. The F_1F_0 -ATPase is a well-described multiunit proton pump, commonly found possessed by LAB species to eliminate overabundant protons at the consumption of ATP. However, with the challenge of gastric acid stimulating the ATP consumption, the insufficient energy supply may undermine this housekeeping function. The essential role of F_1F_0 -ATPases in maintaining the viability of probiotics against a low pH challenge was evidenced in my studies by the sucrose-reinforced microencapsulation intervened by DCCD (an F_1F_0 -ATPase inhibitor, covalent

modifying the Glu 54 residue of the c subunit and hence preventing proton translocation [179, 228]). The presence of metabolisable sugars in the wall matrix significantly increased the survival of the probiotic LAB at the end of the 2-h treatment ($p < 0.01$), providing an average 3-log improvement among all the four examined strains. To confirm the essential role of F_1F_0 -ATPases, a prior treatment of two probiotic strains with DCCD was demonstrated to deeply impact this palliative effect of sucrose due to the specifically-induced malfunction of membrane-bound F_1F_0 -ATPases.

However, by comparing the responses of *L. reuteri* DPC16 and *Bf. lactis* HN019 in the DCCD treatment assay, it also suggested possible diversity of acid-tolerance strategies among strains. The F_1F_0 -ATPase was found to only partially account for the DPC16 strain's survival of a low pH environment in that the DCCD treatment did not annihilate the DPC16 population after the 90 min exposure to SGF. The energy supply may have facilitated some other strategies of this strain in addition to F_1F_0 -ATPase proton pump, to deal with the presence of overabundant protons. By contrast, once deprived of F_1F_0 -ATPases, the HN019 population completely lost their viability much faster in all the corresponding groups, thus indicating the pivotal role of F_1F_0 -ATPase for this strain. Besides the strain-specific divergence, it is noteworthy that without the normal function of F_1F_0 -ATPases, the encapsulation in either the FormE or the AlgC microcapsules was not able to further enhance the survival of the examined probiotics in SGF compared to the non-encapsulated bacteria ($p > 0.05$).

In the current study, lecithin vesicle was successfully incorporated in the probiotic delivery system and compensated the impaired protection against bile salts when the vehicle microcapsules were prepared at a decreased size range. As a direct outcome of this application, the oral dosage of probiotics could be reduced while the requirement on minimal viable count can still be met after the delivery vehicles reach the host's colon.

On the other hand, this application may also be utilised to alleviate the strict requirement for bile tolerance in terms of selection of probiotic strains.

The fluorescent technique utilised in this study to visualise the damage to the probiotics in the microcapsules was also proved competent. This technique allows an instant evaluation on the performance of a microencapsulation formula. From my experiences, it proved to be indicative especially at the early formulation stage. The fluorescent probing technique has been demonstrated in the previous chapter to be successfully combined with flow cytometry (FCM), to perform the detailed and quantitative analysis.

In the current study, although the presence of the protectants promoted a significantly higher survival rate of the probiotics, the strain-specific variance still occurred and was responsible for the final viability. For each challenge assay in this study, the order of stress-resistance of all the four examined strains remained unaltered either with or without the protectants. Protectants for probiotics may take effect either by directly strengthening cellular shock-responses (e.g. in the case of sucrose) or by indirectly relieving environmental stress factors (e.g. lecithin vesicles). However, it is particular strains with diversity of intrinsic traits that take advantage of the positive protections to diverse extents. The results still emphasize the necessity of strain selection in the development of probiotic products, even with appropriate delivery strategies available.

The result of the *in vitro* release of the immobilized probiotic bacteria from the delivery system indicated that the current design of probiotic microcapsule could readily respond to the colonic microbiota-triggered release. It therefore suggests a reasonable application of this type of microcapsules for the colonic delivery of probiotic bacteria. The colonic microfloral enzyme systems prepared in the current study were majorly consisted of extracellular enzymes of the colonic microflora rather than cell-associated enzymes. It has been reported that the degradation efficiency of cell-associated enzyme

is comparatively lower than extracellular enzymes [229]. It may justify the exclusion of cell-associated enzymes in the current study. However, considering the huge number of microorganisms in human microbiota, cell-associated enzymes may still contribute a powerful release-triggering mechanism. It may alter the *in vivo* releasing behaviour of the delivery system, mostly resulting in a more rapid and complete breakdown of polysaccharide matrix, which is worth of future investigations.

In conclusion, when the size of microcapsules falls below 100 μm , the protection to probiotics by the polymer-matrix becomes weak, presumably due to the significantly decreased space which fails to curb or retard the permeation of stress factors. However in the current study, all the examined probiotic strains encapsulated in the sub-100 μm microcapsules greatly benefited from metabolisable sugar and lecithin vesicles which had been incorporated in the microencapsulation formula. The results clearly suggest that sub-100 μm microcapsules can still serve as a competent vehicle for the delivery of probiotics, as long as suitable protectants are present in the wall matrix. It is also noteworthy that the novel use of lecithin vesicles proved to effectively protect the probiotics from disruption by bile acids, indicating a high potential for commercial use.

Chapter 5. Evaluation of the storage stability of freeze-dried probiotic bacteria in the probiotic delivery system, and the inhibitory effect on food-borne pathogens

Following the previous demonstration of the GI protective effect of the probiotic delivery system, this chapter describes the assessment of storage stability of freeze-dried probiotic bacteria in the probiotic delivery system, and the prediction of ambient shelf-life by an accelerated storage test. On the other hand, in order to surrogate any potential change of the probiotic effects caused by the microencapsulation, *L. reuteri* DPC16 was recruited for the comparison between the planktonic and the microencapsulated forms, in terms of the inhibition of food-borne pathogens and the production of its distinctive antimicrobial agent – reuterin.

5.1. Introduction

Probiotics preserved in dried form are preferred for enhanced operational convenience by both consumers and manufacturers [106]. However, their viability during drying process and subsequent storage were reported to be affected by a variety of factors, such as the choice of drying technique, the addition of stabilizers, the presence of ambient polymeric matrixes, etc [230-231]. Although encapsulation has been reported to improve the survival of some LAB strains during drying and following storage [78], inappropriately designed formulae may adversely affect the storage stability and impair the survival of probiotic bacteria [232-233]. Therefore, it is necessary to investigate the

influence of immobilization in the designed probiotic delivery system during prolonged storage.

Since the first reported examples on lactobacilli back in 1970s [234-235], accelerated storage tests have been utilized to quickly and objectively determine the stability of freeze-dried suspensions of lactic acid bacteria (LAB). Based on isothermal kinetics, survival of LAB observed at higher temperatures is used to extrapolate to shelf life at lower storage temperatures. In addition to the shelf-life prediction, such tests have also been performed by some researchers to assess the influence of processing and environmental factors (e.g. water activity, suspension medium, stabilizing additive, and immobilization) that may affect the storage stability of LAB [236-238]. Therefore, in the current study, in order to transcend the limitation of time constraints, we applied this method to evaluate the storage stability of probiotic bacteria in the microcapsule-based delivery system.

Oral administration of probiotic bacteria has been reported to antagonize competing food-borne pathogens and to reduce or prevent specific infectious diseases of the gastrointestinal (GI) tract [239]. The inhibitory mechanisms by probiotics have been proposed in a variety of aspects, including competitive exclusion by competition for binding site, direct production of bacteriocins or inhibitors, modulation of the host's immune responses [240]. However, the host's bio-barriers, such as gastric acidity and bile acids, inevitably challenge the survival of probiotic bacteria and impair their therapeutic functions. To provide extended protection, probiotics are commonly immobilized in polymer matrices [77]. Despite the obvious advantage of increased survival and processing convenience, immobilization may also exert uncertain influence toward preferred probiotic effects. Muthukumarasamy and Holley [241] reported a reduced inhibitory action of the encapsulated *Lactobacillus reuteri* and *Bifidobacterium*

longum against *Escherichia coli* O157:H7 as compared to the non-encapsulated strains. In another study, Brachkova *et al.* [242] suggested that antimicrobial performance of encapsulated probiotic bacteria could be varied with culturing environment, encapsulating protocol and strain. These findings indicate that verification of probiotic effects should be carried out for specific immobilization practices of probiotic strains.

5.2. Materials and methods

5.2.1. Strains and culturing conditions

The probiotic strains *L. reuteri* DPC16 (NZRM#4294) and *L. plantarum* DPC206, and the pathogenic strains: *Salmonella enterica* serovar Typhimurium (ATCC#14028), *E. coli* O157:H7 strain 2988 (ATCC#35150) were provided by Bioactives Research New Zealand (BRNZ, New Zealand). The probiotic strains were anaerobically cultured in deMan-Rogosa-Sharpe (MRS, Difco, USA) broth supplemented with cysteine (0.5 g/L) for 18 h at 37 °C and was counted using MRS agar plate. The pathogenic strains were enriched with Brain Heart Infusion (BHI, BBL, USA) broth, purified with cefixime-tellurite supplemented sorbitol MacConkey (CT-SMAC, Merck, Germany) agar for *E. coli* O157:H7 and xylose lysine deoxycholate (XLD, Oxoid, England) agar for *S. typhimurium*, and counted using MacConkey (Merck, Germany) agar plates aerobically at 37 °C for 24 hours.

5.2.2. Immobilization of the model strains in the probiotic delivery system

Immobilization of the model strains in the probiotic delivery system followed the method described in the previous chapter. The chitosan-coated alginate microcapsules were then recovered by centrifugation, washed with 0.85% (w/v) saline. All procedures were performed under sterile condition.

5.2.3. Production and freeze-drying

Owing to the reported cryo-protective effects and its wide use as the carrier-base for probiotic products, skim milk powder (SMP) was also included for the evaluation of storage stability of the probiotic strains embedded in the microcapsule system.

Two probiotic strains with diverse sensitivity to freeze-drying, i.e. *L. reuteri* DPC16 and *L. plantarum* DPC206, were recruited for this test. Free and microencapsulated cells were suspended either in a control medium containing 2.5% (w/v) fructooligosaccharide (FOS, Sigma, USA) and 2.5% (w/v) lactose (Sigma, USA), or in SMP solution containing 5% (w/v) non-fat skim milk powder (PAMS, New Zealand). The suspensions were deep-frozen at -20 °C for 2 h and at -80 °C overnight, then freeze-dried with FreeZone freeze-dry system (Labconco, USA) at -55 °C under 0.13 mbar for 36 hours. The freeze-dried samples were stored at -80 °C prior to further test.

At the end of freeze-drying, the water activity of all the samples was assayed by an AquaLab 3TE water activity meter (Decagon Devices, USA) to be around 0.13 ± 0.01 .

5.2.4. Accelerated storage test

The freeze-dried samples were dispensed in aluminium foil packets that were vacuum sealed. Accelerated storage test was carried out at 55 °C, 35 °C and 25 °C. At 55 °C, samples were removed at 4-h intervals from 0 to 16 h of exposure; at 35 °C, samples were removed every 48-h from 0 to 192 h; at 25 °C, samples were removed every 120-h from 0 to 480 h. Samples were rehydrated with MRS broth. Microencapsulated bacteria were released, following the previously described method.

During the storage in vacuum package, the water activity of all the freeze-dried samples is considered to remain low and stable.

5.2.5. Kinetics parameters of thermal inactivation

The experimental data at 25 °C, 35 °C and 55 °C were fitted to the kinetic model of thermal inactivation of freeze-dried LAB described previously [234, 236, 243].

Briefly, thermal death of freeze-dried suspensions of LAB was treated as a first-order reaction, i.e.

$$\log N_0 - \log N = \frac{1}{D}t,$$

where N_0 is the initial number of viable bacteria, N is the residual number of viable bacteria after a period t , D is the temperature-dependant kinetic parameter, which numerically equals to the time (in the unit of hours) required for a decimal reduction (1-log drop) in viability to take place. With larger D -values, freeze-dried probiotic bacteria appear to be more stable during storage.

The time-dependant kinetic parameter can also be expressed as a k value, also termed rate constant (specific to certain storage condition) [244]. The k values were calculated from D values following

$$k = \frac{\ln 10}{D}.$$

The k values were further used to relate the reduction rate to the storage temperature.

The effect of temperatures on the reaction rate is derived from the Arrhenius equation,

$$\log k_0 - \log k = \frac{E_a}{R} \cdot \frac{1}{T},$$

where k_0 is an experimental constant that is termed frequency factor, T is the absolute temperature, R is the gas constant and E_a is the energy of activation [245-246]. In such case, $\log k$ follows a linear relation with reciprocal T . The previously calculated k -

values at specific temperatures were applied to obtain the model, which was subsequently used to predict the inactivation kinetic parameters of the probiotic bacteria (e.g. *D* value) at other temperatures (i.e. 4 °C and 20 °C).

To validate the acquired predicting model, the dried samples were also placed at 20 °C, and the numbers of survived probiotic bacteria were determined every week for 11 consecutive weeks. The experimental survival rates were then plotted against the predicted ones for comparison.

Three independent experiments were carried out for each test, and the obtained data were expressed as mean ± standard deviation. Linear regression analysis was conducted to examine the correlation between two factors, such as residual viable count of probiotic bacteria vs. storage period, and inactivation rate constant vs. reciprocal absolute temperature. Where regression coefficient (R^2) is referred, this estimates the goodness of fit to the linear model, 1 being a perfect fit and 0 being a failure of modelling the dataset.

5.2.6. Inhibition of the food-borne pathogens by the probiotic delivery system in a co-culture model

Planktonic samples of DPC16 were prepared at a cell concentration comparable to the microencapsulated sample. Ten millilitre of fresh culture was harvested and re-suspended in 5 mL 0.85% saline. Following the previously acquired optical density calibration curve for this strain, the suspensions were diluted to the equivalent volumetric viable count of the microcapsules. The pathogen suspensions were prepared to a same cell concentration as DPC16 samples following a similar method. To facilitate the co-culture, a modified MRS (mMRS) broth (without tri-ammonium-citrate and sodium acetate, pH 7.2) was used [247]. The mMRS broth was further supplemented

with 250 mM glycerol for the production of reuterin. The optional reducing agent (L-cysteine) was not included to avoid its sulfhydryl group's reaction with reuterin. Five millilitre of DPC16 suspension (for the microcapsules, the volume of inoculation was measured by liquid displacement.) and 5 mL of either pathogen suspension were added into 90 mL mMRS broth. For single culture samples, 5 mL suspension of each strain was added into 95mL mMRS broth. The mixed suspensions were sealed in containers and incubated at 37 °C without further anaerobic treatment. At time intervals of 20 and 40 h, aliquots of the suspension were sampled for the viability of DPC16 and the pathogens. Only 20 h samples were assayed for the content of reuterin using the colorimetric method described by Circle et al. [248].

5.2.7. *In vitro* reuterin production by *L. reuteri* DPC16 immobilized in the probiotic delivery system in a glycerol-water-fermentation system

Reuterin production by the planktonic, the alginate-encapsulated and the chitosan-coated alginate-encapsulated DPC16 cells in an infertile environment was also studied in a glycerol-water-fermentation system supplemented with low molar glucose (20 mM). The alginate-encapsulated DPC16 samples were prepared following the preparation method of the microcapsules described above but without the step of chitosan-coating. Twenty five millilitres of either type of microcapsules were mixed with 25 ml glycerol-water stock (500 mM glycerol in DI water with 40 mM glucose). Similarly, 25 mL planktonic DPC16 suspension was added in 25 ml glycerol water stock for comparison. The reuterin concentration in the supernatant was assayed at 0.5, 1, 2, 3, 4, 8 and 20 h. The viability of DPC16 was enumerated at 0, 3, 8 and 20 h by plating on MRS agar. In order to release immobilized DPC16, the microcapsules were suspended in equal volume of 200 mM sodium citrate solution and exposed to a brief

ultrasonic treatment as described in my previous study [88]. Disintegration of the microcapsules and the released bacteria were confirmed by light microscopy.

5.2.8. Statistical analysis

The results were generated from three independent experiments, each performed in duplicate. Two tailed Student's *t*-test was applied for comparison unless otherwise specified. $P = 0.05$ was selected as the significance level unless otherwise specified.

5.3. Results

5.3.1. Post-freeze-drying survival of the model strains in free and microencapsulated forms with or without the presence of skim milk powder

Post-freeze-drying survival of the model strains in free and microencapsulated forms is shown in Table 5.1. Results indicated that either the microencapsulation or the addition of skim milk powder could independently improve the survival during freeze-drying compared to the unprotected controls. The protected bacteria in both groups only showed an insignificant viability loss after freeze-drying. No negative influence was observed when both protective means were applied. Visual observations of the fluorescent-probe-labelled *L. reuteri* DPC16 also confirmed the lyo-protective effects of SMP and/or microencapsulation. As shown in Figure 5.1, most of the unprotected bacteria were found to have a compromised cell membrane and lack of intracellular enzyme activity, whereas the bacteria protected by either means or both showed a well-preserved integrity and functionality.

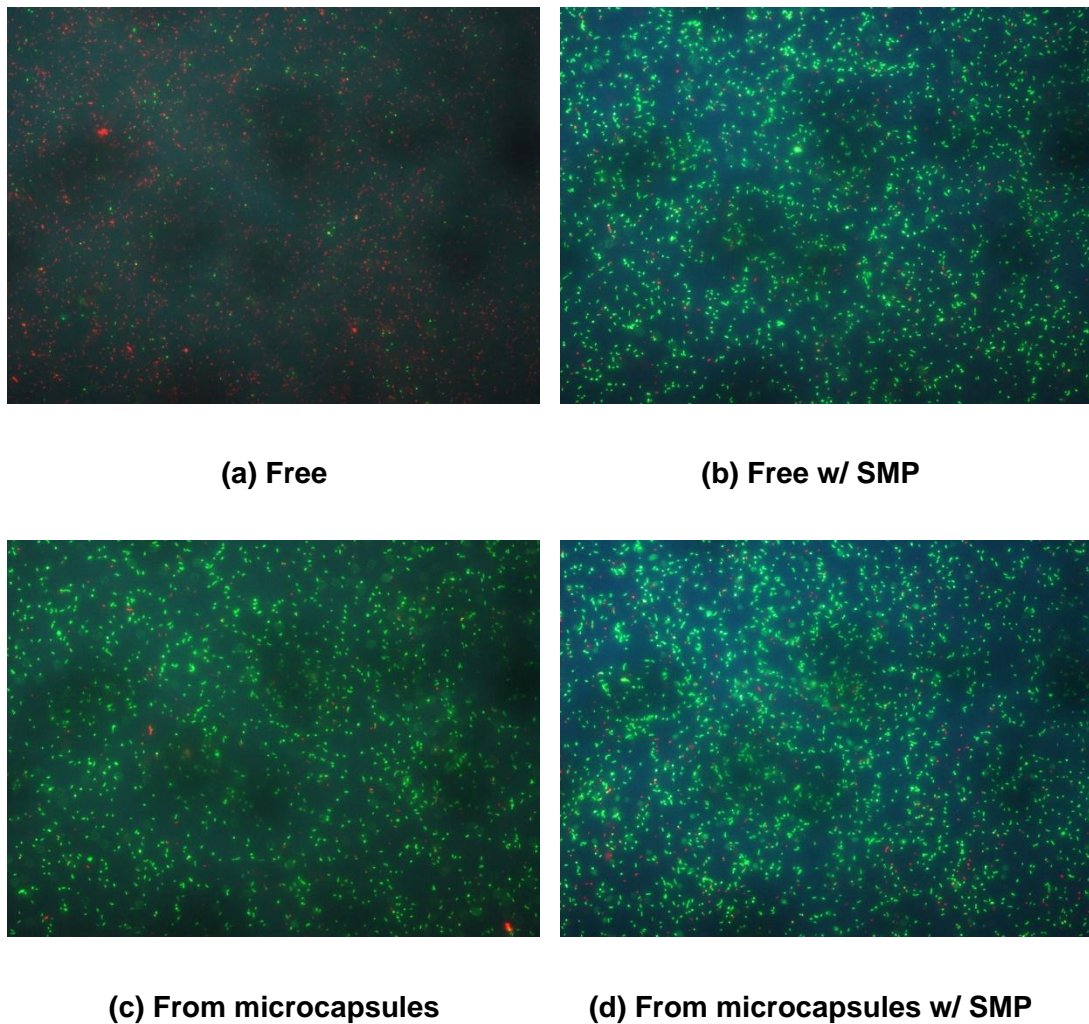


Figure 5.1 Viability assessment of *L. reuteri* DPC16 by PI and cFDA dual staining after freeze-drying as (a) free form, (b) free form with the presence of skim milk powder (SMP), (c) in the microcapsule-based delivery system, and (d) in the microcapsule-based delivery system with the presence of SMP.

Table 5.1 Post-freeze-drying survival (log CFU/g) of the model strains in free and microencapsulated forms with or without the presence of skim milk powder (SMP).

Strain		Free cells			
		w/o SKM		with SKM	
		Log CFU/g	Survival%	Log CFU/g	Survival%
<i>L. reuteri</i>	Initial	9.12 ± 0.28	-	9.01 ± 0.19	-
DPC16	Post-freeze-drying	7.78 ± 0.25	4.6%	8.68 ± 0.18	46.77%
<i>L. plantarum</i>	Initial	9.36 ± 0.29	-	9.28 ± 0.23	-
DPC206	Post-freeze-drying	8.38 ± 0.15	10.5%	9.12 ± 0.21	69.18%

Strain		Microencapsulated cells			
		w/o SKM		with SKM	
		Log CFU/g	Survival%	Log CFU/g	Survival%
<i>L. reuteri</i>	Initial	9.22 ± 0.23	-	9.23 ± 0.25	-
DPC16	Post-freeze-drying	8.79 ± 0.24	37.15%	8.99 ± 0.3	57.54%
<i>L. plantarum</i>	Initial	9.16 ± 0.21	-	9.2 ± 0.22	-
DPC206	Post-freeze-drying	8.96 ± 0.25	63.10%	9.08 ± 0.26	75.86%

5.3.2. Thermal death of the model strains in free and microencapsulated forms with or without the presence of skim milk powder

Table 5.2 and Table 5.3 summarize the decimal thermal reductions of *L. reuteri* DPC16 and *L. plantarum* DPC206, respectively, in free and microencapsulated forms with or without the presence of skim milk powder. Increasing storage temperature induced a faster inactivation of the strains. The protective means either by immobilizing in the microcapsules or by mixing with skim milk powder revealed a lower thermal death compared to free cells. The highest effect of protection was observed when both means were applied in combination.

The two model strains showed different behaviours of thermal inactivation during the accelerated storage, particularly in the absence of protective means. *L. plantarum* DPC206 was found to be more thermo-resistant than *L. reuteri* DPC16. In fact, the lyophilized free *L. plantarum* DPC206 generally gave more than 2-log higher survival rate at all examined temperatures compared to the *L. reuteri* DPC16, which indicated

diversity in intrinsic resistance of these strains. However, the presence of protective means did not only improve the thermal stability for both strains, but it also markedly narrowed the difference of thermal resistance between the two model strains.

Table 5.2 Decimal thermal reduction of *L. reuteri* DPC16 in free and microencapsulated forms with or without the presence of skim milk powder for accelerated storage testing

Temp. (°C)	Storage time (h)	Log N_0 - log N (log CFU/g) (mean ± standard deviation)							
		Free		Free w/ SMP		Encapsulated		Encapsulated w/ SMP	
25	0	0.000	±0.000	0.000	±0.000	0.000	±0.000	0.000	±0.000
	120	1.411	±0.021	0.202	±0.009	0.265	±0.006	0.112	±0.005
	240	2.582	±0.013	0.897	±0.013	0.602	±0.010	0.289	±0.013
	360	3.772	±0.033	0.989	±0.020	0.806	±0.014	0.387	±0.019
	480	5.601	±0.023	1.298	±0.026	1.232	±0.023	0.515	±0.022
35	0	0.000	±0.000	0.000	±0.000	0.000	±0.000	0.000	±0.000
	48	1.702	±0.011	0.276	±0.006	0.311	±0.009	0.149	±0.012
	96	3.389	±0.024	1.053	±0.021	0.788	±0.020	0.339	±0.018
	144	5.034	±0.016	1.411	±0.015	1.157	±0.031	0.522	±0.027
	192	6.231	±0.009	1.918	±0.022	1.571	±0.033	0.645	±0.032
55	0	0.000	±0.000	0.000	±0.000	0.000	±0.000	0.000	±0.000
	4	1.435	±0.015	0.265	±0.010	0.404	±0.010	0.014	±0.002
	8	2.789	±0.023	0.876	±0.023	0.791	±0.019	0.366	±0.010
	12	3.788	±0.008	1.356	±0.030	1.117	±0.028	0.547	±0.018
	16	5.408	±0.031	1.813	±0.024	1.523	±0.030	0.736	±0.019

Table 5.3 Decimal thermal reduction of *L. plantarum* DPC206 in free and microencapsulated forms with or without the presence of skim milk powder for accelerated storage testing

Temp.(°C)	Storage time (h)	Log N_0 - log N (log CFU/g) (mean ± standard deviation)							
		Free		Free w/ SKM		Encapsulated		Encapsulated w/ SKM	
25	0	0.000	±0.000	0.000	±0.000	0.000	±0.000	0.000	±0.000
	120	0.461	±0.011	0.168	±0.018	0.227	±0.006	0.060	±0.013
	240	1.100	±0.016	0.456	±0.022	0.484	±0.012	0.151	±0.016
	360	1.463	±0.021	0.704	±0.018	0.741	±0.013	0.301	±0.018
	480	2.145	±0.033	0.837	±0.020	1.073	±0.019	0.362	±0.022
35	0	0.000	±0.000	0.000	±0.000	0.000	±0.000	0.000	±0.000
	48	0.625	±0.013	0.248	±0.006	0.358	±0.009	0.113	±0.006
	96	1.501	±0.018	0.577	±0.011	0.728	±0.013	0.256	±0.012
	144	2.101	±0.022	1.015	±0.023	1.253	±0.025	0.508	±0.019
	192	2.948	±0.026	1.201	±0.030	1.589	±0.024	0.533	±0.017
55	0	0.000	±0.000	0.000	±0.000	0.000	±0.000	0.000	±0.000
	4	0.553	±0.016	0.293	±0.012	0.151	±0.008	0.136	±0.008
	8	1.137	±0.020	0.638	±0.019	0.642	±0.012	0.281	±0.012
	12	1.783	±0.029	1.026	±0.022	1.153	±0.020	0.456	±0.016
	16	2.181	±0.036	1.111	±0.026	1.409	±0.025	0.574	±0.024

The data of thermal reductions at various temperatures were further illustrated in the plots of loss of viability count (log CFU/g) vs. storage period (h), as shown in Figure 5.2 and Figure 5.3 for *L. reuteri* DPC16 and *L. plantarum* DPC206, respectively. All regressions show good fit to the linear models, indicated by the high R^2 values (>0.9). Parametric D values were directly calculated based on the slope of the fitted model and reported in the following section.

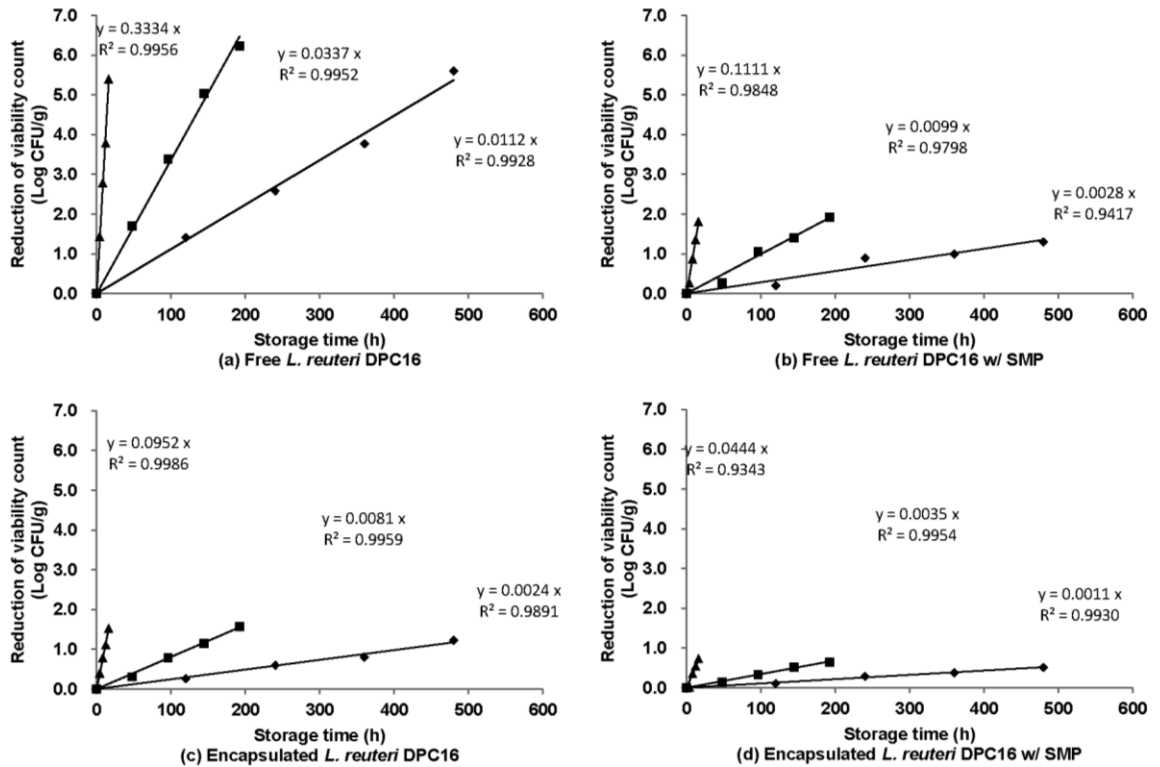


Figure 5.2 Thermal mortality curves of freeze-dried *L. reuteri* DPC16 (a) in free form, (b) in free form with the presence of skim milk powder (SMP), (c) in microencapsulated form, and (d) in microencapsulated form with the presence of skim milk powder at 25 °C (◆), 35 °C (■) and 55 °C (▲), and their linear regressions (model fitting with R^2 denoting the goodness-of-fit).

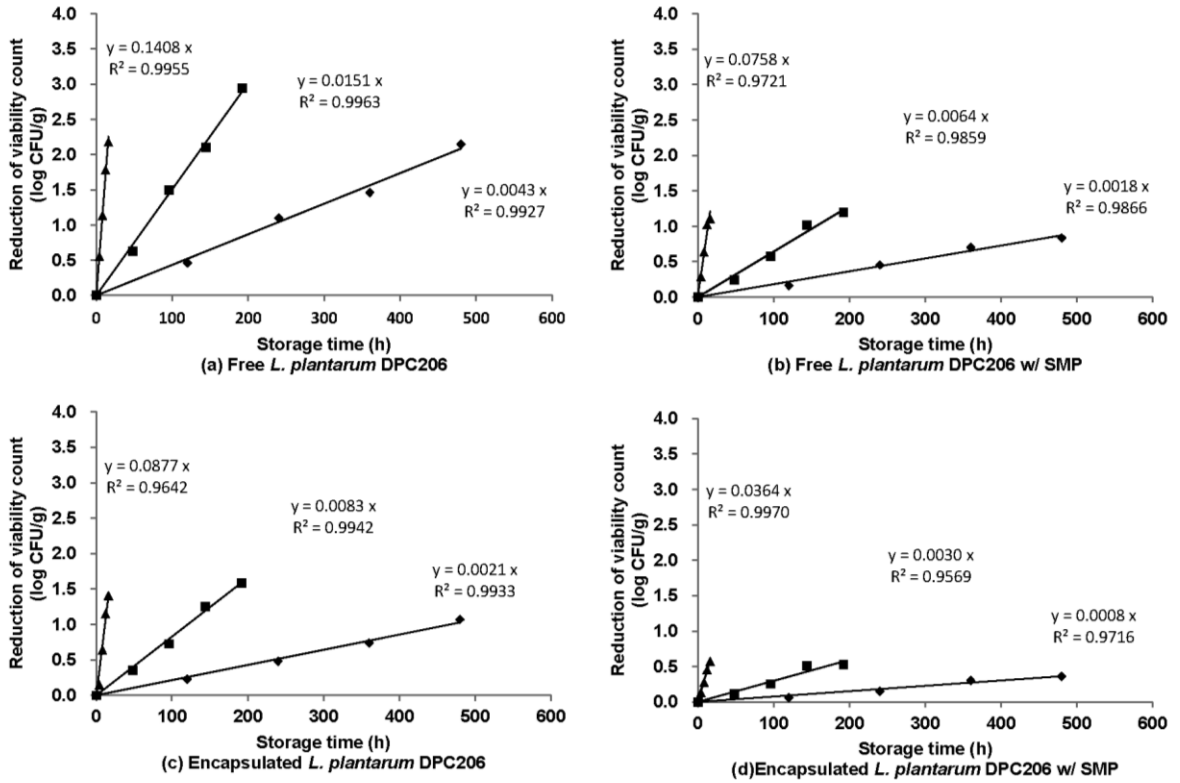


Figure 5.3 Thermal mortality curves of freeze-dried *L. plantarum* DPC206 (a) in free form, (b) in free form with the presence of skim milk powder (SMP), (c) in microencapsulated form, and (d) in microencapsulated form with the presence of skim milk powder at 25 °C (◆), 35 °C (■) and 55 °C (▲), and their linear regressions (model fitting with R^2 denoting the goodness-of-fit).

5.3.3. Determination of the inactivation kinetics and prediction of the stability at 4 °C and 20 °C

The k values and the D values for the thermal inactivation of the two model strains in free and microencapsulated forms, with or without skim milk powder, are calculated and given in Table 5.4 and Table 5.5. The experimental data were used to generate the linear regression models based on the Arrhenius equation for further prediction. The fitting results are shown in Figure 5.4. The D values ranged widely from 3.0 h to 920.2 h for *L. reuteri* DPC16 in different preparations at various temperatures, whereas the range was from 7.1 h to 1327.6 h for *L. plantarum* DPC206. Despite the strain-specific variance, the D values commonly increased with lowering temperature, thus indicating reduced rates of thermal inactivation. The D values were also found to be largely prolonged when the protective means were applied to the model strains. These results indicated that the immobilization and/or the addition of stabilizing skim milk powder could effectively improve the thermal stability of entrapped probiotic bacteria.

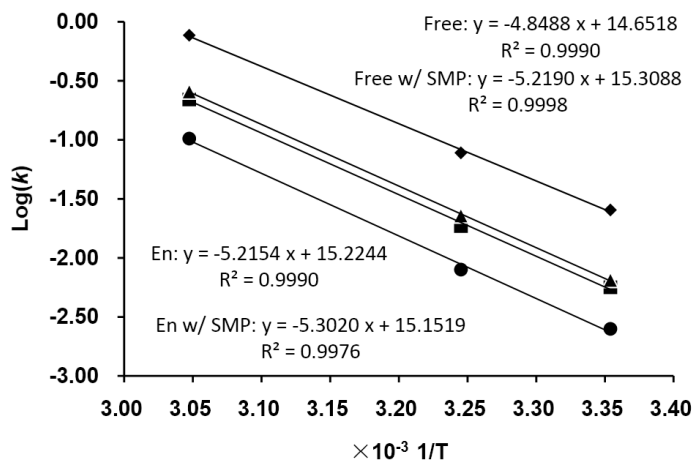
The predicted k values and D values for the thermal inactivation of the two model strains in free and microencapsulated forms with or without skim milk powder at 4 °C and 20 °C were also given in Table 5.4 and Table 5.5. According to the prediction, when both protective means were applied, the duration of decimal reduction in viability at 4 °C was 21913.2 h (approximately 30 months) for *L. reuteri* DPC16 and 33062.0 h (approximately 45 months) for *L. plantarum* DPC206. The enhanced stability was markedly contrasted to the D values of 1606.0 h (approximately 2.2 months) for unprotected free *L. reuteri* DPC16 and 4093.8 h (approximately 5.7 months) for unprotected free *L. plantarum* DPC206.

Table 5.4 Experimental and predicted *D* values and *k* values for the thermal reductions of *L. reuteri* DPC16 in free and microencapsulated forms with or without the presence of skim milk powder at various temperatures.

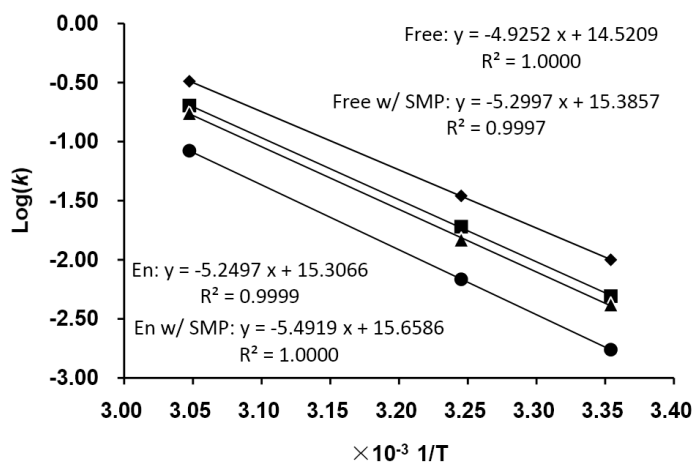
	Temp. (°C)	Free		Free w/ SKM		Encapsulated		Encapsulated w/ SKM	
		<i>D</i> (h)	<i>k</i> (h ⁻¹)	<i>D</i> (h)	<i>k</i> (h ⁻¹)	<i>D</i> (h)	<i>k</i> (h ⁻¹)	<i>D</i> (h)	<i>k</i> (h ⁻¹)
Experimental	55	3.0	0.7675	9.0	0.2565	10.5	0.2195	22.5	0.1025
	35	29.7	0.0775	100.8	0.0229	123.7	0.0186	289.6	0.0080
	25	90.4	0.0255	354.5	0.0065	408.7	0.0056	920.2	0.0025
Predicted	4	1606.0	0.0014	7665.3	0.0003	9033.5	0.0003	21913.2	0.0001
	20	179.3	0.0128	721.3	0.0032	854.7	0.0027	1979.6	0.0012

Table 5.5 Experimental and predicted *D* values and *k* values for the thermal reductions of *L. plantarum* DPC206 in free and microencapsulated forms with or without the presence of skim milk powder at various temperatures.

	Temp. (°C)	Free		Free w/ SKM		Encapsulated		Encapsulated w/ SKM	
		<i>D</i> (h)	<i>k</i> (h ⁻¹)	<i>D</i> (h)	<i>k</i> (h ⁻¹)	<i>D</i> (h)	<i>k</i> (h ⁻¹)	<i>D</i> (h)	<i>k</i> (h ⁻¹)
Experimental	55	7.1	0.3243	13.2	0.1744	11.4	0.2020	27.5	0.0837
	35	66.3	0.0347	155.7	0.0148	120.7	0.0191	336.3	0.0068
	25	230.3	0.0100	550.3	0.0042	467.2	0.0049	1327.6	0.0017
Predicted	4	4093.8	0.0006	12548.9	0.0002	9936.0	0.0002	33062.0	0.0001
	20	438.4	0.0053	1139.5	0.0020	917.0	0.0025	2740.3	0.0008



(a) *L. reuteri* DPC16



(b) *L. plantarum* DPC206

Figure 5.4 Arrhenius plot for the inactivation of the two model strains, i.e. (a) *L. reuteri* DPC16 and (b) *L. plantarum* DPC206, in different preparation forms: free form (Free, \blacklozenge), free form with the presence of skim milk powder (Free w/ SMP, \blacktriangle), microencapsulated form (En, \blacksquare), and microencapsulated form with the presence of skim milk powder (En w/ SMP, \bullet).

To validate the model, comparison between theoretical and actual measurement values of survival rate of the two model strains in various preparations at 20 °C was made and depicted in Figure 5.5. There were no great differences observed, confirming that the theoretical survival rate calculated based on the kinetic parameters can be used as prediction model of stability for the freeze-dried probiotic product.

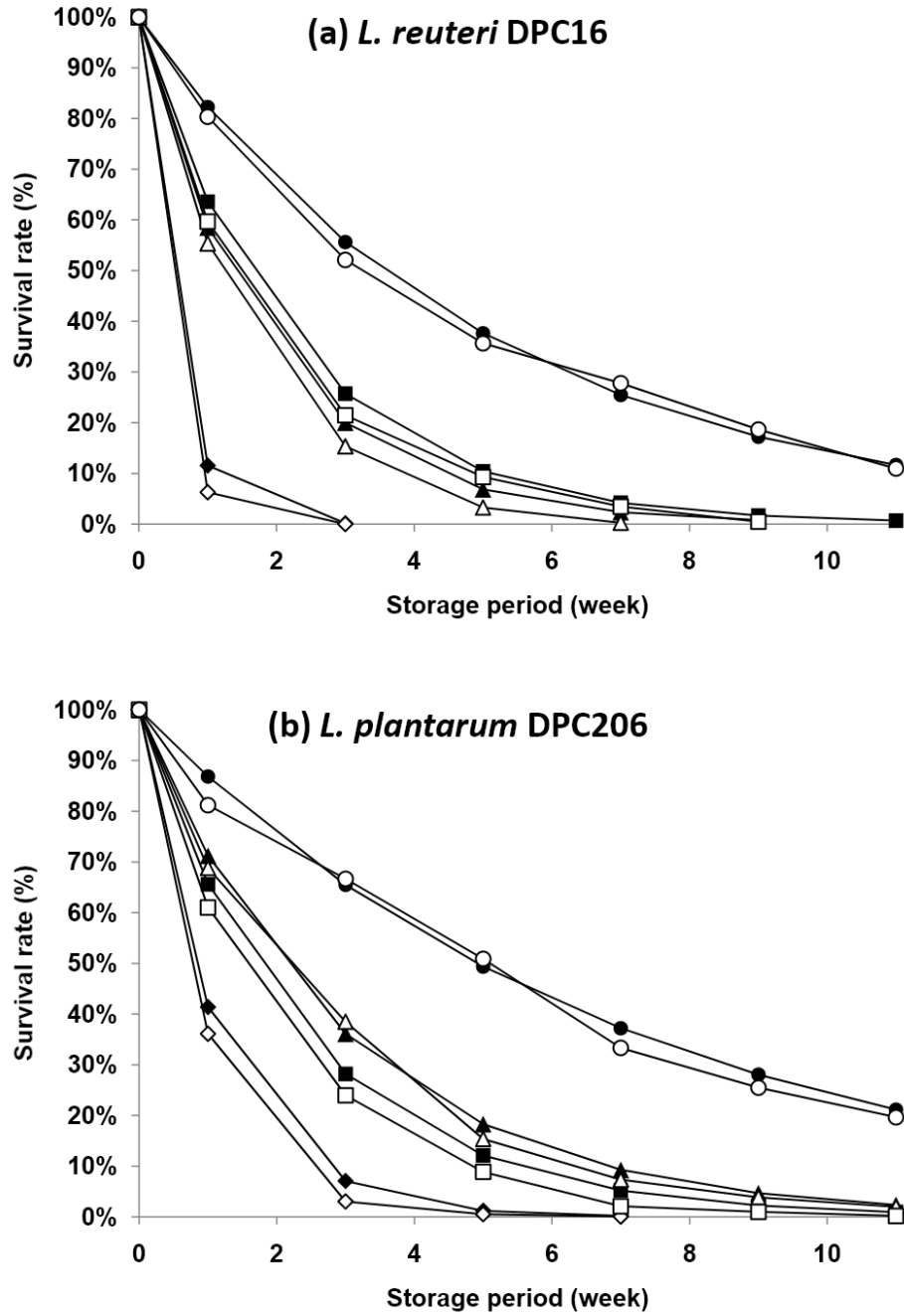


Figure 5.5 Comparison between theoretical and actual measurement values of survival rate at 20 °C of freeze-dried (a) *L. reuteri* DPC16 and (b) *L. plantarum* DPC206. Symbols denote samples prepared as free form (theoretical ◆ and actual ◇), as free form with the presence of skim milk powder (theoretical ▲ and actual △), as microencapsulated form (theoretical ■ and actual □), and as microencapsulated form with the presence of skim milk powder (theoretical ● and actual ○).

5.3.4. Inhibition of the food-borne pathogens by the probiotic delivery system

The viable counts of all strains in the co-culture model and the pH values of the acidified media are listed in Table 5.6. The single culture of the DPC16 strain dropped the pH of mMRS medium to around 3.5 after 20-h incubation, whereas in the case of the single culture of each pathogenic strain the lowered pH values only reached around 4.7. The microencapsulated DPC16 cells delivered a comparable performance of medium acidification compared with the planktonic ones. By the end of 20-h incubation, the medium pH of the planktonic DPC16 was only slightly lower than the one of the encapsulated group and this difference was not statistically significant ($P = 0.1963$). However, also compared to the planktonic DPC16, a 2.75-fold lower CFU count of free cells in the medium for the microencapsulated group at 20 h was meanwhile observed ($P < 0.005$).

Microscopic observation (Figure 5.6) revealed that even after 20-h incubation the microcapsules still remained entire, whereas the dense masses of growing DPC16 cells were commonly observed inside many microcapsules. Meanwhile, the cell releases only occurred at a number of spots on some microcapsules (indicated by the arrows in Figure 5.6), characterizing a spontaneous eruption of a large volume of bacteria into media after a certain critical time point.

The growth of the two food-borne pathogenic strains was found to be sensitive to the presence of *L. reuteri* DPC16. Compared to the single cultures, the viable count of *E. coli* O157:H7 was 3-log lower after 20-h co-incubation ($P < 0.001$), whereas *S. typhimurium* was 2-log lower ($P < 0.001$). By contrast, the viability of DPC16 was only slightly reduced by the presence of *E. coli* O157:H7 (0.22 log drop, $P < 0.05$) and was not significantly affected by the presence of *S. typhimurium* ($P = 0.2886$). The medium pH of co-culture at 20 h was found to be 1-log lower than the single culture of each

pathogenic strain, although it was also slightly higher than in the single culture of DPC16, which could be a result of the competition for fermentable nutrients between the probiotic and the pathogenic strains.

The results from the co-culture model confirmed that this microencapsulation preparation did not affect the inhibitory performance of DPC16 against those two pathogenic strains. In the case of co-culture with *E. coli* O157:H7, both the planktonic and the microencapsulated DPC16 cells dropped the medium pH value to 3.7 after 20-h incubation. More than 3-log reduction in the viable count of *E. coli* O157:H7 was observed in both groups compared to the single culture of *E. coli* O157:H7. By the end of the 40-h incubation, *E. coli* O157:H7 could not be detected by the current enumeration method, indicating a severe reduction of the viability of this strain (to less than 10 CFU/mL). In contrast, the number of viable DPC16 in the medium still remained above 10^8 CFU/mL. On the other hand, the inhibition of *S. typhimurium* provided a more intriguing result. Compared to the planktonic ones, the microencapsulated DPC16 cells further reduced the viable count of *S. typhimurium* by 3-log magnitudes ($P < 0.001$). However, no significant differences were observed in the medium pH values or the reuterin concentrations for the two groups, suggesting the existence of some inhibitory factors other than reuterin.

Table 5.6 Comparison of the inhibitory effect on two food-borne pathogens *E. coli* O157:H7 and *S. typhimurium* by planktonic and microencapsulated *L. reuteri* DPC16.

	PC at 20 h, log(CFU)/mL	Media reuterin concentration at 20 h, mmol/L	Media pH at 20 h	PC at 40 h, log(CFU)/mL
<u>Single culture in mMRS medium</u>				
Encapsulated DPC16	8.65 ± 0.09	67.32 ± 2.30	3.56 ± 0.08	8.49 ± 0.09
Planktonic DPC16	9.09 ± 0.08	70.50 ± 2.81	3.48 ± 0.04	8.33 ± 0.05
<i>S. typhimurium</i>	8.65 ± 0.03	N/A	4.71 ± 0.05	8.13 ± 0.07
<i>E. coli</i> O157:H7	8.80 ± 0.02	N/A	4.78 ± 0.08	8.21 ± 0.11
<u>Co-culture in mMRS medium</u>				
<i>E. coli</i> O157:H7 and planktonic <i>L. reuteri</i> DPC16				
<i>L. reuteri</i> DPC16	8.87 ± 0.03	64.78 ± 1.35	3.70 ± 0.07	8.45 ± 0.04
<i>E. coli</i> O157:H7	5.58 ± 0.09			ND
<i>E. coli</i> O157:H7 and microencapsulated <i>L. reuteri</i> DPC16				
<i>L. reuteri</i> DPC16	8.93 ± 0.10	66.59 ± 1.68	3.70 ± 0.11	8.56 ± 0.06
<i>E. coli</i> O157:H7	5.69 ± 0.12			ND
<i>S. typhimurium</i> and planktonic <i>L. reuteri</i> DPC16				
<i>L. reuteri</i> DPC16	8.97 ± 0.15	64.34 ± 0.96	3.60 ± 0.09	8.48 ± 0.04
<i>S. typhimurium</i>	6.42 ± 0.39			ND
<i>S. typhimurium</i> and microencapsulated <i>L. reuteri</i> DPC16				
<i>L. reuteri</i> DPC16	8.70 ± 0.01	66.32 ± 1.02	3.63 ± 0.12	8.50 ± 0.06
<i>S. typhimurium</i>	3.05 ± 0.07			ND

Note:

1. PC denotes “plate count”; ND denotes “not detected”; N/A denotes “not applicable”.

2. The viability count for each sample is given as “mean ± standard deviation”.

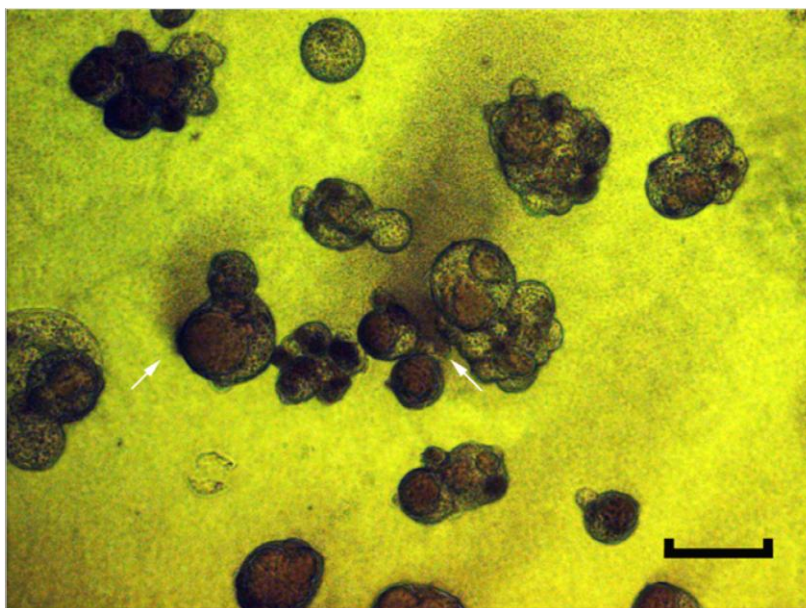


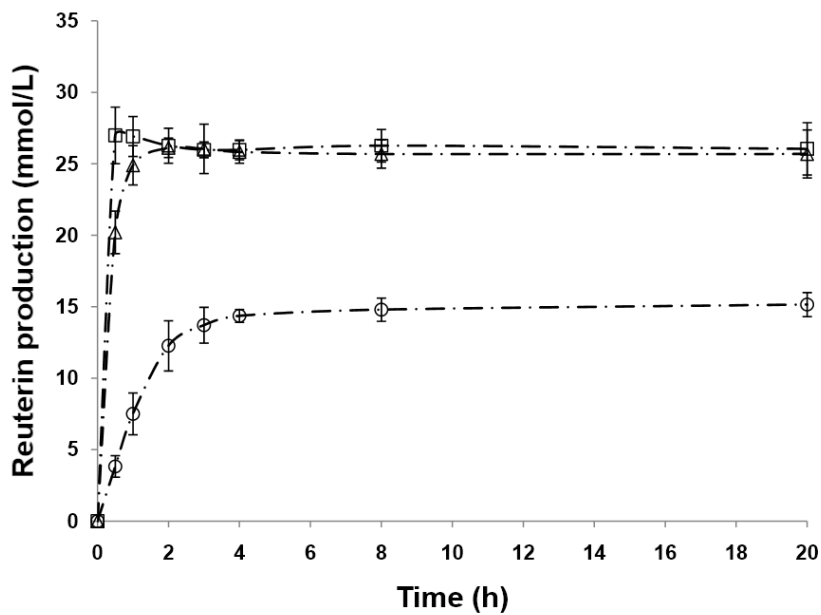
Figure 5.6 Microscopy of newly grown *L. reuteri* DPC16 released from the chitosan-coated alginate microcapsules after 20h incubation at 37 °C in the modified MRS broth. The dark masses in the microcapsules indicate the internal growth of DPC16. The dark cloudy areas surrounding the microcapsules consist of the released DPC16. The white arrows point to the releasing areas. The bar at right bottom corner indicates 100 µm.

5.3.5. *In vitro* reuterin production by *L. reuteri* DPC16 immobilized in the probiotic delivery system

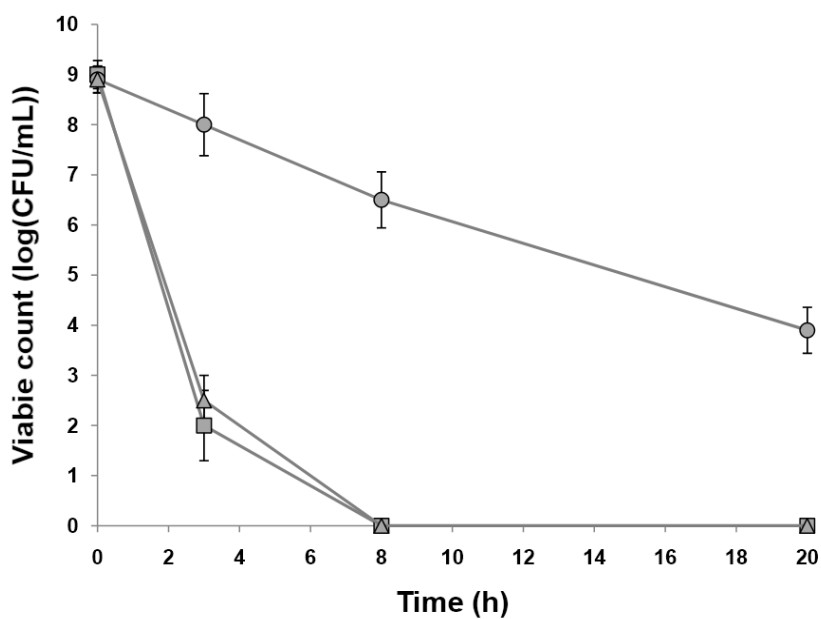
The influence of microencapsulation on the reuterin production and accumulation was compared to the planktonic DPC16 cells using an infertile glycerol-water fermentation system. Figure 5.7(a) shows the time-serial comparison of medium reuterin concentrations among the planktonic, the alginate-encapsulated and the chitosan-coated alginate-encapsulated DPC16 samples. The planktonic DPC16 cells appear to rapidly accumulate a high concentration of reuterin and maintain it for the rest of the examined period. Similarly, the alginate microcapsules without chitosan coating produced a series of reuterin concentrations comparable to the planktonic sample. Only at 0.5-h, the observation revealed a significantly lower reuterin concentration in the alginate-

encapsulated sample as compared to the planktonic one ($P < 0.01$). The results were in agreement with the other reports on immobilizing 10^9 CFU/mL *L. reuteri* bacteria in alginate beads, which showed no difference in the maximum concentration of reuterin compared with the planktonic samples except for a relatively lower production rate at the beginning of fermentation [241, 249]. In contrast, the presence of chitosan-coating reinforced the alginate matrix and suppressed the time-dependent swelling of the uncoated microcapsules. Compared to both the planktonic group and the uncoated alginate microcapsules, the chitosan-coated microcapsules rendered a more moderate reuterin-production rate. The maximum concentration of reuterin was also markedly lower.

On the other hand, by comparing the viability of the DPC16 cells in all groups (Figure 5.7(b)), an improved survival was observed for the DPC16 cells encapsulated in the chitosan-coated microcapsules. By contrast, the accumulation of more reuterin in the other two groups coincided with a quick annihilation of the viable cells. The diverse responses of the three groups suggested that the microencapsulation method could exert marked influence on the availability of glycerol to the immobilized DPC16, and could therefore impact the survival of this microorganism.



(a)



(b)

Figure 5.7 Time-series of (a) the reuterin concentrations (mmol/L) and (b) the viable counts (log(CFU)/mL) in the glycerol-water system produced by the planktonic *L. reuteri* DPC16 (square), the alginate-microencapsulated *L. reuteri* DPC16 (triangle) and the chitosan-coated alginate-microencapsulated *L. reuteri* DPC16 (circle). The y-axis error bars represent the standard deviations.

5.4. Discussion

In the current study, the accelerated storage test was successfully applied to predict the storage stability of probiotic bacteria, and to evaluate the enhanced stabilizing effects by immobilizing probiotic bacteria in the microcapsule-based delivery system. Both probiotic model strains displayed aggravated thermo-sensitivity at elevated temperatures, whereas the sensitivity could be efficiently reduced by the application of the protective means. The activation energy (E_a) values that were determined from the slope of the Arrhenius models falls in the range of 9.62 to 10.90 kcal/mol, which are close to the reported values for various strains [238, 243]. The E_a values were found to consistently increase after preparing the probiotic bacteria in skim milk powder and/or in the delivery system, suggesting that the protective means possess certain mechanisms to restrain the deteriorating reactions of thermal deactivation from taking place. However, the kinetic data *per se* are not able to provide meaningful interpretations on the underlying mechanisms of protection [234]. In addition, similar findings on increased E_a were also reported for the thermo-protective effect of sucrose and glycerol on *Lactococcus* starter cultures [238].

The prediction based on the generated Arrhenius models was validated on both probiotic strains at 20 °C. The results confirmed a reasonable accuracy of the Arrhenius theory. The predicted storage stability at 4 °C indicates an 8-fold improvement in the duration of decimal reduction for both model strains, when they are prepared in the microcapsule-based delivery system and suspended with skim milk powder. It means that a shelf life of approximate 2 years can be expected for so-prepared probiotic products with an initial viable count of 10^9 CFU/g, whereas it may still maintain about 10^8 CFU/g (less than 1-log drop) viable cells at the consumption time before expiration.

It was reported that LAB could produce short chain fatty acids (SCFA) and therefore decrease the pH of the GI tract, creating an inhibitory environment against some pathogenic bacteria [250]. The SCFAs produced by *L. reuteri* DPC16 during fermentation together with the acidification of medium were also confirmed to be partly responsible for the antimicrobial effect of the spent culture medium against a number of Gram positive and negative pathogenic bacteria [251]. Consequently, the microencapsulation preparation was preferred not to affect the capacity of the embedded bacteria to lower environmental pH, which has been supported by the result.

The similar performances of medium acidification indicate comparable cell activities between the free and the microencapsulated groups. Therefore, the difference of cell count in the medium may result from a restrained release of the entrapped DPC16 cells from the microcapsules. Chitosan coating was previously reported to retard cell release from alginate beads (with a diameter of 3.5 mm) immobilizing a *L. lactis* strain [252]. This delayed release was attributed to the strengthened cross-linking between the reversely charged chitosan and alginate macromolecules. Such effect of reinforcement was more pronounced in sub-100 μm Ca^{2+} -alginate microcapsule, owing to the highly increased contact area for the interlinking formation, which also markedly prevented the rapid disintegration of the microcapsules in the gastric fluid [88].

The microscopic observation of the retention of grown cells in the incubated microcapsules was in good agreement with the report that porous solid supports could retain cell growth to a density 10- to 50- folds higher than free-flow ones in liquid nutritive medium [253]. It may also explain the lower cell count in the medium for the microencapsulated sample. Furthermore, during the immobilized incubation, non-specific stress adaptation owing to the quorum-sensing effect at high cell density could also be induced, thus generating a more resistant culture than the originals [253-254]. In

the current study, compared to the planktonic group, the less and slower drop of viable count in the medium for the microencapsulated group may have suggested increased tolerance to the adverse environment among the DPC16 cells grown from the microcapsules.

As shown by the result, the microencapsulated *L. reuteri* DPC16 elicited an enhanced inhibitory effect on *S. typhimurium* as compared to the planktonic ones. Two hypotheses are proposed for this phenomenon. First, the microencapsulation process may have selectively propagated a competitive DPC16 mutant against *S. typhimurium*. Similarly, the enhanced antimicrobial effect was also reported by Zhao et al. [255] for the recovered DPC16 cells from immobilization. Another possibility is that the chitosan coating adsorbed on the Ca²⁺-alginate microcapsules may be responsible for the improved inhibition of *S. typhimurium*. Chitosan was reported to disrupt the barrier property of the outer membrane of Gram-negative bacteria, and this effect was more pronounced in acidic conditions [256]. In my investigation, low-molecular-weight chitosan was used, which shredded more easily from surfaces of eroded microcapsules. Considering the reduced dimension of the microcapsules, the increased surface-to-volume ratio also improved the chances of the erosion and the exposure of chitosan to free-flow *S. typhimurium* cells. However, further investigation is required to elucidate the underlying mechanism.

In addition to SCFAs, reuterin was proven to be another potent antimicrobial factor produced by *L. reuteri* DPC16 [251]. However, reuterin above certain threshold concentration (relative to certain cell concentrations) could also menace the survival of its producing organisms [257-258]. It is in agreement with the finding of substantial loss of viable DPC16 cells during the initial three hours in both the planktonic and the alginate-encapsulated samples. In contrast, the results from the chitosan-coated

microcapsules indicated a reduced availability of substrate glycerol to the immobilized DPC16 cells. Because strong intermolecular hydrogen bonding can occur between –CH₂OH alcoholic groups from glycerol and –NH₂ or as NH₃⁺OOC-CH₃, -CH₂OH and in some extension –NH-CO-CH₃, groups from chitosan, this may lead to strong interactions between chitosan matrix and glycerol, thus restricting the motion of glycerol molecules [259]. We therefore propose that the chitosan coating worked as a barrier to the free diffusion of glycerol into the microcapsules, and therefore reduced the availability of glycerol for reuterin production. The lowered reuterin concentration also allowed the improved survival of the DPC16 cells. Although the chitosan-coated DPC16 microcapsules produced less reuterin, it is noteworthy that reuterin does not require a large volume to take effect. Cleusix et al. [260], after studying the interactions between a *L. reuteri* strain and *E. coli* population using an colonic fermentation model, suggested that the accumulation of reuterin may not happen or necessarily be required *in situ*, whereas a very low reuterin concentration was sufficient to suppress other species.

To conclude, the comparisons of the probiotic strain *L. reuteri* DPC16 between the planktonic and the encapsulated forms were performed in terms of the inhibition of the food-borne pathogens. No attenuated antimicrobial effect was observed for the immobilized DPC16 in the co-culture model. Microencapsulation rendered an enhanced protection on the embedded probiotics, but it may also induce an altered availability of substrates to the immobilized organisms.

Chapter 6. Evaluation of mucoadhesive coatings of chitosan and thiolated chitosan for the probiotic microcapsules

This chapter describes the evaluation of mucoadhesive property of the delivery system. Thiolated chitosan was tested as a novel mucoadhesive coating for its improved mucoadhesion performance.

6.1. Introduction

Polysaccharide microcapsules have been widely reported as useful vehicles for the delivery of probiotic bacteria [77, 261]. They provide the embedded bacteria with enhanced protection against harsh challenges in the upper gastrointestinal (GI) tract. The release of such probiotic microcapsules is expected to occur in the lower GI tract. In particular for the colon-targeted delivery, the generally recruited releasing principle is dependent on the degradation of wall material by endogenous microflora together with consistent erosion by digestive system [262-263]. However, this mechanism requires a relatively long period to initialize the effective release. Therefore, methods to achieve a prolonged retention in the lower GI tract are preferred, thus allowing sufficient time for release and adaptation of the embedded probiotic bacteria.

Among many choices of immobilizing polymers, alginate is widely preferred for its biocompatibility, biodegradability and non-toxicity for cell encapsulation. Divalent calcium ion induced ionotropic gelling of alginate under relatively mild conditions is also commonly applied for preparing immobilized probiotic bacteria for different

applications. Pure alginate, being a hydrophilic polyanion, shows a strong mucoadhesive property. A large number of carboxyl and hydroxyl groups on the backbone of alginate molecule turn to the charged state at a pH above its pK_a (~3.8) [264]. It was suggested that such molecules could help elongate the polymer chain and facilitate the penetration and the entanglement with mucin matrices, thus leading to prolonged adhesion [87].

The Ca^{2+} -induced gelling involves a mechanism of specific and strong packing arrangements between Ca^{2+} cations and long stretches of α -l-guluronic acid (G) units within alginate molecule. Therefore, they can reduce the free mobility and the secondary-bonding capacity of alginate polymers in terms of their interactions with mucin matrices. The mucoadhesion performance of such delivery system hence deserves more consideration. Moreover, relatively stronger Ca^{2+} -alginate gels are usually selected for the delivery of microencapsulated probiotic bacteria to the distal part of the GI tract, thereby preventing the premature release at early stages of passage. Inevitably, this leads to increased extent and strength of the interaction between calcium ions and alginate molecules. Therefore, the mucoadhesive property of such microcapsule should not be taken for granted simply based on the property of the pure polymer. For example, in a study of the mucoadhesive polysaccharide - pectin, Hagesaether et al. [11] observed that zinc-pectinate hydrogel beads showed reduced mucoadhesion along with the increasing extent of cross-linking to Zn^{2+} . Consequently, the authors suggested the importance of doing mucoadhesive measurements on relevant formulations, rather than basing the understanding solely on investigation of polymer solutions.

Chitosan is a polysaccharide consisting of copolymers of glucosamine and N-acetylglucosamine. Its distinctive mucoadhesive properties are mediated by ionic

interactions between the positively charged amino groups, and the negatively charged substructures of the gastrointestinal mucus, e.g. sialic acid [264]. Ionic bonds of polycationic materials were suggested to elicit stronger adhesion than hydrogen bonds and van-der Waals bonds of polyanionic materials [87]. Due to the diverse electric charges, chitosan can intertwine with alginate polymer chain or be adsorbed on alginate surfaces. This phenomenon was utilized to alter the characteristics of alginate gel and provide some new features to the original delivery vehicles [265-266]. Chitosan coating was also reported to increase the survival of some probiotic strains embedded in large Ca^{2+} -alginate beads when they were challenged by GI stress factors [267]. However, the chitosan-induced alteration of mucoadhesive property of Ca^{2+} -alginate microcapsules has only rarely been investigated for the colonic delivery of probiotic bacteria.

Thiolated polymers are a new type of mucoadhesive polymeric materials. Owing to the rich conjugated sulfhydryl functional groups, thiolated polymers were demonstrated to form covalent disulfide bonds with mucus glycoproteins, thus markedly improving the mucoadhesion [156]. Thiolated chitosan was reported to be able to augment the mucoadhesiveness up to 100-fold, compared to unmodified chitosan [268]. The potential use of thiolated chitosan for the improved retention of probiotic microcapsules is hence worthy of evaluation.

In my previous research, a type of sub-100 μm chitosan-coated Ca^{2+} -alginate microcapsule was successfully applied for the delivery of probiotic bacteria [88]. The reduced dimension of microcapsules was suggested to provide more chances for microcapsules to be lodged in surface folds and crevasses of the lower GI tract, whilst minor dislodging stresses imposed on small particles resulted in small adhesive interactions required to keep them in place [87]. The increased surface-to-volume

ratio also allows more mucoadhesive coating materials to be deposited on the surface of the microcapsules in terms of per unit of the core material, thus improving the mucoadhesive performance.

In the current study, the aim was set to study the mucoadhesion enhancement induced by the chitosan or the thiolated chitosan coatings for the colonic delivery of the sub-100 μm probiotic microcapsules.

6.2. Materials and methods

6.2.1. Materials

The materials for microencapsulation including sodium alginate, chitosan (low molecular weight), maltodextrin, ultrafine calcium carbonate were procured from Sigma-Aldrich (Australia). The fluorescent stain carboxyfluorescein di-acetate (cFDA) was procured from Invitrogen Inc (USA). Fluorescein isothiocyanate (FITC) for chitosan labelling was procured from Sigma (Australia). Mucin (Type III) from porcine stomach for rheological synergism assay was procured from Sigma (Australia). The simulated gastric fluid (SGF, pH 1.2) and the simulated intestinal fluid (SIF, pH 6.5) were prepared according to the USP standards.

6.2.2. Preparation of the probiotic microcapsules

The preparation of the sub-100 μm probiotic microcapsules followed the previously described method with some modifications [88]. To simplify the testing conditions, the protectants applied in the original method were not used in this encapsulation formula. *L. reuteri* DPC16 (NZRM#4294) was provided by Bioactives Research New Zealand (Auckland, New Zealand) and used as the model probiotic strain. This strain was routinely cultured anaerobically in deMan-Rogosa-Sharpe (MRS, Difco, USA)

broth supplemented with 0.5 g/L cysteine (Sigma, USA). The probiotic microcapsules loaded with DPC16 had an equivalent cell concentration of 9.27 ± 0.11 log CFU/mL as assayed by serial dilution and plate count on MRS agar plate. Mucoadhesive coating was conferred by suspending the uncoated Ca^{2+} -alginate microcapsules in either 0.8% (w/v) chitosan in acetate buffer (pH 5.5) or 0.8% (w/v) FITC-labelled chitosan in acetate buffer (pH 5.5) or 0.8% (w/v) thiolated chitosan in acetate buffer (pH 5.5) for different purposes of evaluation. Samples were removed from the coating reactors at 5, 20, 180, 720 minutes for the following analyses. The uncoated microcapsules served as the zero-time sample.

6.2.3. Preparation of FITC-conjugated chitosan and flow cytometric (FCM) analysis of the FITC-chitosan coating on the microcapsules

FITC-labelled chitosan was synthesized and the labelling efficiency was evaluated as previously described [269]. In brief, 100 mL dehydrated methanol and 50 mL FITC solution (2 mg/mL in methanol) were mixed into 100 mL chitosan solution (1% w/v in 0.1 M acetic acid). The reaction was carried out in the dark at room temperature for 3 h prior to precipitation in 1 L NaOH (0.1M). The precipitate was filtered and dialyzed in 4 L deionised water with daily replacement until the absence of FITC in the dialysis jar was confirmed by UV-spectrofluorometry (λ_{exc} : 488 nm / λ_{emi} : 515 nm, Jasco FP-6500, Australia). The dialyzed product was then lyophilized. The molar ratio of free amine to FITC-labelled residues was assayed as 9.5:1.

The preparation of FITC-chitosan coated alginate microcapsules followed the same method described in Section 2.2, except that the chitosan in the coating solution was replaced with FITC-chitosan. All FITC-coated microcapsules were washed twice with deionised water. Aliquots of each microcapsule sample (from different durations of

FITC-chitosan coating treatment) were suspended in 2.5 mL deionised water prior to FCM analysis.

FCM analysis was performed with the BD LSR II Flow Cytometer (BD Biosciences, New Zealand). The cytometer was adjusted to a low flow rate in order to count 2,000 fluorescent events. The measurements acquired for each microcapsule included the forward scatter (FSC), the side scatter (SSC) and the green (FL1 for FITC) channels. The FITC was excited by a laser beam at 488 nm and detected at 530 nm. The raw data were analyzed with FlowJo program (v7.6.1, Tree Star, Inc. USA) in the post-run mode.

6.2.4. Zeta-potential of chitosan-coated probiotic microcapsules

Zeta-potential of the chitosan or thiolated chitosan coated microcapsules samples prepared by the method described in Section 2.2 was determined by Zetasizer Nano ZS (Malvern, UK) following the manufacturer's instruction.

6.2.5. Synthesis of thiolated chitosan and its characterization

The thiolated chitosan was synthesized following a method developed by Bernkop-Schnürch et al. [270] with a few modifications as suggested by Masuko et al. [271]. The sample was finally lyophilized at -55 °C and 0.01 mbar (Labconoco Freezone Freeze-drier, USA) and stored at 4 °C for further use. The number of thiol groups on the thiolated chitosan was determined by Ellman's reagent, as previously described by Roldo et al. [272]. The ATR-FTIR analysis of the thiolated chitosan was performed on Bruker TENSOR 37 FTIR spectrometer in a spectral range from 600 cm⁻¹ to 4000 cm⁻¹.

6.2.6. Rheological synergism

The rheological synergism between the mucoadhesive coating polymers and mucin was evaluated via a method previously described by Suknuntha et al. [273] with some modifications. The mucoadhesive interaction between the polymers and mucin was investigated in the SGF and the SIF separately. The final volume of the polymer and mucin mixtures was adjusted to 10 mL, and the mixtures were mixed using a reciprocating shaker until homogeneous. Groups of the final concentrations of the polymer and mucin in the GI fluids are listed in Table 6.1. Concentrations of polymer were lowered for the assays in the SIF due to the reduced solubility of chitosan, and the quick self-gelling behaviour of thiolated chitosan at high concentration at this pH.

Table 6.1 Groups of the final concentrations (w/v) of the polymer (chitosan or thiolated chitosan) and mucin in the GI fluids for the study of mucoadhesion-based rheological synergism in blend system.

#	Mucin	Chitosan	Thiolated chitosan
<i>In simulated gastric fluid (pH 1.2)</i>			
1	5%	0.50%	-
2	5%	0.10%	-
3	5%	0.05%	-
4	5%	-	0.50%
5	5%	-	0.10%
6	5%	-	0.05%
<i>In simulated intestinal fluid (pH 6.5)</i>			
7	5%	0.10%	-
8	5%	0.01%	-
9	5%	-	0.10%
10	5%	-	0.01%

These mixtures of mucin and the polymers were equilibrated at 37.0 ± 0.1 °C for 1 hour. The viscosity measurements were carried out using a Brookfield DV-III Ultra programmable viscometer (Brookfield Engineering Laboratories Inc., USA), equipped

with a CP-40 spindle and a sample adaptor warmed at 37.0 ± 0.1 °C. After loading, samples were allowed to equilibrate in the adaptor for 1 minute prior to testing. The viscosity profile of each sample was collected on a spindle-rotating-speed range from 0 to 250 rpm. The apparent viscosity at a shear rate of 20 s^{-1} (approximate 2.65 rpm) was selected for the estimation of the componential force of mucoadhesion in blend system. All viscosity measurements were performed in triplicate, and data reported as a mean \pm standard deviation.

6.2.7. *Ex vivo* tensile test

The instrumental setting described by Thirawong et al. [153] was recruited in the current study to evaluate the mucoadhesive property of Ca^{2+} -alginate gel with or without the presence of the mucoadhesive coatings. Samples were made by compressing 200-mg alginate powder into flat-faced round disc with a diameter of 12.0 mm using a single punch hydraulic press operated at 8 tonnes for 10 min. The alginate discs were kept in desiccator until further use. The mucoadhesion test was carried out on a texture analyzer (TA.XT plus, Stable Micro System, UK) equipped with a 5 N load cell. The alginate discs were attached to the cylindrical probe (12 mm in diameter) by double-sided adhesive tape. Two types of freshly excised porcine GI tissues (ie, stomach and large intestinal tissues) were obtained from a local slaughterhouse (Auckland, New Zealand). The tissues were washed with deionised water and kept in saline solution at 4 °C prior to use within 3 hours. Before testing, the underlying connective tissues were carefully removed to isolate only the mucosal membrane.

In contrast with the setting by Thirawong et al., my experiment aimed to evaluate the mucoadhesive property of Ca^{2+} cross-linked gel surface of the alginate disc.

Therefore, four types of surfaces were prepared from the alginate discs. The preparation consisted of one or several sequential steps of soaking treatment of the disc surface, which is elaborated in Table 6.2 for each type of surface.

Table 6.2 Soaking treatments for the preparation of the four types of surfaces for the *ex vivo* tensile test.

Surface type	Sequence of the soaking treatments (left to right)			
	In deionised water	In 0.1 M CaCl ₂	In the chitosan coating solution	In the thiolated-chitosan coating solution
Alginate polymer surface	15 min	-	-	-
Ca-alginate gel surface	15 min	10 min	-	-
Chitosan coated Ca-alginate gel surface	15 min	10 min	15 min	-
Thiolated chitosan coated Ca-alginate gel surface	15 min	10 min	-	15 min

After the formation of the desired surface, the alginate disc was rinsed with deionised water. The probe with the disc attached was then immersed in the GI fluid (ie, SGF or SIF) for 10 min for equilibration. To begin the test, the disc was moved downward at 0.5 mm/s to contact with the GI tissue. When the probe touched the GI tissue, the speed of the probe was reduced to 0.1 mm/s while the contact force increased. The probe kept moving until the contact force reached 0.1 N. The contact force was then maintained at this level for 30 s. Subsequently, the probe was withdrawn at 0.1 mm/s to its original position where the disc was completely separated from the below tissue. During the process, force applied on the disc was recorded and mucoadhesion was

observed as the measured force that held down the withdrawing probe (moving up). Two characteristic parameters were calculated from the force vs. time plot using Texture Exponent 32 software. They were the maximum force required to separate the probe from the tissue (i.e. maximum detachment force: F_{\max}) and the total work involved in the probe withdrawal from the tissue (work of adhesion: W_{ad}).

Mucoadhesion at two simulated GI sites (i.e., stomach and colon) were separately tested using the porcine stomach tissue in combination with the SGF, and the porcine colonic tissue in combination with the SIF. Two testing conditions, including tests in the GI fluid (condition A) and tests with the GI fluid removed after the initial equilibration (condition B), were applied.

6.2.8. *In vitro* mucoadhesion of the probiotic microcapsules to the mucin-secreting HT-29-MTX colonic epithelial culture

The mucoadhesion performance of the probiotic microcapsules coated with chitosan or thiolated chitosan was finally surrogated using a well-established model of human mucin-secreting colonic cells, HT29-MTX cells in culture. The HT29-MTX cell line was kindly provided by Bioactives Research New Zealand (Auckland, New Zealand). HT29-MTX cells were routinely grown in Dulbecco's Modified Eagle Medium (DMEM Glutamax, Gibco, USA) containing 4.5 g/L glucose and supplemented with 25 mmol/L HEPES buffer and 10% (v/v) fetal bovine serum (heat inactivated at 60 °C for 45 min, Invitrogen, USA). The cells were kept at 37 °C in controlled atmosphere of 5% CO₂ and 95% air. The culture medium was changed every 2 days.

For adhesion assays, HT29-MTX cells were first seeded into 12-well plates (Costar) at a density of 5×10^4 cells/cm². The cells were allowed to grow until post confluence. For subsequent visual evaluation, the probiotic microcapsules loaded with *L. reuteri*

DPC16 bacteria were labelled with cFDA following a previously described method [88]. The labelled microcapsules were washed, and then suspended with the SIF. The monolayers of HT29-MTX were washed twice with PBS, before suspension in the SIF. Aliquots of probiotic microcapsules (equivalent to 10^9 CFU *L. reuteri* DPC16) were added, and the plates were incubated at 37 °C in the modified atmosphere for 1 h for adhesion to take place. After incubation, each well was gently washed twice with 1 mL SIF to remove the non-adhering microcapsules. Fluorescent microscopic observation was carried out at this stage to visualize the mucoadhesion performance. To estimate the count of *L. reuteri* DPC16 in the adhered microcapsules, the monolayers were trypsinized to separate HT29-MTX cells and the adhered microcapsules from the well. The immobilized *L. reuteri* DPC16 was released by suspending the microcapsules in 0.2 M sodium citrate and exposing to an ultrasonic homogenizer at 20 kHz for 30 s with a 10-s rest interval. The samples were kept on ice at all times to avoid heat. The released bacteria were confirmed by light microscopy and counted by plating on MRS agar. The concentration of HT29-MTX cells in the monolayer was determined by trypsinizing the cells at 37 °C for 10 min, and counting on a hemocytometer.

The probiotic microcapsules, with either chitosan or thiolated chitosan coating treatment for 0, 30, 180, 720 min, were assayed for the performance of adhesion.

6.2.9. Statistical analysis

All experiments were run in triplicate. Comparisons between two groups were carried out with Student's *t* test. A *P* value of 0.05 or less was taken as significant.

6.3. Results

6.3.1. Adsorption of chitosan on alginate microcapsules

Chitosan could be uniformly adsorbed on the surface of alginate microspheres. In Figure 6.1, the green fluorescence uniformly illuminated all the microcapsules, whereas a particular layer near the surface was clearly distinguished by the enhanced fluorescent intensity. The diverse polarities between the two materials were hence proven to be able to induce the formation of chitosan coating.

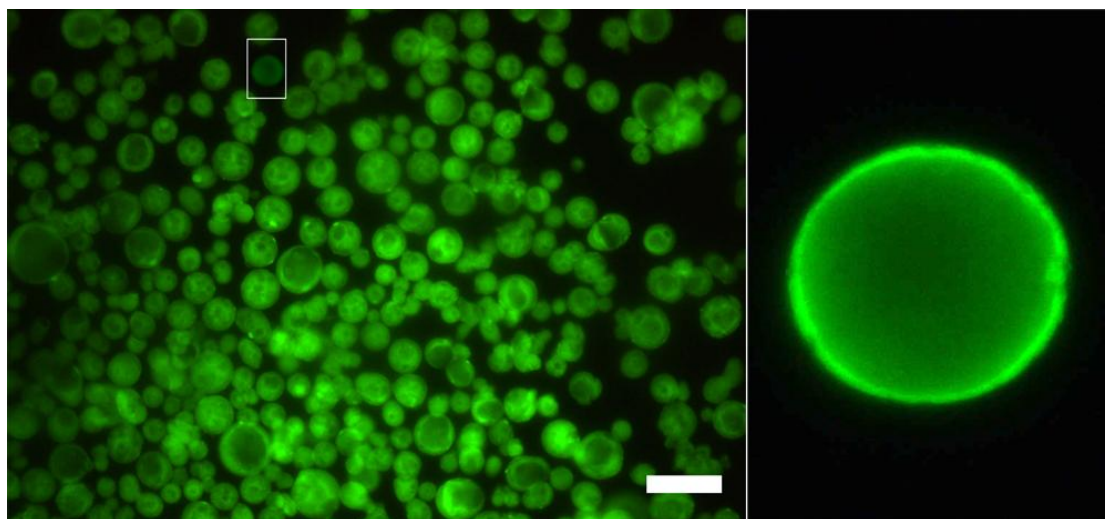


Figure 6.1 The fluorescent microscopy (x100) of the Ca^{2+} -alginate microcapsules coated by FITC-conjugated chitosan. The coating treatment lasted 3 hours. The bar indicates 100 μm . The photo to the right shows the detailed single microcapsule (x400) marked by the white rectangle in the left photo.

The flow cytometric analysis revealed the time-dependant chitosan adsorption on Ca^{2+} -alginate microcapsules. Histograms of FL1 channel in Figure 6.2(a) clearly showed the FITC intensity of microcapsule population moved to higher magnitude with increasing duration of coating treatment. In Figure 6.2(b) and Figure 6.2(c), no significant changes were detected in the FSC (particle size) and the SSC (particle complexity) channels. It evidenced that the increase in the fluorescent intensity was not due to aggregation of microcapsules, but due to increasing amount of FITC-

chitosan adsorbed on the microcapsules. Figure 6.2(d) presents a detected population of microcapsules on the FSC vs. SSC plot. The polygon gate was created to distinguish the subpopulation of single microcapsules and was used for the calculation of average intensity.

The increase of average FITC intensity was plotted against the duration of coating treatment in Figure 6.2(e). The adsorption was found to be faster in the initial 180 min and continue until the end of the examination. In Figure 6.3, the zeta-potential measurement also confirmed an increasing surface charge of microcapsules for both the chitosan coated and the thiolated-chitosan coated samples. Uncoated Ca^{2+} -alginate microcapsules had negative surface charge of -55 mV, while adsorbed chitosan (or thiolated chitosan) rapidly converted the negative surface charge to positive within 30 min. The most rapid increase of surface charge was observed in the initial 180 min and the zeta-potential of coated microcapsules reached around +50 mV at last.

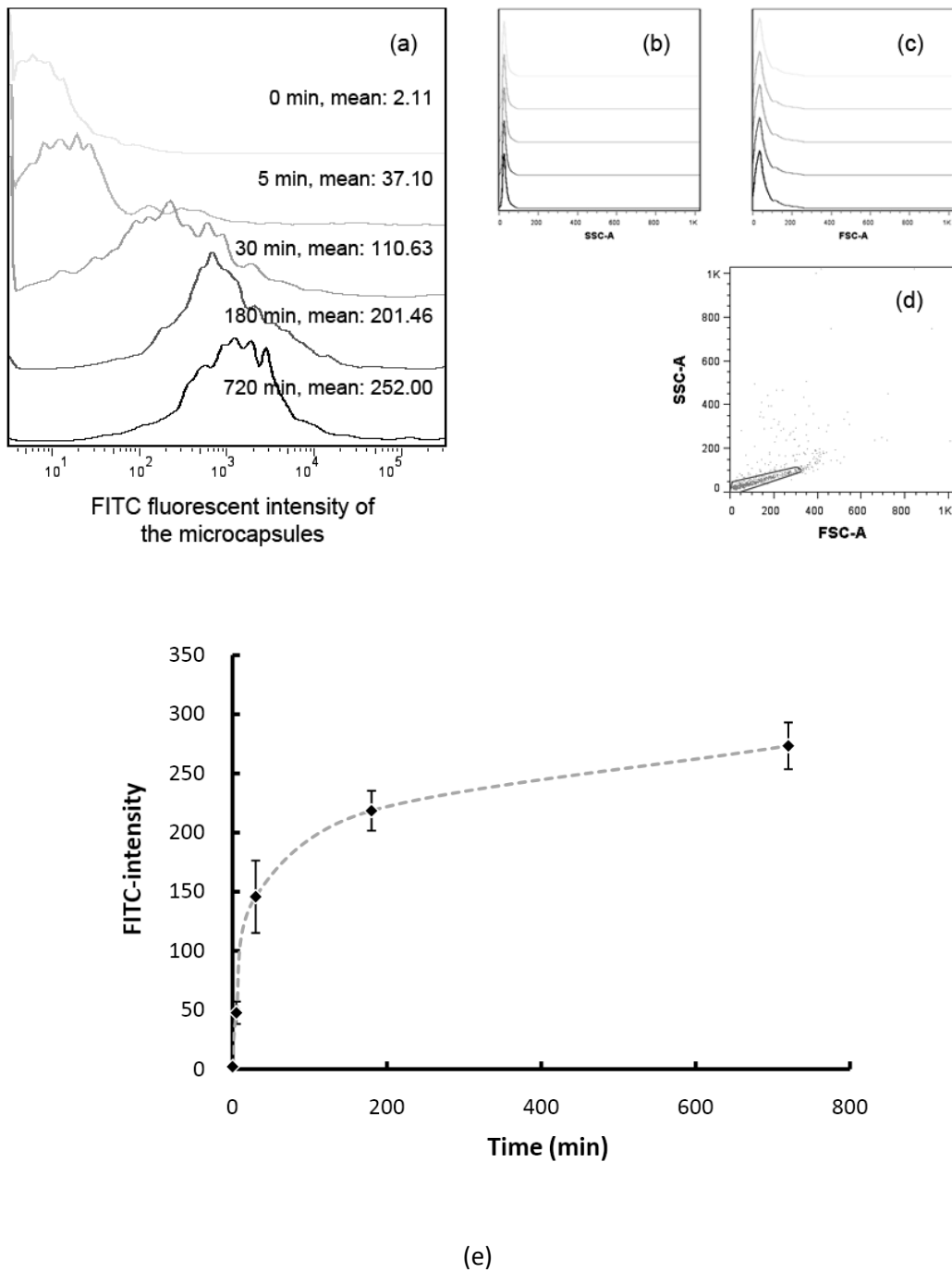


Figure 6.2 Flow cytometric (FCM) analysis of FITC-conjugated chitosan adsorbed on the Ca-alginate microcapsules: (a) the fluorescent intensity of the FITC-chitosan coated microcapsules at different time point of coating treatment; (b) and (c) The histograms of the side scatter (SSC) and the forward scatter (FSC) readings of the samples; (d) the SSC vs. FSC plot of the microcapsules detected by FCM; and (e) average FITC-fluorescent intensities of the microcapsules that were exposed to various durations of coating treatment.

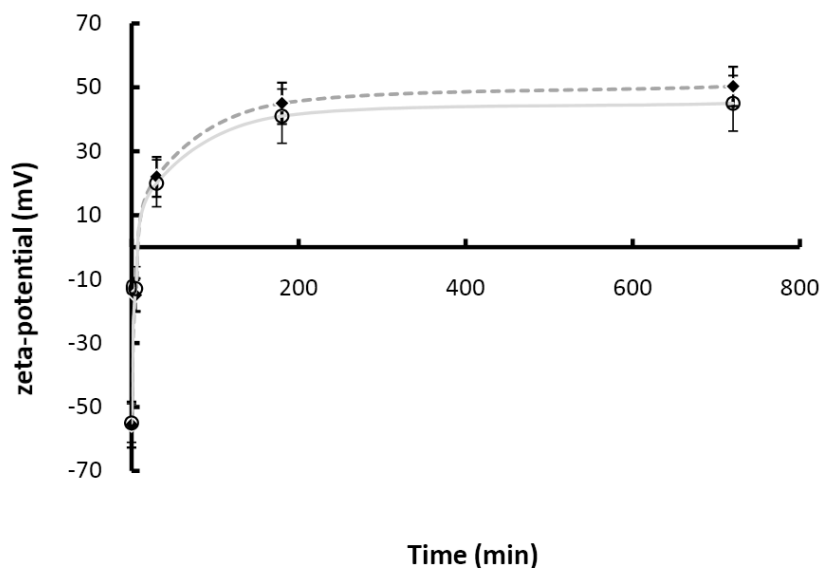


Figure 6.3 Zeta-potential of the chitosan or the thiolated chitosan coated microcapsules that were exposed to different duration of the coating treatments.

6.3.2. Synthesis of thiolated chitosan and confirmation of the presence of thiol groups

The ATR-FTIR spectra of original chitosan, thiolated chitosan and 2-iminothiolane (the thiolating agent) were illustrated in Figure 6.4. The spectrum of thiolated chitosan shares a lot of common features with the one of original chitosan. The successful conjugation of thiol groups into thiolated chitosan was clearly evidenced by the additional peaks at $\sim 2550\text{ cm}^{-1}$ and $\sim 709\text{ cm}^{-1}$, which were assigned to S-H stretch and C-S stretch, respectively [274]. Compared to original chitosan, the peaks of amine and amide of thiolated chitosan slightly shifted from 1629 cm^{-1} and 1525 cm^{-1} to 1635 cm^{-1} and 1553 cm^{-1} , respectively, which agreed with the report by Jiang et al. [275]. In addition, the thiol content of thiolated chitosan was estimated by Ellman's reagent as $130 \pm 16\text{ }\mu\text{mol/g}$.

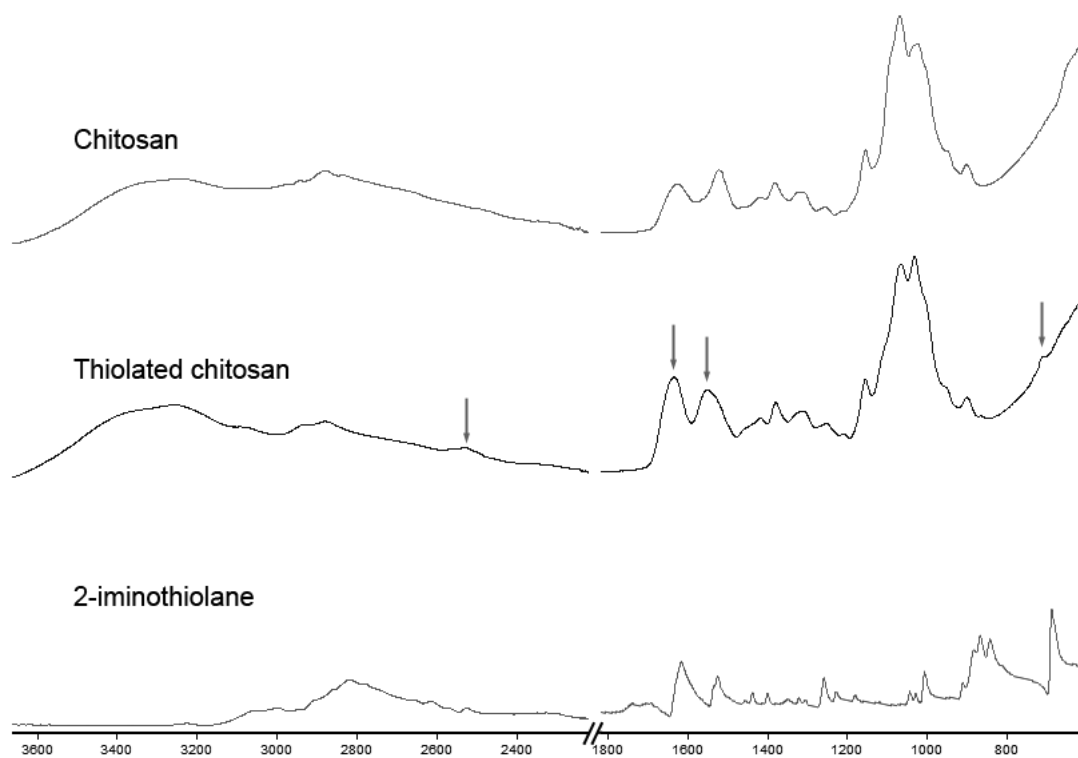


Figure 6.4 ATR-FTIR spectra of original chitosan, thiolated chitosan and 2-iminothiolane (the thiolating agent).

6.3.3. Evaluation of the bio-/muco-adhesion of chitosan and thiolated chitosan

6.3.3.1. Viscosity synergism of polymers and mucin

The method of viscosity measurements described by Suknuntha et al. [273] was used to evaluate the mucoadhesive interactions between mucin and polymers (chitosan and thiolated chitosan). The componential force of mucoadhesion in the system was estimated based on the change of measured viscosity according to the following equations:

$$\eta_{ad} = \eta_t - \eta_m - \eta_p,$$

$$F = \eta_{ad}\sigma,$$

where η_t is the total viscosity of the blend system, η_m and η_p are the componential viscosities of pure mucin and polymer, respectively, η_{ad} is the componential viscosity

contributed by mucoadhesive interactions, F is the calculated force of mucoadhesion at the shear rate σ (in this case 20 s^{-1}).

The viscosity and mucoadhesion data describing the mixture systems in either SGF or SIF are listed in Table 6.3. Force of mucoadhesion was found to increase with the concentration of the mucoadhesive polymer. The force was also higher in SIF (pH 6.5) than in SGF (pH 1.2). It indicates that both mucoadhesive materials can render stronger adhesion to mucus in near neutral environment (e.g., the lower GI tract). In addition, thiolated chitosan was found to elicit stronger mucoadhesion than the original chitosan at all concentrations, in both SGF and SIF.

Table 6.3 Viscosity of mucin (η_m) plus polymer (η_p), the blend system (η_t), the calculated viscosity of mucoadhesion (η_{ad}) and the calculated force of mucoadhesion (F). Test was done in SGF and SIF with 5% mucin and various concentrations of chitosan or thiolated chitosan at 37 °C using a shear rate of 20 s⁻¹. Measured results are presented as mean \pm standard deviation (n =3).

Combination of mucin and polymer	Measured viscosity		calculated η_{ad}	Calculated F (dyne/cm)
	$\eta_m + \eta_p$	η_t		
<i>In SGF pH 1.2</i>				
Mucin 5% + Chitosan 0.5%	26.12 \pm 0.13	31.77 \pm 0.53	5.65	1.13
Mucin 5% + Chitosan 0.1%	22.83 \pm 0.15	26.17 \pm 0.38	3.33	0.67
Mucin 5% + Chitosan 0.05%	22.23 \pm 0.32	25.23 \pm 0.32	3.00	0.60
Mucin 5% + Thiolated Chitosan 0.5%	61.97 \pm 1.00	71.52 \pm 0.47	9.56	1.91
Mucin 5% + Thiolated Chitosan 0.1%	30.07 \pm 0.40	36.43 \pm 0.45	6.37	1.27
Mucin 5% + Thiolated Chitosan 0.05%	26.13 \pm 0.32	31.50 \pm 0.50	5.36	1.07
<i>In SIF pH 6.5</i>				
Mucin 5% + Chitosan 0.1%	38.80 \pm 0.26	74.77 \pm 0.32	35.97	7.19
Mucin 5% + Chitosan 0.01%	19.78 \pm 0.19	45.63 \pm 0.40	25.85	5.17
Mucin 5% + Thiolated Chitosan 0.1%	48.94 \pm 0.05	94.40 \pm 0.69	45.46	9.09
Mucin 5% + Thiolated Chitosan 0.01%	20.74 \pm 0.28	51.36 \pm 0.41	30.63	6.13

The flow behaviour of blend system (polymer and mucin) was also fitted to the Ostwald-de Waele rheological model (also known as power law model):

$$\eta = K\dot{\gamma}^{n-1},$$

where η denotes the viscosity of the blend system, $\dot{\gamma}$ denotes the shear rate. Consistency K and flow index n are two key parameters characterizing individual system.

The values of K and n of all samples are listed in Table 6.4. The n values are all less than 1 indicating that these samples exhibited a non-Newtonian pseudoplastic (shear thinning) behaviour. K is numerically equal to the viscosity of the blend system at a shear rate of 1 s^{-1} . Greater K values were observed in the presence of the polymers when compared to mucin alone in both SGF and SIF, which demonstrated good synergism between these polymers and mucin. Also as shown by the results, K values became larger when increasing the concentration of polymer. Such increase of K value was more pronounced in SIF even at reduced concentration of the polymers, suggesting a feature of site-response. In addition, thiolated chitosan samples uniformly gave higher K values compared to original chitosan, thus indicating a moderately superior mucoadhesive property.

Table 6.4 Power law index (n) and consistency index (K) of chitosan or thiolated chitosan at various concentrations in SGF or SIF with or without mucin, derived from the Ostwald-de Waele rheological model (mean \pm standard deviation, $n = 3$).

Sample	Flow behaviour index n		Consistency index K	
	Polymer	Polymer+Mucin	Polymer	Polymer+Mucin
<i>In SGF pH 1.2</i>				
Mucin 5%	-	-	0.75 \pm 0.02	46.70 \pm 2.89
Mucin 5% + Chitosan 0.5%	0.57 \pm 0.02	0.72 \pm 0.02	14.19 \pm 1.23	74.62 \pm 3.01
Mucin 5% + Chitosan 0.1%	0.59 \pm 0.01	0.73 \pm 0.01	2.84 \pm 0.12	58.49 \pm 2.19
Mucin 5% + Chitosan 0.05%	0.59 \pm 0.01	0.74 \pm 0.02	1.42 \pm 0.09	55.57 \pm 1.90
Mucin 5% + Thiolated Chitosan 0.5%	0.62 \pm 0.02	0.54 \pm 0.01	113.23 \pm 6.77	245.04 \pm 19.45
Mucin 5% + Thiolated Chitosan 0.1%	0.64 \pm 0.01	0.64 \pm 0.01	22.65 \pm 1.59	117.28 \pm 10.23
Mucin 5% + Thiolated Chitosan 0.05%	0.65 \pm 0.02	0.66 \pm 0.02	11.32 \pm 1.05	88.73 \pm 3.89
<i>In SIF pH 6.5</i>				
Mucin 5%	-	-	0.80 \pm 0.02	32.34 \pm 1.29
Mucin 5% + Chitosan 0.1%	0.29 \pm 0.01	0.53 \pm 0.01	165.14 \pm 20.34	302.43 \pm 24.33
Mucin 5% + Chitosan 0.01%	0.31 \pm 0.02	0.63 \pm 0.02	16.51 \pm 2.01	139.69 \pm 8.65
Mucin 5% + Thiolated Chitosan 0.1%	0.27 \pm 0.01	0.53 \pm 0.01	264.38 \pm 18.73	386.41 \pm 21.48
Mucin 5% + Thiolated Chitosan 0.01%	0.29 \pm 0.02	0.67 \pm 0.02	26.44 \pm 2.27	93.36 \pm 5.15

6.3.3.2. Mucoadhesion of various alginate-gel surfaces assayed by *ex vivo* tensile test using freshly excised porcine tissue strip model

The results of the *ex vivo* mucoadhesion assay of the four types of mucoadhesive surfaces were given in Table 6.5.

Greater total work was observed under Condition B (i.e., the GI fluid was only used for equilibrating the surface and the tissue, and was removed before the test) among all samples compared to Condition A (i.e., the test took place in the presence of the GI fluid). It conforms to the finding by Varum et al. [276], which suggested that stronger mucoadhesion occurred when the hydrating fluid came from the mucus layers, rather than from the surrounding medium.

Calcium ion cross-linked alginate gel generally displayed the lowest mucoadhesion among all the four types of surfaces. In particular, nearly no effect of mucoadhesion was observed for Ca²⁺-alginate surface to the porcine colonic tissue in SIF. The finding therefore supports the argument that Ca²⁺-alginate microcapsule may not be a competent mucoadhesive vehicle for the purpose of prolonged retention of probiotic bacteria.

On the other hand, coating of chitosan or thiolated chitosan conferred the Ca²⁺-alginate surface an improved mucoadhesiveness, especially in environments simulating the colon. Considering the case of mucoadhesion to porcine colonic tissue under Condition A, both coatings markedly raised the F_{\max} and W_{ad} compared to the near absence of mucoadhesion on the uncoated Ca²⁺-alginate surface. The enhancement under Condition B also reached 2.4-fold via chitosan coating and 3.1-fold via thiolated chitosan coating. However, in the case of adhesion to porcine stomach mucus, the difference between the uncoated Ca²⁺-alginate surface and the

chitosan coated Ca^{2+} -alginate surface was only subtle ($P > 0.05$). By contrast, the thiolated chitosan coating elicited a significantly higher effect of mucoadhesion compared to the other two ($P < 0.01$).

For comparison, alginate surface without any treatment was also evaluated for its mucoadhesiveness. It exhibited an improved mucoadhesion at elevated medium pH values. It also displayed the highest mucoadhesion to the colonic tissue among all samples.

Table 6.5 The maximum detachment force and the total work to detach certain mucoadhesive surface from porcine GI tissue, as measured by a texture analyzer.

Four types of mucoadhesive surfaces included alginate, Ca²⁺-alginate, chitosan coated Ca²⁺-alginate and thiolated chitosan coated Ca²⁺-alginate. Two testing conditions were Condition A (i.e., the surface and the animal tissue were equilibrated in the GI fluid and the detachment took place in the presence of the GI fluid.) and Condition B (i.e., the surface and the animal tissue were equilibrated in the GI fluid, but the detachment took place after the GI fluid was removed.).

Surface type	SGF (pH 1.5), porcine stomach tissue		SIF (pH 6.8), porcine colonic tissue	
	Maximum detachment force (mN)	Total work (μ J)	Maximum detachment force (mN)	Total work (μ J)
<i>Condition A:</i>				
Alginate	6.96 \pm 5.70	3.91 \pm 5.52	77.86 \pm 11.01	54.50 \pm 11.00
Ca-alginate	8.95 \pm 0.81	1.94 \pm 2.00	3.87 \pm 0.78	0.02 \pm 0.01
Chitosan coated Ca-alginate	10.43 \pm 1.24	2.00 \pm 0.12	20.46 \pm 3.18	5.85 \pm 0.59
Thiolated chitosan coated Ca-alginate	20.36 \pm 1.56	4.00 \pm 0.70	25.38 \pm 1.91	8.30 \pm 1.07
<i>Condition B:</i>				
Alginate	92.51 \pm 17.17	55.88 \pm 5.94	134.78 \pm 25.44	145.65 \pm 10.91
Ca-alginate	34.80 \pm 2.86	41.62 \pm 6.27	25.54 \pm 2.37	25.74 \pm 0.95
Chitosan coated Ca-alginate	23.23 \pm 1.40	32.10 \pm 0.54	48.35 \pm 2.66	37.54 \pm 2.01
Thiolated chitosan coated Ca-alginate	30.89 \pm 2.00	33.61 \pm 3.42	61.32 \pm 4.68	48.26 \pm 5.00

6.3.3.3. Adhesion of the chitosan and the thiolated chitosan coated probiotic microcapsules to mucin-secreting HT-29-MTX colonic epithelial monolayer

The data showing the capability of the microcapsules to adhere to the mucin-secreting HT-29-MTX colonic epithelial monolayer are given in Table 6.6. Photos of the microscopic observations are also presented in Figure 6.5 for visual evaluation. The results clearly show that the extra coatings of chitosan or thiolated chitosan significantly improve the adhesion of the microcapsules to the model colonic epithelial monolayer. The adhesion efficiency was also found to increase with the duration of coating treatment. Compared with chitosan, thiolated chitosan coating was able to provide improved performance of mucoadhesion, thus retaining more *L. reuteri* DPC16 to the epithelial monolayer.

Table 6.6 Counts of *L. reuteri* DPC16 released from the adhered microcapsules with chitosan coating (A) or thiolated chitosan coating (B) to HT29-MTX monolayer. Durations of exposure to each coating solution (A or B) were 0, 30, 180 and 720 min for sample 1 to 4 respectively. Results were given as mean \pm standard deviation (n = 3) and the average percentage of total applied bacteria (1×10^9 CFU).

#	Coating duration (min)	Chitosan coating (A)		Thiolated chitosan coating (B)	
		Count of <i>L. reuteri</i> DPC16 in adhered microcapsules (log CFU/mL)	% of total applied bacteria	Count of <i>L. reuteri</i> DPC16 in adhered microcapsules (log CFU/mL)	% of total applied bacteria
1	0	4.66 \pm 0.03	0.00%	4.67 \pm 0.06	0.00%
2	30	6.76 \pm 0.02	0.57%	6.91 \pm 0.01	0.82%
3	180	8.25 \pm 0.02	17.98%	8.42 \pm 0.05	26.21%
4	720	8.58 \pm 0.02	38.30%	8.69 \pm 0.02	48.62%

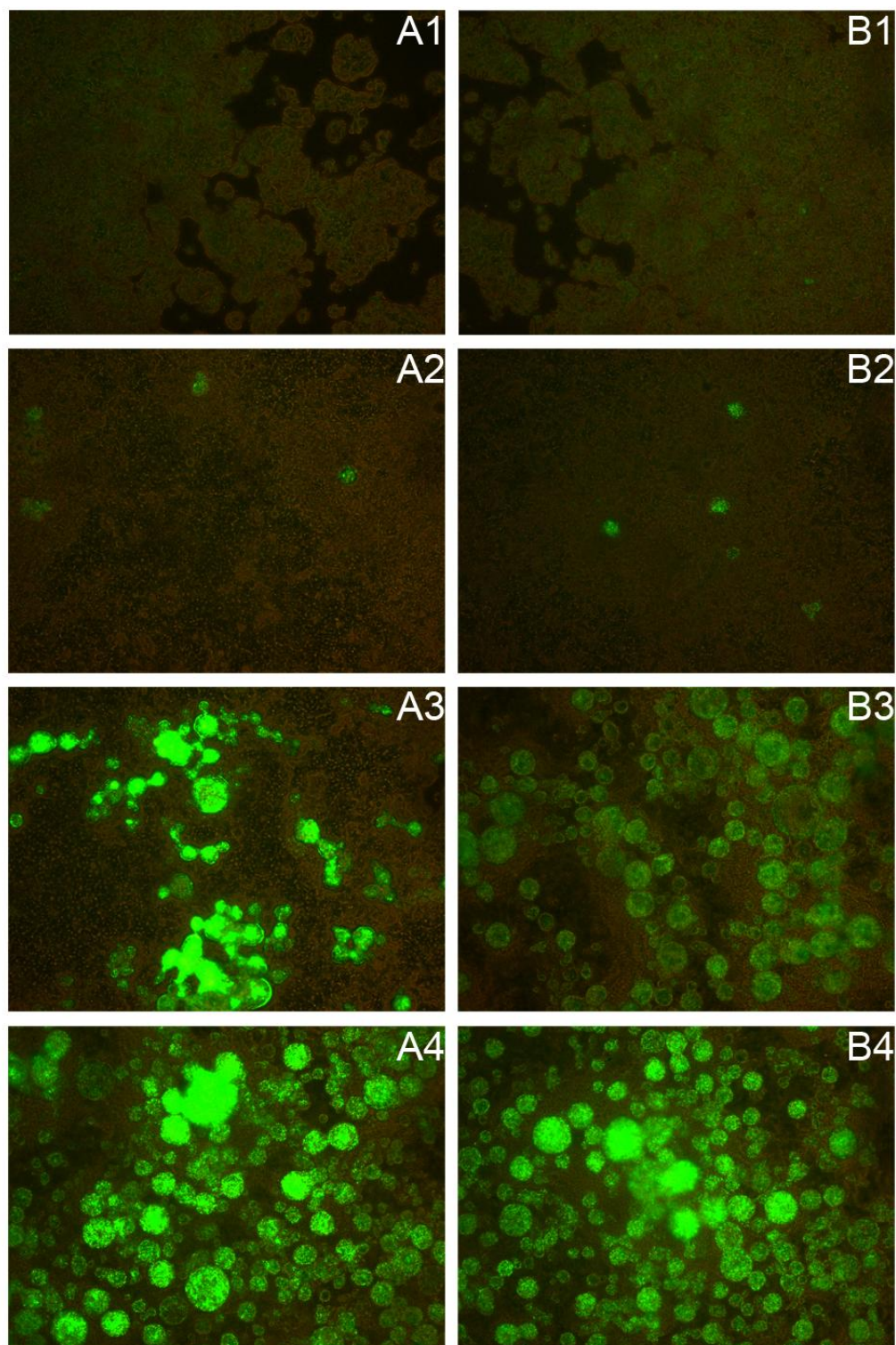


Figure 6.5 Epi-fluorescent microscopy of the adhered microcapsules to HT29-MTX monolayer. The microcapsules immobilized cF-labelled *L. reuteri* DPC16 (green fluorescence). A's denote samples with chitosan coating and B's denote samples with thiolated chitosan coating. Numbers 1 to 4 indicate the various durations of exposure to the according coating solution: 0, 30, 180 and 720, respectively.

6.4. Discussion

In the current study, the reduction in mucoadhesive property of Ca^{2+} cross-linked alginate gel was innovatively demonstrated in the *ex vivo* tensile test, using the texture analyzer. It therefore justifies the need of extra mucoadhesive coating on alginate-based probiotic microcapsule, in order to achieve desired retention in the GI tract. Although chitosan coating was previously reported to reinforce alginate vehicles for the delivery of probiotics and improve the survival of immobilized bacteria [88, 269], its contribution in enhancing the mucoadhesive property of such delivery vehicle was, to the best of my knowledge, for the first time, evaluated in the current study. Thiolated chitosan, as a second generation of mucoadhesive material which can form strong covalent bonds with mucin, was also evaluated for its potential use in probiotic microcapsules. The results confirmed the enhancement of mucoadhesion performance achieved by chitosan and thiolated chitosan coatings. Thiolated chitosan also displayed significantly higher mucoadhesiveness in comparison with unmodified chitosan. Interestingly, Bernkop-Schnürch et al [270] reported that Chitosan-TBA (the thiolated chitosan via 2-iminothiolane, the same type of thiolated chitosan as prepared in the current study) could reach more than 140 folds improvement of its mucoadhesive property, as compared to unmodified chitosan. However, such a high improvement ratio was not observed in my study, although the thiol contents of the two thiolated chitosan samples were of similar level ($\sim 100 \mu\text{mol/g}$). This discrepancy could result from the different experimental designs or the dissimilarity between the testing formulations. But it may also be open to other explanation. Davidovich-Pinhas et al. [277] claimed that hydration could lead to deactivation of conjugated thiol groups due to formation of inter-molecular disulfide junctions, before they contacted active bond-forming sites in mucin. This could be true considering my own case, whereby we allowed an

equilibration period (in the GI fluid) before performing each detachment test. However, it was also suggested that thiol-disulfide exchange reaction (i.e., intermolecular disulfide bonds of polymer reacting with thiol groups in mucin polymer.) could still happen to mediate the interaction between polymer and mucin [156], although the extent may be very limited. Nevertheless, the extra coating of chitosan was demonstrated to achieve improved mucoadhesion, even without the capacity to form strong disulfide bonds with mucin.

In the *in vitro* adhesion to HT29-MTX colonic epithelial monolayer, the mucoadhesive coating of chitosan or thiolated chitosan significantly enhance the mucoadhesive property of the probiotic microcapsule. It is considered to render the ingested probiotic bacteria some extra support, after they have been exposed to the challenges in the upper GI tract. The adhesion of probiotic strains to intestinal mucosa could be affected due to the alteration in the structures present on the surface of the bacteria. It was demonstrated that industrial processing, prolonged storage and exposure to the bio-barriers of the GI tract could induce conformational changes in cell membrane of probiotic strains and therefore reduce their adhesion particularly of sensitive strains in the lower GI tract [278-280]. Prolonged retention provided by the probiotic delivery system is hence an advantage, considering the exhausted state of those strains when they reach the site of function. For comparison, the model probiotic strain *L. reuteri* that we used in the current study was reported to have an adhesion efficiency of approximate 14 CFU/epithelial cell to HT-29 monolayer [255], which equals a concentration of 6.82 log CFU/mL (estimated calculation based on a HT-29 cell count of 4.8×10^5 cells as measured in the current assay). Referring to the results of probiotic microcapsules, 30-min treatment of coating with either chitosan or thiolated chitosan could achieved a

concentration of similar level (6.76 – 6.91 log CFU/mL). Prolong coating treatment above 3 h could further elicit more than 80 - 150 fold enhancement.

The coating of chitosan or thiolated chitosan on the surface of Ca²⁺-alginate microsphere is due to the electrostatic interaction between the reversely charged polyelectrolytes. The zeta-potential analysis revealed that the adsorption could continue, even after the maximum (+50 mV) was reached at around 3 hours. The results were consistent with the findings by Guo and Gemeinhart [281] who also suggested that subsequent layers of chitosan were formed on the first monomolecular adsorption layer, and intertwinement of separate chitosan molecules could be achieved through hydrophobic interaction, van der Waal's forces and hydrogen bonds. The multi-layer feature of chitosan coating can partly explain the reinforced strength of the sub-100 probiotic microcapsules, which have an increased coating-material-to-core-material ratio.

This enhancement of mucoadhesive property induced by chitosan and thiolated chitosan coatings was demonstrated to be markedly higher in an environment of with a near neutral pH (pH 6.5) and less ambient water. Considering that the amine groups of chitosan and thiolated chitosan, the thiol groups in thiolated chitosan and the functional groups of mucin (e.g. sialic acids and sulfate groups) are mainly ionized at this pH, the electric attraction between the reversely charged macromolecules and the formation of disulfide bonds are expected to reach the optimum states, thus improving the mucoadhesion performance. On the other hand, under a near neutral pH, chitosan and mucin macromolecules are characterized by a more extended conformation, which further favours the interactions between them [282]. Regarding the role of medium water, Varum et al. [276] indicated that stronger interactions occurred when the hydrating fluid came from the mucus layers rather than from the surrounding medium.

It hence justifies that the chitosan or thiolated chitosan coated probiotic microcapsules may show the preferential mucoadhesion to colonic epithelia, where the environmental pH is slight acid neutral, water content is largely mucin-bound (due to the significant absorption of water at colon), and the depth of mucus layer is increased.

In conclusion, cross-linking with calcium ions reduced the mucoadhesive property of alginate hydrogel. Chitosan and thiolated chitosan could be adsorbed on sub-100 μm Ca^{2+} -alginate microcapsule and substantially improved the mucoadhesion performance of the system. The coated system was demonstrated to deliver markedly higher amount of probiotic bacteria to the *in vitro* model of colonic mucosa. The coatings were also found to exert significantly stronger mucoadhesion to colonic mucosa tissue at slight acid neutral pH with less ambient water, which conforms to the physiological environment of the colon, thus supporting prolonged retention in this region.

Chapter 7. General discussion and future directions

All the specific aspects of the current research project have been described and discussed in the previous chapters. In the final chapter, we intend to summarize the main findings and discuss the work and the future directions in a broader context.

7.1. General discussion and conclusions

Since the last decade, research into the health promoting potential of lactic acid bacteria has been receiving much attention by both academic and industrial researchers in New Zealand. Probiotic technologies that focus on enhancing shelf-stability and *in-vivo* efficacy, such as microencapsulation, are also the popular subject of active research in New Zealand [2]. On the other hand, the improved level of consumer awareness of different types of probiotics and the health claims for probiotic products also drive research efforts into the development of efficient technologies for the delivery of probiotic benefits to end-consumers [283]. Probiotics can be delivered commercially either as nutritional supplements, pharmaceuticals or foods. International standards require that products that are claimed to be “probiotic products” contain a minimum of 10^7 viable probiotic bacteria per gram of product or 10^9 cells per serving size when consumed [261]. However, many products fail to meet these requirements due to inactivation of probiotic cells in food products during storage, even at refrigerating temperatures. Consequently, the industrial demand for technologies ensuring stability of probiotics in foods remains strong. That also leads to the development of immobilized

cell technology to produce probiotics with increased cell resistance to environmental stress factors [76, 261].

In the current research, the goal was to develop a colonic delivery system for probiotic bacteria based on chitosan coated Ca^{2+} -alginate microcapsules, which are also characterized by the reduced dimension of sub-100 μm and enhanced mucoadhesiveness. As suggested in the review, the reduced size of sub-100 μm may provide multiple advantages for the colonic delivery of probiotics featuring prolonged retention in the lower GI tract. However, it was also demonstrated that reducing the size of microcapsules almost depleted the physical protection of chitosan-reinforced Ca^{2+} -alginate matrix on all the examined probiotic strains, when such probiotic microcapsules were exposed to the challenges of the simulated human bio-barriers, i.e. gastric acid and bile salts. To overcome the drawback, two selected protectants (sucrose and lecithin vesicles) were proposed to reinforce protection in the GI tract. Flow cytometry, in combination with fluorescent-probes, was recruited to quantitatively compare the physiological damages inflicted by GI stress factors in the presence or the absence of the protectants. The results showed a universally positive improvement in GI survival among all the examined LAB strains. After being incorporated into the wall materials of the microcapsules, these protectants were confirmed to compensate for the otherwise attenuated protection by polymeric matrix of reduced dimension. The novel probiotic delivery system based on sub-100 μm polysaccharide microcapsules was demonstrated to be a competent vehicle for the delivery of probiotics if the proper modifications were applied [88].

Another poorly addressed issue by previous studies is the mucoadhesive property of polysaccharide-based probiotic delivery systems. Probiotic delivery system is preferred to have a prolonged retention in the lower GI tract, whereby entrapped probiotic cells

can be efficiently and continuously released so as to achieve longer transient existence or better colonisation. Mucoadhesive materials are often utilized to reach such prolonged retention in many pharmaceutical applications. Natural polysaccharides, such as alginate and pectin, display intrinsic mucoadhesive property. Probiotic delivery systems based on these polysaccharides are apparently considered to inherit the mucoadhesive property by many researchers. However, this is not always true. My study on the Ca^{2+} -alginate gel showed that the ionotropic gelling reaction between calcium ions and alginate molecules sharply lowered the mucoadhesive performance of the gels. It therefore justified my seeking alternative materials for enhanced mucoadhesion. Chitosan and thiolated chitosan coatings were evaluated for this purpose. The results from several different *in vitro* methods collectively indicated that the mucoadhesive property of the coated systems was markedly increased compared to the uncoated counterparts. Interestingly, the mucoadhesive property of the coated gel systems also showed significant variation in response to environmental pH and water content. Higher mucoadhesion occurred at near-neutral pH with less ambient water, which conforms to the physiological environment of colon. It therefore indicates the potential of the current design for targeted adhesion to colonic mucosa.

In addition, stability of probiotic bacteria in the delivery system during possessing and subsequent storage was evaluated by freeze-drying the model strains and exposing them to an accelerated storage test. This part of research may contribute to the development of probiotic products with a satisfactory shelf-stability in the future. The accelerated storage test proved to be a reliable modelling technique for the prediction of shelf-stability of probiotics, whilst it was also demonstrated to be useful for the evaluation of different strategies for preserving these probiotic cells.

Intriguingly, in one of the current studies, the probiotic delivery system induced an altered behaviour of the entrapped model strain *L. reuteri* DPC16 in regard to its *in vitro* productivity of the metabolite - reuterin. Nevertheless, it may not constitute a real problem, in that we also demonstrated that the entrapped bacteria could be efficiently and rapidly released in colon. However, it is worth a consideration that probiotic functionality in encapsulation may be subject to variation. *In vivo* confirmation should be obtained especially for preferred therapeutic effects in pharmaceutical applications.

In conclusion, the four objectives identified at the beginning of the project (as listed in Section 1.2) have been achieved and individually elaborated in the previous chapters. The novel colonic delivery system for probiotic LAB was successfully developed according to the specified requirements and proved to be effective and efficient.

7.2. Future directions

As above mentioned, the *in vivo* confirmation of probiotic effects for the delivery system was beyond the scope of this research because of time constraints. In particular, it may be better to seek such confirmation in terms of individual strains, for which prophylactic or therapeutic functions are known. It will also be very promising to test this probiotic delivery system in inflammatory-bowel-disease (IBD) induced animal models, since probiotics have been suggested to render a positive influence.

The many ingredients in the formula of wall materials and the multiple parameters in the process of preparing the microcapsule-based probiotic delivery system open up the possibility of optimisation. Response surface methodology (RSM) in combination with design of experiments (DOE) may serve as useful tools for this practise.

Unfortunately, we did not achieve an investigation into the *in vivo* distribution of the probiotic delivery systems in the lower GI tract via γ -scintiphotography technology, due

to time and resource constraints. This will be left for future research, which surely will provide concrete evidence for the performance of the probiotic delivery system in the real world.

Bibliography

1. FAO/WHO. Expert consultation report on evaluation of health and nutritional properties of probiotics in food including powder milk with live lactic acid bacteria. Cordoba, Argentina. 2001.
2. Crittenden R, Bird AR, Gopal P, Henriksson A, Lee YK, Playne MJ. Probiotic research in Australia, New Zealand and the Asia-Pacific region. *Curr Pharm Des.* 2005;11(1):37-53
3. Champagne CP, Fustier P. Microencapsulation for the improved delivery of bioactive compounds into foods. *Curr Opin Biotechnol.* 2007;18(2):184-90. [doi:10.1016/j.copbio.2007.03.001]
4. Kailasapathy K. Microencapsulation of probiotic bacteria: technology and potential applications. *Curr Issues Intest Microbiol.* 2002;3(2):39-48
5. Kim KI, Yoon YH, Baek YJ. Effects of rehydration media and immobilization in Ca-alginate on the survival of *Lactobacillus casei* and *Bifidobacterium bifidum*. *Korean Journal of Dairy Science.* 1996;18
6. Reuter G. Probiotics - possibilities and limitations of their application in food, animal feed, and in pharmaceutical preparations for men and animals. *Berl Munch Tierarztl Wochenschr.* 2001;114:410-9
7. Bezirtzoglou E, Stavropoulou E. Immunology and probiotic impact of the newborn and young children intestinal microflora. *Anaerobe.* 2011;17(6):369-74. [doi:10.1016/j.anaerobe.2011.03.010]
8. Lin DC. Probiotics as functional foods. *Nutr Clin Pract.* 2003;18(6):497-506. [doi:10.1177/0115426503018006497]
9. Sheil B, McCarthy J, O'Mahony L, Bennett MW, Ryan P, Fitzgibbon JJ, et al. Is the mucosal route of administration essential for probiotic function?

- Subcutaneous administration is associated with attenuation of murine colitis and arthritis. *Gut*. 2004;53(5):694-700. [doi:10.1136/gut.2003.027789]
10. Gueniche A, Cathelineau AC, Bastien P, Esdaile J, Martin R, Queille Roussel C, et al. *Vitreoscilla filiformis* biomass improves seborrheic dermatitis. *J Eur Acad Dermatol Venereol*. 2008;22(8):1014-5. [doi:10.1111/j.1468-3083.2007.02508.x]
 11. Gueniche A, Knaudt B, Schuck E, Volz T, Bastien P, Martin R, et al. Effects of nonpathogenic gram-negative bacterium *Vitreoscilla filiformis* lysate on atopic dermatitis: a prospective, randomized, double-blind, placebo-controlled clinical study. *Br J Dermatol*. 2008;159(6):1357-63. [doi:10.1111/j.1365-2133.2008.08836.x]
 12. Peral MC, Martinez MA, Valdez JC. Bacteriotherapy with *Lactobacillus plantarum* in burns. *Int Wound J*. 2009;6(1):73-81. [doi:10.1111/j.1742-481X.2008.00577.x]
 13. Grozdanov L, Raasch C, Schulze J, Sonnenborn U, Gottschalk G, Hacker J, et al. Analysis of the genome structure of the non-pathogenic probiotic *Escherichia coli* strain Nissle1917. *J Bacteriol*. 2004;186:5432-41
 14. Große C, Scherer J, Koch D, Otto M, Taudte N, Grass G. A new ferrous iron-uptake transporter, EfeuU(YcdN), from *Escherichia coli*. *Mol Microbiol*. 2006;62:120-31
 15. Corr SC, Li Y, Riedel CU, O'Toole PW, Hill C, Gahan CGM. Bacteriocin production as a mechanism for the antiinfective activity of *Lactobacillus salivarius* UCC118. *Proc Natl Acad Sci USA*. 2007;104:7617-21
 16. Oelschlaeger TA. Mechanisms of probiotic actions - a review. *Int J Med Microbiol*. 2010;300(1):57-62
 17. Lomax AR, Calder PC. Probiotics, immune function, infection and inflammation: a review of the evidence from studies conducted in humans. *Curr Pharm Des*. 2009;15:1428-518
 18. Pagnini C, Saeed R, Bamias G, Arseneau KO, Pizarro TT, Cominelli F. Probiotics promote gut health through stimulation of epithelial innate immunity. *Proc Natl Acad Sci USA*. 2010;107(1):454-9. [doi:10.1073/pnas.0910307107]

19. Corcoran BM, Stanton C, Fitzgerald G, Ross RP. Life under stress: the probiotic stress response and how it may be manipulated. *Curr Pharm Des.* 2008;14(14):1382-99
20. Gardiner GE, O'Sullivan E, Kelly J, Auty MA, Fitzgerald GF, Collins JK. Comparative survival rates of human derived probiotic *Lactobacillus paracasei* and *L. salivarius* strains during heat treatment and spray drying. *Appl Environ Microbiol.* 2000;66:2605-12
21. Simpson PJ, Stanton C, Fitzgerald GF, Ross RP. Intrinsic tolerance of *Bifidobacterium* species to heat and oxygen and survival following spray drying and storage. *J Appl Microbiol.* 2005;99:493-501
22. van de Guchte M, Serror P, Chervaux C, Smokvina T, Ehrlich SD, Maguin E. Stress responses in lactic acid bacteria. *Antonie Van Leeuwenhoek.* 2002;82:187-216
23. Fernandez Murga ML, De Ruiz Holgado AP, De Valdez GF. Survival rate and enzyme activities of *Lactobacillus acidophilus* following frozen storage. *Cryobiology.* 1998;36:315-9
24. Dumont F, Marechal PA, Gervais P. Cell size and water permeability as determining factors for cell viability after freezing at different cooling rates. *Appl Environ Microbiol.* 2004;70:268-72
25. Arany CB, Hackney CR, Duncan SE, Kator H, Webster J, Pierson M, et al. Improved recovery of stressed *Bifidobacterium* from water and frozen yogurt. *J Food Prot.* 1995;58(10):1142-6
26. Miyoshi A, Rochat T, Gratadoux JJ, Le Loir Y, Oliveira SC, Langella P, et al. Oxidative stress in *Lactococcus lactis*. *Genetics and Molecular Research.* 2003;2(4):348-59
27. Vido K, Diemer H, Van Dorsselaer A, Leize E, Juillard V, Gruss A, et al. Roles of thioredoxin reductase during the aerobic life of *Lactococcus lactis*. *J Bacteriol.* 2005;187(2):601-10. [doi:10.1128/jb.187.2.601-610.2005]
28. Santivarangkna C, Kulozik U, Foerst P. Effect of carbohydrates on the survival of *Lactobacillus helveticus* during vacuum drying. *Lett Appl Microbiol.* 2006;42(3):271-6. [doi:10.1111/j.1472-765X.2005.01835.x]

29. Buitink J, Leprince O. Intracellular glasses and seed survival in the dry state. *C R Biol.* 2008;331(10):788-95. [doi:10.1016/j.crv.2008.08.002]
30. Crowe JH, Carpenter JF, Crowe LM. The role of vitrification anhydrobiosis. *Annu Rev Physiol.* 1998;60(1):73-103. [doi:10.1146/annurev.physiol.60.1.73]
31. Aguilera JM, Karel M. Preservation of biological materials under desiccation. *Crit Rev Food Sci Nutr.* 1997;37(3):287-309
32. Higl B, Kurtmann L, Carlsen CU, Ratjen J, Forst P, Skibsted LH, et al. Impact of water activity, temperature, and physical state on the storage stability of *Lactobacillus paracasei* ssp. *paracasei* freeze-dried in a lactose matrix. *Biotechnol Prog.* 2007;23(4):794-800. [doi:10.1021/bp070089d]
33. Castro HP, Teixeira PM, Kirby R. Storage of lyophilized cultures of *Lactobacillus bulgaricus* under different relative humidities and atmospheres. *Appl Microbiol Biotechnol.* 1995;44(1):172-6
34. Castro HP, Teixeira PM, Kirby R. Changes in the cell membrane of *Lactobacillus bulgaricus* during storage following freeze-drying. *Biotechnology Letters.* 1996;18(1):99-104
35. Teixeira P, Castro H, Kirby R. Evidence of membrane lipid oxidation of spray-dried *Lactobacillus bulgaricus* during storage. *Lett Appl Microbiol.* 1996;22(1):34-8
36. Borst JW, Visser NV, Kouptsova O, Visser AJ. Oxidation of unsaturated phospholipids in membrane bilayer mixtures is accompanied by membrane fluidity changes. *Biochim Biophys Acta.* 2000;1487(1):61-73
37. In 't Veld G, Driessen AJ, Konings WN. Effect of the unsaturation of phospholipid acyl chains on leucine transport of *Lactococcus lactis* and membrane permeability. *Biochim Biophys Acta.* 1992;1108(1):31-9
38. Hood SK, Zottola EA. Effect of low pH on the ability of *Lactobacillus acidophilus* to survive and adhere to human intestinal cells. *J Food Sci.* 1988;53:1514-6
39. Dunne C, Murphy L, Flynn S, O'Mahony L, O'Halloran S, Feeney M, et al. Probiotics: from myth to reality. Demonstration of functionality in animal models of disease and in human clinical trials. *Antonie Van Leeuwenhoek.* 1999;76(1-4):279-92

40. Heuman DM, Bajaj RS, Lin Q. Adsorption of mixtures of bile salt taurine conjugates to lecithin-cholesterol membranes: implications for bile salt toxicity and cytoprotection. *J Lipid Res.* 1996;37(3):562-73
41. Coleman R, Lowe PJ, Billington D. Membrane lipid composition and susceptibility to bile salt damage. *Biochimica et Biophysica Acta (BBA) - Biomembranes.* 1980;599(1):294-300. [doi:10.1016/0005-2736(80)90075-9]
42. Zárte G, Gonzalez S, Chaia AP, Oliver G. Effect of bile on the beta-galactosidase activity of dairy propionibacteria. *Lait.* 2000;80(2):267-76
43. Gómez Zavaglia A, Kociubinski G, Pérez P, Disalvo E, De Antoni G. Effect of bile on the lipid composition and surface properties of bifidobacteria. *J Appl Microbiol.* 2002;93(5):794-9. [doi:10.1046/j.1365-2672.2002.01747.x]
44. Waar K, van der Mei HC, Harmsen HJM, Degener JE, Busscher HJ. Adhesion to bile drain materials and physicochemical surface properties of *Enterococcus faecalis* strains grown in the presence of bile. *Appl Environ Microbiol.* 2002;68(8):3855-8. [doi:10.1128/aem.68.8.3855-3858.2002]
45. Hofmann M, Schumann C, Zimmer G, Henzel K, Locher U, Leuschner U. LUV's lipid composition modulates diffusion of bile acids. *Chem Phys Lipids.* 2001;110(2):165-71. [doi:10.1016/S0009-3084(01)00131-1]
46. Schubert R, Jaroni H, Schoelmerich J, Schmidt KH. Studies on the mechanism of bile salt-induced liposomal membrane damage. *Digestion.* 1983;28(3):181-90
47. Cabral DJ, Small DM, Lilly HS, Hamilton JA. Transbilayer movement of bile acids in model membranes. *Biochemistry (Mosc).* 1987;26(7):1801-4. [doi:10.1021/bi00381a002]
48. Grill JP, Cayuela C, Antoine JM, Schneider F. Isolation and characterization of a *Lactobacillus amylovorus* mutant depleted in conjugated bile salt hydrolase activity: relation between activity and bile salt resistance. *J Appl Microbiol.* 2000;89(4):553-63. [doi:10.1046/j.1365-2672.2000.01147.x]
49. Floch MH, Binder HJ, Filburn B, Gershengoren W. The effect of bile acids on intestinal microflora. *The American Journal of Clinical Nutrition.* 1972;25(12):1418-26
50. Percy-Robb IW, Collee JG. Bile acids: a pH dependent antibacterial system in the gut? *BMJ.* 1972;3(5830):813-5. [doi:10.1136/bmj.3.5830.813]

51. Ouwehand AC, Tölkkö S, Salminen S. The effect of digestive enzymes on the adhesion of probiotic bacteria *in vitro*. *Journal of Food Science*. 2001;66(6):856-9. [doi:10.1111/j.1365-2621.2001.tb15186.x]
52. Izquierdo E, Medina M, Ennahar S, Marchioni E, Sanz Y. Resistance to simulated gastrointestinal conditions and adhesion to mucus as probiotic criteria for *Bifidobacterium longum* strains. *Curr Microbiol*. 2008;56(6):613-8. [doi:10.1007/s00284-008-9135-7]
53. Fuller R. Probiotics-the scientific basis. London, UK: Chapman and Hall; 1992.
54. Ross RP, Desmond C, Fitzgerald GF, Stanton C. Overcoming the technological hurdles in the development of probiotic foods. *J Appl Microbiol*. 2005;98(6):1410-7
55. Ouwehand AC, Søndberg Svendsen L, Leyer G. Probiotics: from strain to product. In: *Probiotics and Health Claims*: Wiley-Blackwell; 2011. p. 37-48.
56. Bunthof CJ, Bloemen K, Breeuwer P, Rombouts FM, Abee T. Flow cytometric assessment of viability of lactic acid bacteria. *Appl Environ Microbiol*. 2001;67(5):2326-35
57. Amor KB, Breeuwer P, Verbaarschot P, Rombouts FM, Akkermans ADL, De Vos WM, et al. Multiparametric flow cytometry and cell sorting for the assessment of viable, injured, and dead *bifidobacterium* cells during bile salt stress. *Appl Environ Microbiol*. 2002;68(11):5209-16
58. Bunthof CJ, Abee T. Development of a flow cytometric method to analyze subpopulations of bacteria in probiotic products and dairy starters. *Appl Environ Microbiol*. 2002;68(6):2934-42
59. O'Sullivan O, O'Callaghan J, Sangrador-Vegas A, McAuliffe O, Slattery L, Kaleta P, et al. Comparative genomics of lactic acid bacteria reveals a niche-specific gene set. *BMC Microbiol*. 2009;9:50. [doi:10.1186/1471-2180-9-50]
60. Kim WS, Perl L, Park JH, Tandianus JE, Dunn NW. Assessment of stress response of the probiotic *Lactobacillus acidophilus*. *Curr Microbiol*. 2001;43(5):346-50. [doi:10.1007/s002840010314]
61. Shah NP. Symposium: Probiotic bacteria: Selective enumeration and survival in dairy foods. *J Dairy Sci*. 2000;83(4):894-907

62. Klaenhammer TR, Kullen MJ. Selection and design of probiotics. *Int J Food Microbiol.* 1999;50:45-57
63. Prasad J, McJarrow P, Gopal P. Heat and osmotic stress responses of probiotic *Lactobacillus rhamnosus* HN001 (DR20) in relation to viability after drying. *Appl Environ Microbiol.* 2003;69(2):917-25
64. Desmond C, Fitzgerald GF, Stanton C, Ross RP. Improved stress tolerance of GroESL-overproducing *Lactococcus lactis* and probiotic *Lactobacillus paracasei* NFBC 338. *Appl Environ Microbiol.* 2004;70(10):5929-36. [doi:10.1128/aem.70.10.5929-5936.2004]
65. Corcoran BM, Ross RP, Fitzgerald GF, Dockery P, Stanton C. Enhanced survival of GroESL-overproducing *Lactobacillus paracasei* NFBC 338 under stressful conditions induced by drying. *Appl Environ Microbiol.* 2006;72(7):5104-7. [doi:10.1128/aem.02626-05]
66. Miller CW, Nguyen MH, Rooney M, Kailasapathy K. The influence of packaging materials on the dissolved oxygen content of probiotic yoghurt. *Packaging Technology and Science.* 2002;15(3):133-8
67. Liu SQ, Tsao M. Enhancement of survival of probiotic and non-probiotic lactic acid bacteria by yeasts in fermented milk under non-refrigerated conditions. *Int J Food Microbiol.* 2009;135(1):34-8. [doi:10.1016/j.ijfoodmicro.2009.07.017]
68. Mortazavian A, Razavi SH, Ehsani MR, Sohrabvandi S. Principles and methods of microencapsulation of probiotic microorganisms. *Iranian Journal of Biotechnology.* 2007;5(1)
69. Miranda FJR. Colloidal-scale self-assembly of microcapsules for food: Wageningen University; 2010.
70. Gilliland SE, Walker DK. Factors to consider when selecting a culture of *Lactobacillus acidophilus* as a dietary adjunct to produce a hypocholesterolemic effect in humans. *J Dairy Sci.* 1990;73(4):905-11. [doi:10.3168/jds.S0022-0302(90)78747-4]
71. Brazel CS. Microencapsulation: offering solutions for the food industry. *Cereal Foods World.* 1999;44(6):388-93
72. Kim B-S, Baez CE, Atala A. Biomaterials for tissue engineering. *World J Urol.* 2000;18(1):2-9. [doi:10.1007/s003450050002]

73. Tønnesen HH, Karlsen J. Alginate in drug delivery systems. *Drug Dev Ind Pharm.* 2002;28(6):621-30. [doi:10.1081/DDC-120003853]
74. Kuang SS, Oliveira JC, Crean AM. Microencapsulation as a tool for incorporating bioactive ingredients into food. *Crit Rev Food Sci Nutr.* 2010;50(10):951-68. [doi:10.1080/10408390903044222]
75. Hogan SA, McNamee BF, O'Riordan ED, O'Sullivan M. Emulsification and microencapsulation properties of sodium caseinate/carbohydrate blends. *Internantional Dairy Journal.* 2001;11(3):137-44
76. Doleyres Y, Lacroix C. Technologies with free and immobilised cells for probiotic bifidobacteria production and protection. *Internantional Dairy Journal.* 2005;15(10):973-88
77. Anal AK, Singh H. Recent advances in microencapsulation of probiotics for industrial applications and targeted delivery. *Trends in Food Science & Technology.* 2007;18(5):240-51
78. Vidhyalakshmi R, Bhakayaraj R, Subhasree RS. Encapsulation "The future of probiotics"-a review. *Advances in Biological Research.* 2009;3(3-4):96-103
79. Rabanel J-M, Banquy X, Zouaoui H, Mokhtar M, Hildgen P. Progress technology in microencapsulation methods for cell therapy. *Biotechnol Prog.* 2009;25(4):946-63
80. Li Y, Xu SN, Li K, Lu YQ. Comparative investigation of molecules releasing from intra-hollow calcium-alginate capsules using fluorimetry. *Spectroscopy and Spectral Analysis.* 2011;31(4):1069-73
81. Sohail A, Turner MS, Coombes A, Bostrom T, Bhandari B. Survivability of probiotics encapsulated in alginate gel microbeads using a novel impinging aerosols method. *Int J Food Microbiol.* 2011;145(1):162-8. [doi:10.1016/j.ijfoodmicro.2010.12.007]
82. Ma Y, Pacan JC, Wang Q, Xu Y, Huang X, Korenevsky A, et al. Microencapsulation of bacteriophage felix O1 into chitosan-alginate microspheres for oral delivery. *Appl Environ Microbiol.* 2008;74(15):4799-805. [doi:10.1128/AEM.00246-08]
83. Chavarri M, Maranon I, Ares R, Ibanez FC, Marzo F, Villaran Mdel C. Microencapsulation of a probiotic and prebiotic in alginate-chitosan capsules

- improves survival in simulated gastro-intestinal conditions. *Int J Food Microbiol.* 2010;142(1-2):185-9. [doi:10.1016/j.ijfoodmicro.2010.06.022]
84. Annan NT, Borza AD, Hansen LT. Encapsulation in alginate-coated gelatin microspheres improves survival of the probiotic *Bifidobacterium adolescentis* 15703T during exposure to simulated gastro-intestinal conditions. *Food Research International.* 2008;41(2):184-93. [doi:10.1016/j.foodres.2007.11.001]
85. Abdelkader H, Youssef-Abdalla O, Salem H. Formulation of controlled-release baclofen matrix tablets. II. Influence of some hydrophobic excipients on the release rate and *in vitro* evaluation. *AAPS PharmSciTech.* 2008;9(2):675-83. [doi:10.1208/s12249-008-9094-0]
86. Tyle P. Effect of size, shape and hardness of particles in suspension on oral texture and palatability. *Acta Psychol (Amst).* 1993;84(1):111-8. [doi:10.1016/0001-6918(93)90077-5]
87. Smart JD. The basics and underlying mechanisms of mucoadhesion. *Advanced Drug Delivery Reviews.* 2005;57(11):1556-68. [doi:10.1016/j.addr.2005.07.001]
88. Chen S, Zhao Q, Ferguson LR, Shu Q, Weir I, Garg S. Development of a novel probiotic delivery system based on microencapsulation with protectants. *Appl Microbiol Biotechnol.* 2012;93(4):1447-57. [doi:10.1007/s00253-011-3609-4]
89. Kramer M, Obermajer N, Matijašić BB, Rogelj I, Kmetec V. Quantification of live and dead probiotic bacteria in lyophilised product by real-time PCR and by flow cytometry. *Appl Microbiol Biotechnol.* 2009;84(6):1137-47
90. Giao MS, Wilks SA, Azevedo NF, Vieira MJ, Keevil CW. Validation of SYTO 9/propidium iodide uptake for rapid detection of viable but noncultivable *Legionella pneumophila*. *Microb Ecol.* 2009;58(1):56-62
91. Shapiro HM. *Practical flow cytometry.* 4th ed. New York: A.R.Liss, Inc; 2006.
92. Shi L, Günther S, Hübschmann T, Wick LY, Harms H, Müller S. Limits of propidium iodide as a cell viability indicator for environmental bacteria. *Cytometry Part A.* 2007;71A(8):592-8. [doi:10.1002/cyto.a.20402]
93. Haugland RP. *Handbook of fluorescent probes and research chemicals.* Eugene, O R: Molecular Probes, Inc.; 2006.

94. Robinson JP, Darzynkiewicz Z, Dean PN, Orfao A, Ribinovitch PS, Stewart CC, et al., editors. *Current Protocols in Cytometry*. New York: Wiley; 2007.
95. D íaz M, Herrero M, Garc ía LA, Quir ós C. Application of flow cytometry to industrial microbial bioprocesses. *Biochemical Engineering Journal*. 2009
96. Lehtinen J, Nuutila J, Lilius EM. Green fluorescent protein-propidium iodide (GFP-PI) based assay for flow cytometric measurement of bacterial viability. *Cytometry Part A*. 2004;60(2):165-72. [doi:10.1002/cyto.a.20026]
97. Falcioni T, Papa S, Gasol JM. Evaluating the flow-cytometric nucleic acid double-staining protocol in realistic situations of planktonic bacterial death. *Appl Environ Microbiol*. 2008;74(6):1767-79. [doi:10.1128/aem.01668-07]
98. Malacrin P, Zapparoli G, Torriani S, Dellaglio F. Rapid detection of viable yeasts and bacteria in wine by flow cytometry. *J Microbiol Methods*. 2001;45(2):127-34
99. Quiros C, Herrero M, Garcia LA, Diaz M. Application of flow cytometry to segregated kinetic modeling based on the physiological states of microorganisms. *Appl Environ Microbiol*. 2007;73(12):3993-4000. [doi:10.1128/aem.00171-07]
100. Reis A, da Silva TL, Kent CA, Kosseva M, Roseiro JC, Hewitt CJ. Monitoring population dynamics of the thermophilic *Bacillus licheniformis* CCM1 1034 in batch and continuous cultures using multi-parameter flow cytometry. *J Biotechnol*. 2005;115(2):199-210
101. Deere D, Porter J, Edwards C, Pickup R. Evaluation of the suitability of *bis*-(1,3-dibutylbarbituric acid) trimethine oxonol, (diBA-C4(3) -), for the flow cytometric assessment of bacterial viability. *FEMS Microbiol Lett*. 1995;130(2-3):165-9
102. Button DK, Robertson BR. Determination of DNA content of aquatic bacteria by flow cytometry. *Appl Environ Microbiol*. 2001;67(4):1636-45. [doi:10.1128/aem.67.4.1636-1645.2001]
103. Chen S, Ferguson LR, Shu Q, Garg S. The application of flow cytometry to the characterisation of a probiotic strain *Lactobacillus reuteri* DPC16 and the evaluation of sugar preservatives for its lyophilization. *LWT - Food Science and Technology*. 2011;44(9):1873-9. [doi:10.1016/j.lwt.2011.05.006]

104. Rault A, Béal C, Ghorbal S, Ogier J-C, Bouix M. Multiparametric flow cytometry allows rapid assessment and comparison of lactic acid bacteria viability after freezing and during frozen storage. *Cryobiology*. 2007;55(1):35-43
105. Ananta E, Volkert M, Knorr D. Cellular injuries and storage stability of spray-dried *Lactobacillus rhamnosus* GG. *International Dairy Journal*. 2005;15(4):399-409. [doi:10.1016/j.idairyj.2004.08.004]
106. Muller JA, Ross RP, Fitzgerald GF, Stanton C. Manufacture of probiotic bacteria. Charalampopoulos D, Rastall RA, editors. In: *Prebiotics and Probiotics Science and Technology*: Springer New York; 2009. p. 725-59.
107. Christine E. Physiology of the colorectal barrier. *Advanced Drug Delivery Reviews*. 1997;28(2):173-90. [doi:10.1016/S0169-409X(97)00071-9]
108. Gotch F, Nadell J, Edelman IS. Gastrointestinal water and electrolytes. IV. The equilibration of deuterium oxide (D₂O) in gastrointestinal contents and the proportion of total body water (T.B.W.) in the gastrointestinal tract. *J Clin Invest*. 1957;36(2):289-96. [doi:10.1172/JCI103423]
109. Schiller C, Fröhlich CP, Giessmann T, Siegmund W, MÖnnikes H, Hosten N, et al. Intestinal fluid volumes and transit of dosage forms as assessed by magnetic resonance imaging. *Aliment Pharmacol Ther*. 2005;22(10):971-9. [doi:10.1111/j.1365-2036.2005.02683.x]
110. Rajilic-Stojanovic M, Smidt H, de Vos WM. Diversity of the human gastrointestinal tract microbiota revisited. *Environ Microbiol*. 2007;9(9):2125-36. [doi:10.1111/j.1462-2920.2007.01369.x]
111. McConnell EL, Fadda HM, Basit AW. Gut instincts: Explorations in intestinal physiology and drug delivery. *Int J Pharm*. 2008;364(2):213-26
112. Coupe AJ, Davis SS, Wilding IR. Variation in gastrointestinal transit of pharmaceutical dosage forms in healthy subjects. *Pharm Res*. 1991;8(3):360-4
113. Rao CV. Nitric oxide signaling in colon cancer chemoprevention. *Mutation Research-Fundamental and Molecular Mechanisms of Mutagenesis*. 2004;555(1-2):107-19

114. Evans DF, Pye G, Bramley R, Clark AG, Dyson TJ, Hardcastle JD. Measurement of gastrointestinal pH profiles in normal ambulant human subjects. *Gut*. 1988;29(8):1035-41
115. Sasaki Y, Hada R, Nakajima H, Fukuda S, Munakata A. Improved localizing method of radiopill in measurement of entire gastrointestinal pH profiles: colonic luminal pH in normal subjects and patients with Crohn's disease. *Am J Gastroenterol*. 1997;92(1):114-8
116. Press AG, Hauptmann IA, Hauptmann L, Fuchs B, Fuchs M, Ewe K, et al. Gastrointestinal pH profiles in patients with inflammatory bowel disease. *Aliment Pharmacol Ther*. 1998;12(7):673-8
117. Gazzaniga A, Maroni A, Sangalli ME, Zema L. Time-controlled oral delivery systems for colon targeting. *Expert Opinion on Drug Delivery*. 2006;3(5):583-97. [doi:doi:10.1517/17425247.3.5.583]
118. Yang L, Chu JS, Fix JA. Colon-specific drug delivery: new approaches and *in vitro/in vivo* evaluation. *Int J Pharm*. 2002;235(1-2):1-15
119. Shibata N, Ohno T, Shimokawa T, Hu Z, Yoshikawa Y, Koga K, et al. Application of pressure-controlled colon delivery capsule to oral administration of glycyrrhizin in dogs. *J Pharm Pharmacol*. 2001;53(4):441-7
120. Xu J, Mahowald MA, Ley RE, Lozupone CA, Hamady M, Martens EC, et al. Evolution of symbiotic bacteria in the distal human intestine. *PLoS Biol*. 2007;5(7):e156. [doi:10.1371/journal.pbio.0050156]
121. Xu J, Bjursell MK, Himrod J, Deng S, Carmichael LK, Chiang HC, et al. A genomic view of the human-Bacteroides thetaiotaomicron symbiosis. *Science*. 2003;299(5615):2074-6. [doi:10.1126/science.1080029
299/5615/2074 [pii]]
122. Kosaraju SL. Colon targeted delivery systems: review of polysaccharides for encapsulation and delivery. *Crit Rev Food Sci Nutr*. 2005;45(4):251-8. [doi:10.1080/10408690490478091]
123. McConnell EL, Liu F, Basit AW. Colonic treatments and targets: issues and opportunities. *J Drug Target*. 2009;17(5):335-63. [doi:doi:10.1080/10611860902839502]

124. Salyers AA, West SE, Vercellotti JR, Wilkins TD. Fermentation of mucins and plant polysaccharides by anaerobic bacteria from the human colon. *Appl Environ Microbiol.* 1977;34(5):529-33
125. Crociani F, Alessandrini A, Mucci MM, Biavati B. Degradation of complex carbohydrates by *Bifidobacterium* spp. *Int J Food Microbiol.* 1994;24(1-2):199-210
126. Hopkins MJ, Englyst HN, Macfarlane S, Furrrie E, Macfarlane GT, McBain AJ. Degradation of cross-linked and non-cross-linked arabinoxylans by the intestinal microbiota in children. *Appl Environ Microbiol.* 2003;69(11):6354-60
127. Gibson GR, Macfarlane S, Cummings JH. The fermentability of polysaccharides by mixed human faecal bacteria in relation to their suitability as bulk-forming laxatives. *Lett Appl Microbiol.* 1990;11(5):251-4. [doi:10.1111/j.1472-765X.1990.tb00174.x]
128. McConnell EL, Murdan S, Basit AW. An investigation into the digestion of chitosan (noncrosslinked and crosslinked) by human colonic bacteria. *J Pharm Sci.* 2008;97(9):3820-9. [doi:10.1002/jps.21271]
129. Simonsen L, Hovgaard L, Mortensen PB, Brøndsted H. Dextran hydrogels for colon-specific drug delivery. V. Degradation in human intestinal incubation models. *Eur J Pharm Sci.* 1995;3(6):329-37. [doi:10.1016/0928-0987(95)00023-6]
130. Ross AH, Eastwood MA, Brydon WG, Anderson JR, Anderson DM. A study of the effects of dietary gum arabic in humans. *Am J Clin Nutr.* 1983;37(3):368-75
131. Cherbut C. Inulin and oligofructose in the dietary fibre concept. *Br J Nutr.* 2002;87 Suppl 2:S159-62. [doi:10.1079/BJNBJN2002532]
132. Nyman M. Fermentation and bulking capacity of indigestible carbohydrates: the case of inulin and oligofructose. *Br J Nutr.* 2002;87 Suppl 2:S163-8. [doi:10.1079/BJNBJN/2002533]
133. Salyers AA, Palmer JK, Wilkins TD. Degradation of polysaccharides by intestinal bacterial enzymes. *Am J Clin Nutr.* 1978;31(10 Suppl):S128-S30
134. Rochet V, Bernalier A. Utilization of algal polysaccharides by human colonic bacteria, in axenic culture or in association with hydrogenotrophic microorganisms. *Reprod Nutr Dev.* 1997;37(2):221-9

135. Hartemink R, Van Laere KMJ, Mertens AKC, Rombouts FM. Fermentation of xyloglucan by intestinal bacteria. *Anaerobe*. 1996;2(4):223-30. [doi:10.1006/anae.1996.0031]
136. Palframan RJ, Gibson GR, Rastall RA. Carbohydrate preferences of *Bifidobacterium* species isolated from the human gut. *Curr Issues Intest Microbiol*. 2003;4(2):71-5
137. Cu Y, Saltzman WM. Mathematical modeling of molecular diffusion through mucus. *Adv Drug Deliv Rev*. 2009;61(2):101-14. [doi:10.1016/j.addr.2008.09.006]
138. Atuma C, Strugala V, Allen A, Holm L. The adherent gastrointestinal mucus gel layer: thickness and physical state *in vivo*. *Am J Physiol Gastrointest Liver Physiol*. 2001;280(5):G922-9
139. Johansson MEV, Phillipson M, Petersson J, Velcich A, Holm L, Hansson GC. The inner of the two Muc2 mucin-dependent mucus layers in colon is devoid of bacteria. *Proceedings of the National Academy of Sciences*. 2008;105(39):15064-9. [doi:10.1073/pnas.0803124105]
140. Corfield AP, Carroll D, Myerscough N, Probert CS. Mucins in the gastrointestinal tract in health and disease. *Frontiers in bioscience : a journal and virtual library*. 2001;6:D1321-57
141. Dixon J, Strugala V, Griffin SM, Welfare MR, Dettmar PW, Allen A, et al. Esophageal mucin: an adherent mucus gel barrier is absent in the normal esophagus but present in columnar-lined Barrett's esophagus. *The American Journal of Gastroenterology*. 2001;96(9):2575-83. [doi:10.1016/S0002-9270(01)02721-6]
142. Sarosiek J, McCallum RW. Mechanisms of oesophageal mucosal defence. *Best Practice & Research Clinical Gastroenterology*. 2000;14(5):701-17
143. Jordan N, Newton J, Pearson J, Allen A. A novel method for the visualization of the *in situ* mucus layer in rat and man. *Clin Sci*. 1998;95(1):97-106
144. Newton JL, Jordan N, Oliver L, Strugala V, Pearson J, James OFW, et al. *Helicobacter pylori in vivo* causes structural changes in the adherent gastric mucus layer but barrier thickness is not compromised. *Gut*. 1998;43(4):470-5. [doi:10.1136/gut.43.4.470]

145. Pullan RD, Thomas GA, Rhodes M, Newcombe RG, Williams GT, Allen A, et al. Thickness of adherent mucus gel on colonic mucosa in humans and its relevance to colitis. *Gut*. 1994;35(3):353-9. [doi:10.1136/gut.35.3.353]
146. Rubinstein A, Tirosh B. Mucus gel thickness and turnover in the gastrointestinal tract of the rat: response to cholinergic stimulus and implication for mucoadhesion. *Pharm Res*. 1994;11(6):794-9
147. Ahuja A, Khar RK, Ali J. Mucoadhesive drug delivery systems. *Drug Dev Ind Pharm*. 1997;23(5):489-515. [doi:10.3109/03639049709148498]
148. Mathiowitz E, Chickering DE, Lehr CM. Bioadhesive drug delivery systems: fundamentals, novel approaches, and development: Informa HealthCare; 1999.
149. Peppas NA, Sahlin JJ. Hydrogels as mucoadhesive and bioadhesive materials: a review. *Biomaterials*. 1996;17(16):1553-61. [doi:10.1016/0142-9612(95)00307-X]
150. Kinloch AJ, editor. Adhesion and adhesives science and technology. 2nd rev. edn. ed. ed: Chapman and Hall; 1987.
151. Mikos AG, Peppas NA, editors. Scaling concepts and molecular theories of adhesion of synthetic polymers to glycoprotein networks: CRC Press; 1990.
152. Chowdary KPR, Srinivasa Rao Y. Mucoadhesive microspheres for controlled drug delivery. *Biol Pharm Bull*. 2004;27(11):1717-24
153. Thirawong N, Nunthanid J, Puttipipatkachorn S, Sriamornsak P. Mucoadhesive properties of various pectins on gastrointestinal mucosa: An *in vitro* evaluation using texture analyzer. *Eur J Pharm Biopharm*. 2007;67(1):132-40
154. Bernkop-Schnürch A, Schwarz V, Steininger S. Polymers with thiol groups: a new generation of mucoadhesive polymers? *Pharm Res*. 1999;16(6):876-81. [doi:10.1023/a:1018830204170]
155. Perez-Vilar J. Gastrointestinal mucus gel barrier. In: *Oral Delivery of Macromolecular Drugs*2009. p. 21-48.
156. Leitner VM, Walker GF, Bernkop-Schnürch A. Thiolated polymers: evidence for the formation of disulphide bonds with mucus glycoproteins. *Eur J Pharm Biopharm*. 2003;56(2):207-14. [doi:10.1016/S0939-6411(03)00061-4]

157. Dhaliwal S, Jain S, Singh H, Tiwary A. Mucoadhesive microspheres for gastroretentive delivery of acyclovir: *in vitro* and *in vivo* evaluation. *The AAPS Journal*. 2008;10(2):322-30. [doi:10.1208/s12248-008-9039-2]
158. Bernkop-Schnürch A, Kast CE, Guggi D. Permeation enhancing polymers in oral delivery of hydrophilic macromolecules: thiomers/GSH systems. *J Controlled Release*. 2003;93(2):95-103. [doi:10.1016/j.jconrel.2003.05.001]
159. Guggi D, Krauland AH, Bernkop-Schnürch A. Systemic peptide delivery via the stomach: *in vivo* evaluation of an oral dosage form for salmon calcitonin. *J Controlled Release*. 2003;92(1-2):125-35. [doi:10.1016/S0168-3659(03)00299-2]
160. Bernkop-Schnürch A. Mucoadhesive systems in oral drug delivery. *Drug discovery today: Technologies*. 2005;2(1):83-7
161. Hoyer H, Schlocker W, Krum K, Bernkop-Schnürch A. Preparation and evaluation of microparticles from thiolated polymers via air jet milling. *Eur J Pharm Biopharm*. 2008;69(2):476-85. [doi:10.1016/j.ejpb.2008.01.009]
162. Millotti G, Samberger C, Frohlich E, Bernkop-Schnürch A. Chitosan-graft-6-mercaptopyridonic acid: synthesis, characterization, and biocompatibility. *Biomacromolecules*. 2009;10(11):3023-7. [doi:10.1021/bm9006248]
163. Guggi D, Langoth N, Hoffer MH, Wirth M, Bernkop-Schnürch A. Comparative evaluation of cytotoxicity of a glucosamine-TBA conjugate and a chitosan-TBA conjugate. *Int J Pharm*. 2004;278(2):353-60. [doi:10.1016/j.ijpharm.2004.03.016]
164. Lowman AM, Peppas NA. Analysis of the complexation/decomplexation phenomena in graft copolymer networks. *Macromolecules*. 1997;30(17):4959-65
165. De Ascentiis A, deGrazia JL, Bowman CN, Colombo P, Peppas NA. Mucoadhesion of poly(2-hydroxyethyl methacrylate) is improved when linear poly(ethylene oxide) chains are added to the polymer network. *J Controlled Release*. 1995;33(1):197-201
166. Huang Y, Leobandung W, Foss A, Peppas NA. Molecular aspects of muco- and bioadhesion: tethered structures and site-specific surfaces. *J Controlled Release*. 2000;65(1-2):63-71

167. Sahlin JJ, Peppas NA. Enhanced hydrogel adhesion by polymer interdiffusion: use of linear poly (ethylene glycol) as an adhesion promoter. *J Biomater Sci Polym Ed.* 1997;8(6):421-36
168. Chickering DE, Mathiowitz E. Bioadhesive microspheres: I. A novel electrobalance-based method to study adhesive interactions between individual microspheres and intestinal mucosa. *J Controlled Release.* 1995;34(3):251-62
169. Andrews GP, Lavery TP, Jones DS. Mucoadhesive polymeric platforms for controlled drug delivery. *Eur J Pharm Biopharm.* 2009;71(3):505-18
170. Anande NM, Jain SK, Jain NK. Con-A conjugated mucoadhesive microspheres for the colonic delivery of diloxanide furoate. *Int J Pharm.* 2008;359(1-2):182-9
171. Albrecht K, Greindl M, Kremser C, Wolf C, Debbage P, Bernkop-Schnürch A. Comparative *in vivo* mucoadhesion studies of thiomers formulations using magnetic resonance imaging and fluorescence detection. *J Controlled Release.* 2006;115(1):78-84
172. Vanderpool C, Yan F, Polk DB. Mechanisms of probiotic action: Implications for therapeutic applications in inflammatory bowel diseases. *Inflamm Bowel Dis.* 2008;14(11):1585-96. [doi:10.1002/ibd.20525]
173. Begley M, Gahan CGM, Hill C. The interaction between bacteria and bile. *FEMS Microbiol Rev.* 2005;29(4):625-51
174. Cotter PD, Hill C. Surviving the acid test: responses of gram-positive bacteria to low pH. *Microbiol Mol Biol Rev.* 2003;67(3):429
175. Kashket ER. Bioenergetics of lactic acid bacteria: cytoplasmic pH and osmotolerance. *FEMS Microbiol Lett.* 1987;46(3):233-44. [doi:10.1111/j.1574-6968.1987.tb02463.x]
176. Jin LZ, Ho YW, Abdullah N, Jalaludin S. Acid and bile tolerance of *Lactobacillus* isolated from chicken intestine. *Lett Appl Microbiol.* 1998;27(3):183-5. [doi:10.1046/j.1472-765X.1998.00405.x]
177. Jacobsen CN, Nielsen VR, Hayford AE, Møller PL, Michaelsen KF, Pærregaard A, et al. Screening of probiotic activities of forty-seven strains of *Lactobacillus* spp. by *in vitro* techniques and evaluation of the colonization ability of five selected strains in humans. *Appl Environ Microbiol.* 1999;65(11):4949-56

178. Charalampopoulos D, Pandiella SS, Webb C. Evaluation of the effect of malt, wheat and barley extracts on the viability of potentially probiotic lactic acid bacteria under acidic conditions. *Int J Food Microbiol.* 2003;82(2):133-41. [doi:10.1016/S0168-1605(02)00248-9]
179. Corcoran BM, Stanton C, Fitzgerald GF, Ross RP. Survival of probiotic lactobacilli in acidic environments is enhanced in the presence of metabolizable sugars. *Appl Environ Microbiol.* 2005;71(6):3060
180. Lorca GL, Font de Valdez G. Acid tolerance mediated by membrane ATPases in *Lactobacillus acidophilus*. *Biotechnology Letters.* 2001;23(10):777-80
181. Giannella RA, Broitman SA, Zamcheck N. Gastric acid barrier to ingested microorganisms in man: studies *in vivo* and *in vitro*. *Gut.* 1972;13(4):251-6. [doi:10.1136/gut.13.4.251]
182. Kurdi P, Kawanishi K, Mizutani K, Yokota A. Mechanism of growth inhibition by free bile acids in lactobacilli and bifidobacteria. *J Bacteriol.* 2006;188(5):1979-86. [doi:10.1128/jb.188.5.1979-1986.2006]
183. Lahtinen SJ, Ouwehand AC, Reinikainen JP, Korpela JM, Sandholm J, Salminen SJ. Intrinsic properties of so-called dormant probiotic bacteria, determined by flow cytometric viability assays. *Appl Environ Microbiol.* 2006;72(7):5132-4. [doi:10.1128/aem.02897-05]
184. Ouwehand AC, Kirjavainen PV, Shortt C, Salminen S. Probiotics: mechanisms and established effects. *International Dairy Journal.* 1999;9(1):43-52. [doi:10.1016/S0958-6946(99)00043-6]
185. Lahtinen SJ, Ahokoski H, Reinikainen JP, Gueimonde M, Nurmi J, Ouwehand AC, et al. Degradation of 16S rRNA and attributes of viability of viable but nonculturable probiotic bacteria. *Lett Appl Microbiol.* 2008;46(6):693-8. [doi:10.1111/j.1472-765X.2008.02374.x]
186. Sträuber H, Müller S. Viability states of bacteria—Specific mechanisms of selected probes. *Cytometry Part A.* 2010;77A(7):623-34. [doi:10.1002/cyto.a.20920]
187. Ananta E, Heinz V, Knorr D. Assessment of high pressure induced damage on *Lactobacillus rhamnosus* GG by flow cytometry. *Food Microbiology.* 2004;21(5):567-77

188. Ananta E, Knorr D. Comparison of inactivation pathways of thermal or high pressure inactivated *Lactobacillus rhamnosus* ATCC 53103 by flow cytometry analysis. *Food Microbiology*. 2009;26(5):542-6
189. Ananta E, Voigt D, Zenker M, Heinz V, Knorr D. Cellular injuries upon exposure of *Escherichia coli* and *Lactobacillus rhamnosus* to high-intensity ultrasound. *J Appl Microbiol*. 2005;99(2):271-8. [doi:10.1111/j.1365-2672.2005.02619.x]
190. Papadimitriou K, Pratsinis H, Nebe-von-Caron G, Kleetsas D, Tsakalidou E. Rapid assessment of the physiological status of *Streptococcus macedonicus* by flow cytometry and fluorescence probes. *Int J Food Microbiol*. 2006;111(3):197-205. [doi:10.1016/j.ijfoodmicro.2006.04.042]
191. Hope MJ, Bally MB, Webb G, Cullis PR. Production of large unilamellar vesicles by a rapid extrusion procedure. Characterization of size distribution, trapped volume and ability to maintain a membrane potential. *Biochimica et Biophysica Acta (BBA)-Biomembranes*. 1985;812(1):55-65
192. Bunthof CJ, van den Braak S, Breeuwer P, Rombouts FM, Abee T. Rapid fluorescence assessment of the viability of stressed *Lactococcus lactis*. *Appl Environ Microbiol*. 1999;65(8):3681-9
193. Gardiner GE, O'Sullivan E, Kelly J, Auty MAE, Fitzgerald GF, Collins JK, et al. Comparative survival rates of human-derived probiotic *Lactobacillus paracasei* and *L. salivarius* strains during heat treatment and spray drying. *Appl Environ Microbiol*. 2000;66(6):2605-12. [doi:10.1128/aem.66.6.2605-2612.2000]
194. Hartke A, Bouche S, Gansel X, Boutibonnes P, Auffray Y. Starvation-Induced stress resistance in *Lactococcus lactis* subsp. *lactis* IL1403. *Appl Environ Microbiol*. 1994;60(9):3474-8
195. Papadimitriou K, Pratsinis H, Nebe-von-Caron G, Kleetsas D, Tsakalidou E. Acid tolerance of *Streptococcus macedonicus* as assessed by flow cytometry and single-cell sorting. *Appl Environ Microbiol*. 2007;73(2):465-76. [doi:10.1128/aem.01244-06]
196. Chen X, Sun Z, Meng H, Zhang H. The acid tolerance association with expression of H⁺-ATPase in *Lactobacillus casei*. *International Journal of Dairy Technology*. 2009;62(2):272-6

197. Gobbetti M, Fox PF, Stepaniak L. Isolation and characterization of a tributyrin esterase from *Lactobacillus plantarum* 2739. *J Dairy Sci.* 1997;80(12):3099-106. [doi:10.3168/jds.S0022-0302(97)76280-5]
198. Wang X, Geng X, Egashira Y, Sanada H. Purification and characterization of a feruloyl esterase from the intestinal bacterium *Lactobacillus acidophilus*. *Appl Environ Microbiol.* 2004;70(4):2367-72. [doi:10.1128/aem.70.4.2367-2372.2004]
199. Choi YJC, Lee BL. Culture conditions for the production of esterase from *Lactobacillus casei* CL96. *Bioprocess and Biosystems Engineering.* 2001;24(1):59-63. [doi:10.1007/s004490100233]
200. Madenci D, Egelhaaf SU. Self-assembly in aqueous bile salt solutions. *Current Opinion in Colloid & Interface Science.* 2010;15(1-2):109-15
201. Leng J, Egelhaaf SU, Cates ME. Kinetics of the micelle-to-vesicle transition: aqueous lecithin-bile salt mixtures. *Biophys J.* 2003;85(3):1624-46
202. Pártay LB, Sega M, Jedlovszky P. A two-step aggregation scheme of bile acid salts, as seen from computer simulations. *Colloids for Nano-and Biotechnology.* 2008:181-7
203. Nichols JW, Ozarowski J. Sizing of lecithin-bile salt mixed micelles by size-exclusion high-performance liquid chromatography. *Biochemistry (Mosc).* 1990;29(19):4600-6. [doi:10.1021/bi00471a014]
204. Carey MC, Small DM. The characteristics of mixed micellar solutions with particular reference to bile. *Am J Med.* 1970;49(5):590-608. [doi:10.1016/S0002-9343(70)80127-9]
205. Donovan JM, Timofeyeva N, Carey MC. Influence of total lipid concentration, bile salt:lecithin ratio, and cholesterol content on inter-mixed micellar/vesicular (non-lecithin-associated) bile salt concentrations in model bile. *J Lipid Res.* 1991;32(9):1501-12
206. Hatakka K, Mutanen M, Holma R, Saxelin M, Korpela R. *Lactobacillus rhamnosus* LC705 together with *Propionibacterium freudenreichii* ssp *shermanii* JS administered in capsules is ineffective in lowering serum lipids. *J Am Coll Nutr.* 2008;27(4):441

207. Ooi LG, Liong MT. Cholesterol-lowering effects of probiotics and prebiotics: a review of *in vivo* and *in vitro* findings. *International journal of molecular sciences*. 2010;11(6):23. [doi:10.3390/ijms11062499]
208. Kekkonen RA, Lummela N, Karjalainen H, Latvala S, Tynkkynen S, Järvenpää S, et al. Probiotic intervention has strain-specific anti-inflammatory effects in healthy adults. *World Journal of Gastroenterology*. 2008;14(13). [doi:10.3748/wjg.14.2029]
209. de Vrese M, Marteau PR. Probiotics and prebiotics: effects on diarrhea. *J Nutr*. 2007;137(3):803S-11
210. Drouault S, Corthier G, Ehrlich SD, Renault P. Survival, physiology, and lysis of *Lactococcus lactis* in the digestive tract. *Appl Environ Microbiol*. 1999;65(11):4881-6
211. Masco L, Crockaert C, Van Hoorde K, Swings J, Huys G. In vitro assessment of the gastrointestinal transit tolerance of taxonomic reference strains from human origin and probiotic product isolates of *Bifidobacterium*. *J Dairy Sci*. 2007;90(8):3572-8. [doi:10.3168/jds.2006-548]
212. Waddington L, Cyr T, Hefford M, Hansen L, Kalmokoff M. Understanding the acid tolerance response of bifidobacteria. *J Appl Microbiol*. 2010;108(4):1408-20
213. Charalampopoulos D, Rastall RA, O'Flaherty S, Goh YJ, Klaenhammer TR. Genomics of probiotic bacteria. In: *Prebiotics and Probiotics Science and Technology*: Springer New York; 2009. p. 681-723.
214. Sánchez B, De Los Reyes-Gavilán CG, Margolles A. The F₁F₀-ATPase of *Bifidobacterium animalis* is involved in bile tolerance. *Environ Microbiol*. 2006;8(10):1825-33. [doi:10.1111/j.1462-2920.2006.01067.x]
215. Narain PK, DeMaria EJ, Heuman DM. Lecithin protects against plasma membrane disruption by bile salts. *J Surg Res*. 1998;78(2):131-6
216. Sagawa H, Tazuma S, Kajiyama G. Protection against hydrophobic bile salt-induced cell membrane damage by liposomes and hydrophilic bile salts. *American Journal of Physiology- Gastrointestinal and Liver Physiology*. 1993;264(5):835

217. Leroy F, Falony G, Vuyst L. Latest developments in probiotics. In: Meat Biotechnology. U.S.A: Springer; 2008. p. 217-29.
218. Lee K-Y, Heo T-R. Survival of *Bifidobacterium longum* immobilized in calcium alginate beads in simulated gastric juices and bile salt solution. Appl Environ Microbiol. 2000;66(2):869-73. [doi:10.1128/aem.66.2.869-873.2000]
219. Hansen LT, Allan-Wojtas PM, Jin YL, Paulson AT. Survival of Ca-alginate microencapsulated *Bifidobacterium* spp. in milk and simulated gastrointestinal conditions. Food Microbiology. 2002;19(1):35-45
220. Chandramouli V, Kailasapathy K, Peiris P, Jones M. An improved method of microencapsulation and its evaluation to protect *Lactobacillus* spp. in simulated gastric conditions. J Microbiol Methods. 2004;56(1):27-35
221. Cui JH, Goh JS, Kim PH, Choi SH, Lee BJ. Survival and stability of bifidobacteria loaded in alginate poly-*l*-lysine microparticles. Int J Pharm. 2000;210(1-2):51-9
222. Larisch B, Poncelet D, Champagne C, Neufeld R. Microencapsulation of *Lactococcus lactis* subsp. *cremoris*. J Microencapsul. 1994;11(2):189-95
223. Prizont R, Konigsberg N. Identification of bacterial glycosidases in rat cecal contents. Dig Dis Sci. 1981;26(9):773-7. [doi:10.1007/bf01309607]
224. Munteanu M, Ritter H. Enzymatic polysaccharide degradation. In: Biocatalysis in polymer chemistry: Wiley-VCH Verlag GmbH & Co. KGaA; 2010. p. 389-420.
225. Sheu TY, Marshall RT. Microentrapment of lactobacilli in calcium alginate gels. Journal of Food Science. 1993;58(3):557-61. [doi:10.1111/j.1365-2621.1993.tb04323.x]
226. Li X-Y, Jin L-J, McAllister TA, Stanford K, Xu J-Y, Lu Y-N, et al. Chitosan-alginate microcapsules for oral delivery of egg yolk immunoglobulin (IgY). Journal of Agricultural and Food Chemistry. 2007;55(8):2911-7. [doi:10.1021/jf062900q]
227. Silva CM, Ribeiro AJ, Figueiredo M, Ferreira D, Veiga F. Microencapsulation of hemoglobin in chitosan-coated alginate microspheres prepared by emulsification/internal gelation. The AAPS Journal. 2005;7(4):903-13

228. Cotter P, Gahan C, Hill C. Analysis of the role of the *Listeria monocytogenes* F₀F₁-ATPase operon in the acid tolerance response. *Int J Food Microbiol.* 2000;60(2-3):137-46
229. Zhang H, Neau SH. In vitro degradation of chitosan by bacterial enzymes from rat cecal and colonic contents. *Biomaterials.* 2002;23(13):2761-6. [doi:10.1016/S0142-9612(02)00011-X]
230. Meng XC, Stanton C, Fitzgerald GF, Daly C, Ross RP. Anhydrobiotics: The challenges of drying probiotic cultures. *Food Chemistry.* 2008;106(4):1406-16. [doi:10.1016/j.foodchem.2007.04.076]
231. Strasser S, Neureiter M, Geppl M, Braun R, Danner H. Influence of lyophilization, fluidized bed drying, addition of protectants, and storage on the viability of lactic acid bacteria. *J Appl Microbiol.* 2009;107(1):167-77. [doi:10.1111/j.1365-2672.2009.04192.x]
232. Weinbreck F, Bodnár I, Marco ML. Can encapsulation lengthen the shelf-life of probiotic bacteria in dry products? *Int J Food Microbiol.* 2010;136(3):364-7. [doi:10.1016/j.ijfoodmicro.2009.11.004]
233. Ying DY, Sanguansri L, Weerakkody R, Singh TK, Leischtfeld SF, Gantenbein-Demarchi C, et al. Tocopherol and ascorbate have contrasting effects on the viability of microencapsulated *Lactobacillus rhamnosus* GG. *Journal of Agricultural and Food Chemistry.* 2011;59(19):10556-63. [doi:10.1021/jf202358m]
234. Mitic S, Otenhajmer I, Damjanovic V. Predicting the stabilities of freeze-dried suspensions of *Lactobacillus acidophilus* by the accelerated storage test. *Cryobiology.* 1974;11(2):116-20. [doi:10.1016/0011-2240(74)90300-9]
235. Damjanović V, Radulović D. Predicting the stability of freeze-dried *Lactobacillus bifidus* by the accelerated storage test. *Cryobiology.* 1968;5(2):101-4. [doi:10.1016/S0011-2240(68)80150-6]
236. Tsen J-H, Lin Y-P, Huang H-Y, King VA-E. Accelerated storage testing of freeze-dried immobilized *Lactobacillus acidophilus*-fermented banana media. *Journal of Food Processing and Preservation.* 2007;31(6):688-701. [doi:10.1111/j.1745-4549.2007.00160.x]
237. Abe F, Miyauchi H, Uchijima A, Yaeshima T, Iwatsuki K. Effects of storage temperature and water activity on the survival of bifidobacteria in powder form.

- International Journal of Dairy Technology. 2009;62(2):234-9. [doi:10.1111/j.1471-0307.2009.00464.x]
238. Achour M, Mtimet N, Cornelius C, Zgouli S, Mahjoub A, Thonart P, et al. Application of the accelerated shelf life testing method (ASLT) to study the survival rates of freeze-dried *Lactococcus* starter cultures. J Chem Technol Biotechnol. 2001;76(6):624-8. [doi:10.1002/jctb.427]
239. Petrof EO. Probiotics and gastrointestinal disease: clinical evidence and basic science. Anti-inflammatory & anti-allergy agents in medicinal chemistry. 2009;8(3):260
240. Corr SC, Hill C, Gahan CGM. Understanding the mechanisms by which probiotics inhibit gastrointestinal pathogens. Steve LT, editor. In: Adv Food Nutr Res: Academic Press; 2009. p. 1-15.
241. Muthukumarasamy P, Holley RA. Survival of *Escherichia coli* O157:H7 in dry fermented sausages containing micro-encapsulated probiotic lactic acid bacteria. Food Microbiology. 2007;24(1):82-8. [doi:10.1016/j.fm.2006.03.004]
242. Brachkova MI, Duarte MA, Pinto JF. Preservation of viability and antibacterial activity of *Lactobacillus* spp. in calcium alginate beads. Eur J Pharm Sci. 2010;41(5):589-96
243. Yao AA, Bera F, Franz C, Holzapfel W, Thonart P. Survival rate analysis of freeze-dried lactic acid bacteria using the Arrhenius and z -value models. J Food Prot. 2008;71(2):431-4
244. Toledo RT. Fundamentals of food process engineering. In: Thermal process calculations. 2nd ed. New York, NY: Van Nostrand Reinhold; 1991.
245. Eisenberg DS, Crothers DM. Physical chemistry with applications to the life sciences. In: Chemical and biochemical kinetics. Menlo Park, CA: Benjamin/Cummings Pub. Co.; 1979.
246. Saguy I, Karel M. Modeling of quality deterioration during food processing and storage. Food Technology. 1980;34(2):78-85
247. Annuk H, Shchepetova J, Kullisaar T, Songisepp E, Zilmer M, Mikelsaar M. Characterization of intestinal lactobacilli as putative probiotic candidates. J Appl Microbiol. 2003;94(3):403-12. [doi:10.1046/j.1365-2672.2003.01847.x]

248. Circle SJ, Stone L, Boruff CS. Acrolein determination by means of tryptophane. *Ind Eng Chem Anal Ed.* 1945;17:259-62
249. Zamudio-Jaramillo MA, Hernandez-Mendoza A, Robles VJ, Mendoza-Garcia PG, Espinosa-de-los-Monteros JJ, Garcia HS. Reuterin production by *Lactobacillus reuteri* NRRL B-14171 immobilized in alginate. *J Chem Technol Biotechnol.* 2009;84(1):100-5. [doi:10.1002/jctb.2012]
250. Ogawa M, Shimizu K, Nomoto K, Tanaka R, Hamabata T, Yamasaki S, et al. Inhibition of in vitro growth of Shiga toxin-producing *Escherichia coli* O157:H7 by probiotic *Lactobacillus* strains due to production of lactic acid. *Int J Food Microbiol.* 2001;68(1-2):135-40. [doi:10.1016/S0168-1605(01)00465-2]
251. Bian L, Molan A-L, Maddox I, Shu Q. Antimicrobial activity of *Lactobacillus reuteri* DPC16 supernatants against selected food borne pathogens. *World Journal of Microbiology and Biotechnology.* 2011;27(4):991-8. [doi:10.1007/s11274-010-0543-z]
252. Klinkenberg G, Lystad KQ, Levine DW, Dyrset N. Cell release from alginate immobilized *Lactococcus lactis* ssp. *lactis* in chitosan and alginate coated beads. *J Dairy Sci.* 2001;84(5):1118-27
253. Lacroix C, Yildirim S. Fermentation technologies for the production of probiotics with high viability and functionality. *Curr Opin Biotechnol.* 2007;18(2):176-83. [doi:10.1016/j.copbio.2007.02.002]
254. Lacroix C, Grattepanche F, Doleyres Y, Bergmaier D. Immobilised cell technologies for the dairy industry. Nedović V, Willaert R, editors. In: *Applications of cell immobilisation biotechnology*: Springer Netherlands; 2005. p. 295-319.
255. Zhao Q, Mutukumira A, Lee S, Maddox I, Shu Q. Functional properties of free and encapsulated *Lactobacillus reuteri* DPC16 during and after passage through a simulated gastrointestinal tract. *World Journal of Microbiology and Biotechnology.* 2012;28(1):61-70. [doi:10.1007/s11274-011-0792-5]
256. Helander IM, Nurmiäho-Lassila EL, Ahvenainen R, Rhoades J, Roller S. Chitosan disrupts the barrier properties of the outer membrane of Gram-negative bacteria. *Int J Food Microbiol.* 2001;71(2-3):235-44. [doi:10.1016/S0168-1605(01)00609-2]

257. Talarico TL, Casas IA, Chung TC, Dobrogosz WJ. Production and isolation of reuterin, a growth inhibitor produced by *Lactobacillus reuteri*. *Antimicrob Agents Chemother*. 1988;32(12):1854-8. [doi:10.1128/aac.]
258. Rasch M, Barker GC, Sachau K, Jakobsen M, Arneborg N. Characterisation and modelling of oscillatory behaviour related to reuterin production by *Lactobacillus reuteri*. *Int J Food Microbiol*. 2002;73(2-3):383-94. [doi:10.1016/S0168-1605(01)00661-4]
259. Quijada-Garrido I, Iglesias-González V, Mazón-Arechederra JM, Barrales-Rienda JM. The role played by the interactions of small molecules with chitosan and their transition temperatures. *Glass-forming liquids: 1,2,3-Propantriol (glycerol). Carbohydrate Polymers*. 2007;68(1):173-86. [doi:10.1016/j.carbpol.2006.07.025]
260. Cleusix V, Lacroix C, Vollenweider S, Le Blay G. Glycerol induces reuterin production and decreases *Escherichia coli* population in an *in vitro* model of colonic fermentation with immobilized human feces. *FEMS Microbiology Ecology*. 2008;63(1):56-64. [doi:10.1111/j.1574-6941.2007.00412.x]
261. Manojlović V, Nedović VA, Kailasapathy K, Zuidam NJ. Encapsulation of probiotics for use in food products. Zuidam NJ, Nedovic V, editors. In: *Encapsulation technologies for active food ingredients and food processing*: Springer New York; 2010. p. 269-302.
262. Patel MM. Cutting-edge technologies in colon-targeted drug delivery systems. *Expert Opinion on Drug Delivery*. 2011;8(10):1247-58. [doi:10.1517/17425247.2011.597739]
263. Philip AK, Philip B. Colon targeted drug delivery systems: a review on primary and novel approaches. *Oman Med J*. 2010;25(2):70-8
264. George M, Abraham TE. Polyionic hydrocolloids for the intestinal delivery of protein drugs: Alginate and chitosan — a review. *J Controlled Release*. 2006;114(1):1-14. [doi:10.1016/j.jconrel.2006.04.017]
265. Shu XZ, Zhu KJ. The release behavior of brilliant blue from calcium–alginate gel beads coated by chitosan: the preparation method effect. *Eur J Pharm Biopharm*. 2002;53(2):193-201. [doi:10.1016/S0939-6411(01)00247-8]

266. Ribeiro AJ, Silva C, Ferreira D, Veiga F. Chitosan-reinforced alginate microspheres obtained through the emulsification/internal gelation technique. *Eur J Pharm Sci.* 2005;25(1):31-40. [doi:10.1016/j.ejps.2005.01.016]
267. Krasaekoopt W, Bhandari B, Deeth H. The influence of coating materials on some properties of alginate beads and survivability of microencapsulated probiotic bacteria. *International Dairy Journal.* 2004;14(8):737-43. [doi:10.1016/j.idairyj.2004.01.004]
268. Bernkop-Schnürch A, Hornof M, Guggi D. Thiolated chitosans. *Eur J Pharm Biopharm.* 2004;57(1):9-17. [doi:10.1016/S0939-6411(03)00147-4]
269. Cook MT, Tzortzis G, Charalampopoulos D, Khutoryanskiy VV. Production and evaluation of dry alginate-chitosan microcapsules as an enteric delivery vehicle for probiotic bacteria. *Biomacromolecules.* 2011;12(7):2834-40. [doi:10.1021/bm200576h]
270. Bernkop-Schnürch A, Hornof M, Zoidl T. Thiolated polymers—thiomers: synthesis and *in vitro* evaluation of chitosan–2-iminothiolane conjugates. *Int J Pharm.* 2003;260(2):229-37. [doi:10.1016/S0378-5173(03)00271-0]
271. Masuko T, Minami A, Iwasaki N, Majima T, Nishimura S-I, Lee YC. Thiolation of chitosan. Attachment of proteins via thioether formation. *Biomacromolecules.* 2005;6(2):880-4. [doi:10.1021/bm049352e]
272. Roldo M, Hornof M, Caliceti P, Bernkop-Schnürch A. Mucoadhesive thiolated chitosans as platforms for oral controlled drug delivery: synthesis and *in vitro* evaluation. *Eur J Pharm Biopharm.* 2004;57(1):115-21. [doi:10.1016/S0939-6411(03)00157-7]
273. Suknuntha K, Tantishaiyakul V, Worakul N, Taweepreda W. Characterization of muco- and bioadhesive properties of chitosan, PVP, and chitosan/PVP blends and release of amoxicillin from alginate beads coated with chitosan/PVP. *Drug Dev Ind Pharm.* 2011;37(4):408-18. [doi:10.3109/03639045.2010.518149]
274. Coates J. Interpretation of infrared spectra, a practical approach. In: *Encyclopedia of Analytical Chemistry*: John Wiley & Sons, Ltd; 2006.
275. Jiang HL, Artoe R, Quan JS, Yoo MK, Kim YK, Kim IY, et al. Alginate-coated thiolated chitosan microspheres for an oral drug delivery system *in vitro*. *Key Engineering Materials.* 2007;342-343:433-6

276. Varum FJO, Veiga F, Sousa JS, Basit AW. An investigation into the role of mucus thickness on mucoadhesion in the gastrointestinal tract of pig. *Eur J Pharm Sci.* 2010;40(4):335-41. [doi:10.1016/j.ejps.2010.04.007]
277. Davidovich-Pinhas M, Harari O, Bianco-Peled H. Evaluating the mucoadhesive properties of drug delivery systems based on hydrated thiolated alginate. *J Controlled Release.* 2009;136(1):38-44. [doi:10.1016/j.jconrel.2009.01.029]
278. Golowczyc MA, Silva J, Teixeira P, De Antoni GL, Abraham AG. Cellular injuries of spray-dried *Lactobacillus* spp. isolated from kefir and their impact on probiotic properties. *Int J Food Microbiol.* 2011;144(3):556-60. [doi:10.1016/j.ijfoodmicro.2010.11.005]
279. Deepika G, Rastall RA, Charalampopoulos D. Effect of food models and low-temperature storage on the adhesion of *Lactobacillus rhamnosus* GG to caco-2 cells. *Journal of Agricultural and Food Chemistry.* 2011;59(16):8661-6. [doi:10.1021/jf2018287]
280. Ouwehand AC, Tuomola EM, Tödkkö S, Salminen S. Assessment of adhesion properties of novel probiotic strains to human intestinal mucus. *Int J Food Microbiol.* 2001;64(1-2):119-26. [doi:10.1016/S0168-1605(00)00440-2]
281. Guo C, Gemeinhart RA. Understanding the adsorption mechanism of chitosan onto poly(lactide-co-glycolide) particles. *Eur J Pharm Biopharm.* 2008;70(2):597-604. [doi:10.1016/j.ejpb.2008.06.008]
282. Rossi S, Ferrari F, Bonferoni MC, Caramella C. Characterization of chitosan hydrochloride–mucin rheological interaction: influence of polymer concentration and polymer:mucin weight ratio. *Eur J Pharm Sci.* 2001;12(4):479-85. [doi:10.1016/S0928-0987(00)00194-9]
283. Granato D, Branco GF, Nazzaro F, Cruz AG, Faria JAF. Functional foods and nondairy probiotic food development: trends, concepts, and products. *Comprehensive Reviews in Food Science and Food Safety.* 2010;9(3):292-302. [doi:10.1111/j.1541-4337.2010.00110.x]

Publications and presentations

Publications

- **Chen S**, Ferguson LR, Shu Q, Garg S. The application of flow cytometry to the characterisation of a probiotic strain *Lactobacillus reuteri* DPC16 and the evaluation of sugar preservatives for its lyophilization. **LWT - Food Science and Technology**. 2011;44:1873-9. [doi:10.1016/j.lwt.2011.05.006]
- **Chen S**, Zhao Q, Ferguson LR, Shu Q, Weir I, Garg S. Development of a novel probiotic delivery system based on microencapsulation with protectants. **Applied Microbiology and Biotechnology**. 2012;93:1447-57. [doi:10.1007/s00253-011-3609-4]
- **Chen S**, Cao Y, Ferguson LR, Shu Q, Garg S. Flow cytometric assessment of the protectants for enhanced *in vitro* survival of probiotic lactic acid bacteria through simulated human gastro-intestinal stresses. **Applied Microbiology and Biotechnology**. 2012;95:345-56. [doi: 10.1007/s00253-012-4030-3]
- **Chen S**, Cao Y, Ferguson LR, Shu Q, Garg S. The effect of immobilization of probiotic *Lactobacillus reuteri* DPC16 in sub-100 µm microcapsule on food-borne pathogens. **World Journal of Microbiology and Biotechnology**. 2012;28:2447-52. [doi: 10.1007/s11274-012-1046-x]
- **Chen S**, Cao Y, Ferguson LR, Shu Q, Garg S. Evaluation of mucoadhesive coatings of chitosan and thiolated chitosan for the colonic delivery of microencapsulated probiotic bacteria. 2012; Epub ahead of print. [doi: 10.3109/02652048.2012.700959]

Presentations (Poster)

- **Chen S**, Shu Q, Liu A, Riddle P, Ferguson LR, Garg S. Modelling the cellular integrity of microencapsulated and lyophilised *Lactobacillus reuteri* DPC16 and optimising processing parameters for enhanced cell viability. **HealthX 2008 Conference**. 12th September 2008, Auckland, New Zealand.
- **Chen S**, Tian H, Ferguson LR, Shu Q, Garg S. Characterisation of a novel probiotic strain – *Lactobacillus reuteri* DPC16. **APSA 2008 Conference**. 6th-9th December 2008, Canberra, Australia.
- **Chen S**, Ferguson LR, Garg S, Shu Q. Application of flow cytometry to the characterisation of stress resistance of the probiotic strain *Lactobacillus reuteri* DPC16 and evaluation of sugars as preservative for this strain to survive lyophilisation. **NZBIO Conference 2010**. 22nd-24th March 2010, Auckland, New Zealand.